



January 2018

Isolation And Characterization Of Stem Cell Population In Human Proximal Tubule Cells And The Effect Of Cadmium In The Isolated Proximal Tubule Stem/progenitor Cell Line.

Swojani Shrestha

Follow this and additional works at: <https://commons.und.edu/theses>

Recommended Citation

Shrestha, Swojani, "Isolation And Characterization Of Stem Cell Population In Human Proximal Tubule Cells And The Effect Of Cadmium In The Isolated Proximal Tubule Stem/progenitor Cell Line." (2018). *Theses and Dissertations*. 2347.
<https://commons.und.edu/theses/2347>

This Dissertation is brought to you for free and open access by the Theses, Dissertations, and Senior Projects at UND Scholarly Commons. It has been accepted for inclusion in Theses and Dissertations by an authorized administrator of UND Scholarly Commons. For more information, please contact zeinebyousif@library.und.edu.

ISOLATION AND CHARACTERIZATION OF STEM CELL POPULATION IN HUMAN
PROXIMAL TUBULE CELLS AND THE EFFECT OF CADMIUM IN THE ISOLATED
PROXIMAL TUBULE STEM/PROGENITOR CELL LINE.

by

Swojani Shrestha
Bachelor of Science, Minnesota State University Moorhead, 2013

A Dissertation
Submitted to the Graduate Faculty

of the

University of North Dakota

in partial fulfillment of the requirements

for the degree of

Doctor of Philosophy

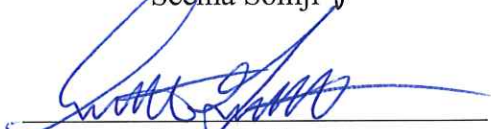
Grand Forks, North Dakota

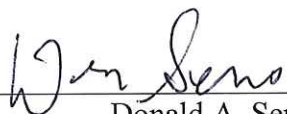
August
2018

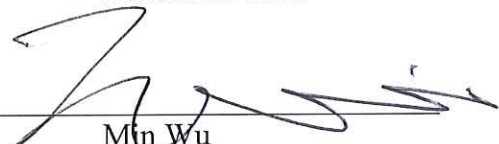
c 2018 Swojani Shrestha

This dissertation, submitted by Swojani Shrestha in partial fulfillment of the requirements for the Degree of Doctor of Philosophy from the University of North Dakota, has been read by the Faculty Advisory Committee under whom the work has been done and is hereby approved.


Seema Somji



Scott H. Garrett

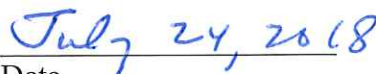

Donald A. Sens


Min Wu


Tristan Darland

This dissertation is being submitted by the appointed advisory committee as having met all the requirements of the School of Graduate Studies at the University of North Dakota and is hereby approved.


Grant McGimpsey
Dean of the School of Graduate Studies


Date

PERMISSION

Title Isolation and characterization of stem cell population from human proximal tubule cells and the effect of cadmium in isolated proximal tubule stem/progenitor cell lines

Department Biochemistry and Molecular Biology

Degree Doctor of Philosophy

In presenting this dissertation in partial fulfillment of the requirements for a graduate degree from the University of North Dakota, I agree that the library of this University shall make it freely available for inspection. I further agree that permission for extensive copying for scholarly purposes may be granted by the professor who supervised my dissertation work or, in his absence, by the Chairperson of the department or the dean of the School of Graduate Studies. It is understood that any copying or publication or other use of this dissertation or part thereof for financial gain shall not be allowed without my written permission. It is also understood that due recognition shall be given to me and to the University of North Dakota in any scholarly use which may be made of any material in my dissertation.

Swojani Shrestha
Jun, 2018

TABLE OF CONTENTS

LIST OF FIGURES.....	iv
LIST OF TABLES.....	v
ACKNOWLEDGEMENTS.....	vi
ABSTRACT.....	vii
CHAPTER	
I. INTRODUCTION.....	1
The Kidney.....	1
Proximal Tubule Cells of the Kidney, Their Functions and Significance.....	2
Cadmium Toxicity.....	4
Kidney Tubule Regeneration Theories.....	6
Stem/Progenitor Cells in Kidney.....	8
Markers of Stem/Progenitor Cells in Human Proximal Tubule Cells.....	8
Studies on Isolation of Stem/Progenitor Cells of Human Proximal Tubule Cells.....	9
Role of Stem/Progenitor Cells in Tubular Regeneration.....	11
Significance of <i>In-vitro</i> Cell Culture Models.....	12
Cell Culture Models.....	15
Rationale/Hypothesis.....	17

II.	METHODS.....	20
	Cell Culture.....	20
	RNA Isolation.....	20
	Real Time PCR.....	21
	Microarray Analysis of Global Gene Expression.....	22
	Determination of Cell Viability by DAPI Staining.....	22
	Western Blot.....	23
	Determination of LDH release.....	25
	Caspase-3 assay.....	25
	Florescence Activated Cell Sorting.....	26
	Transepithelial Resistance Measurement.....	27
	Spheroids Culture.....	28
	Thick and Thin Layer Matrigel coated Cell Growth.....	28
	Immunofluorescence.....	29
	MTT growth assay.....	30
	Exposure of Cell-lines to Cd ²⁺ and Determination of Cell Population.....	30
	Subcutaneous Injection of Cell-Lines.....	31
	Immunohistochemistry.....	31
	Statistical Analysis.....	33
III.	RESULTS.....	34

Global Gene Expression Pattern of HK-2, HPT and RPTEC/TERT1 Cells.....	34
Expression of CD24 and CD133 in the HK-2, HPT and RPTEC/TERT1 Cells.....	42
Expression of Cadherins, Claudins and Occludin in the HK-2, HPT and RPTEC/TERT1 Cell Isolates.....	45
Mode of Cell Death in RPTEC/TERT1 Cells in Response to Cd ²⁺ - Induced Toxicity.....	48
Isolation of CD133+CD24+ and CD24+ Cell Population from RPTEC/TERT1 Cell Cultures.....	50
Expression of CD133 and CD24 Markers in RPTEC/TERT1, CD133+CD24+ and CD24+ Cells Cultures.....	54
Morphology, Transepithelial Resistance and Growth Rate Determination of RPTEC/TERT, CD133+CD24+ and CD24+ Cells.....	56
Ki67 Expression in RPTEC/TERT1, CD133+CD24+ and CD24+ cells.....	58
Expression of AQP-1 and CAL Markers in RPTEC/TERT1, CD133+CD24+ and CD24+ Cells.....	60
Ability of RPTEC/TERT1, CD133+CD24+ and CD24+ Cells to Form Spheroids.....	61
Change in CD133+CD24+ and CD24+ Cell Population after Exposure to Cd ²⁺ for 34 Days.....	63
Growth of RPTEC/TERT1, CD133+CD24+, CD24+ and HPT Cells with Matrigel in Culture Plates.....	68
Histology and Immunohistochemical staining of tubular structures formed by various populations of RPTEC/TERT1 cells.....	71
IV. DISCUSSION.....	77

Characteristic Features of <i>In-Vitro</i> Human Proximal Epithelial Cell Culture.....	77
Immortalized RPTEC/TERT1 Cells as a Model System to Study Human Proximal Tubule Cells.....	79
Mode of Cell Death after Cadmium Insult in RPTEC/TERT1 Cells...	82
Expression of CD133 and CD24 Markers in Primary Human Proximal Tubule Cultures.....	83
Characterization of CD133+CD24+ and CD24+ Cells isolated from RPTEC/TERT1 Cells.....	83
Exposure to Cadmium decreases CD24+ Cell Population while increases CD133+CD24+ Cell Population.....	85
Ki67 Expression in Cultured RPTEC/TERT1 after Cadmium Insult..	87
Demonstration of the ability of various populations of cells to form tubular structures <i>in-vitro</i> and <i>in-vivo</i>	87
REFERENCES.....	92

LIST OF FIGURES

Figure	Page
I-1. Three regions of the kidney.....	1
I-2. Parts of the nephron.....	2
I-3. Regeneration mechanism in epithelial tubular cells after injury.....	7
I-4. Schematic of dome formation.....	13
III-1. Hierarchical clustering of various proximal tubule cell transcriptomes.....	35
III-2. Principal component analysis using all 67,528 non-control transcript clusters.....	37
III-3. Venn diagram showing differentially expressed genes in HK-2 cells and RPTEC/TERT1 cells in comparison to mortal human proximal tubule cell (HPT) isolates.....	38
III-4. Transposed principal component analysis after performing discriminant analysis of pre-defined groups.....	39
III-5. Hierarchical clustering of transcript cluster expression after statistical filtering.....	41
III-6. Flow cytometry analysis of CD24 and CD133 populations in proximal tubule cells.....	43
III-7. Expression of stem cell markers in cultures of human proximal tubule cells.....	44
III-8. Expression of cadherins in cultures of human proximal tubule cells.....	46
III-9. Expression of tight junction proteins in cultures of human proximal tubule cells.....	47
III-10. Effect of Cd ⁺² on RPTEC/TERT1 cells.....	48

III-11. Effect of Cd ⁺² on HK-2 cells.....	49
III-12. Flow cytometry analysis of CD133+CD24+ and CD24+ populations in RPTEC/TERT1 cells ran in triplicate.....	51
III-13. Flow cytometry analysis of CD133+CD24+ cells to test purity at each passage number.....	52
III-14. Flow cytometry analysis of CD24+ cells to test purity at each passage number.....	53
III-15. Expression of CD133 and CD24 in various populations of renal tubular cells.....	55
III-16. Light level microscopy of different proximal tubular cell cultures after sorting.....	56
III-17. Transepithelial resistance measurement of RPTEC/TERT1, CD133+CD24+ and CD24+ cells.....	57
III-18. Determination of growth rates of various populations of renal tubular cells..	58
III-19. Flow cytometric analysis of number of cells stained positive for Ki67 in fully confluent cultures RPTEC/TERT1, CD133+CD24+ and CD24+ cells.....	59
III-20. Expression of aquaporin-1 (AQP-1) and calbindin (CAL) in various populations of renal tubular cells.....	61
III-21. Light level microscopy of spheroids generated from RPTEC/TERT1, CD133+CD24+, CD24+ cells.....	62
III-22. Effect of Cd ⁺² on the viability RPTEC/TERT1 cells exposed to 0, 4.5, 9, 13.5, 18, 27 and 45 µM Cd ⁺² for 16 days.....	63
III-23. Light level microscopy of CD133+CD24+ cells treated with 4.5 and 9µM Cd ²⁺ for 34 days.....	64
III-24. Light level microscopy of CD24+ cells treated with 4.5 and 9µM Cd ²⁺ for 34 days.....	65
III-25. Effect of cadmium on the viability RPTEC/TERT1 cells.....	67

III-26. Effect of cadmium on the viability of various populations of renal tubular cells.....	67
III-27. Light level microscopy of RPTEC/TERT1 cells plated with matrigel in a 48-well plate.....	68
III-28. Light level microscopy of CD133+CD24+ cells plated with matrigel in a 48-well plate.....	69
III-29. Light level microscopy of CD24+ cells plated with matrigel in a 48-well plate.....	69
III-30. Light level microscopy of HPT cells plated with matrigel in a 48-well plate..	70
III-31. Light level microscopy of RPTEC/TERT1, CD133+CD24+ and CD24+ cells plated on the surface of thin matrigel coated 48-well plate.....	70
III-32. Immunohistochemical analysis of proximal tubule stem cell markers in subcutaneous nodules formed in immuno-compromised mice.....	72
III-33. Immunohistochemical analysis of tubular markers in subcutaneous nodules formed in immuno-compromised mice.....	73
III-34. Immunohistochemical analysis of keratin proteins, filament protein and nephron development marker in subcutaneous nodules formed in immuno-compromised mice.....	74

LIST OF TABLES

Table	Page
II-1. List of primary antibodies used for western blot.....	24
II-2. List of primary antibodies used for immunofluorescence.....	30
II-3. List of primary antibodies used for immunohistochemistry.....	32

ACKNOWLEDGEMENTS

I would first like to thank Dr. Don Sens who accepted me as a graduate student in his lab and provided me with an opportunity to gain extensive knowledge and training on science and research. Without Dr. Joe Provost, my undergraduate advisor, I would have never imagined going to graduate school, so much thanks to him. I would like to thank my advisors Dr. Seema Somji as well as Dr. Scott Garrett for providing insightful guidance on my research, training on different cellular and molecular biology techniques and being available anytime to answer my questions. My special thanks to Dr. Seema Somji for believing in my potentials and providing me with tremendous encouragement throughout my graduate degree career. I am overwhelmed and fortunate to be a part of this department who recognized my abilities and allowed me to thrive as a researcher.

I would like to thank Dr. Jane Dunlevy for training me with her expertise in confocal microscopy and Dr. Zhou and Ms. Wang for helping me with animal handling techniques and taking immunohistological images. I would like to thank Dr. Min Wu and Dr. Kathy Sukalski for giving their time to talk about how to succeed in graduate school when I first started the program. I would like to extend many thanks to Dr. Tristan Darland for his willingness to become my faculty at large. Thank you to Steve for providing me extensive training on flow cytometry.

I am extremely grateful and thankful to Dr. Mary Ann Sens and Dr. Don Sens for the support they offered me during my difficult times. I will never be able to repay their kindness.

I considered myself extremely lucky for having one of the most amazing lab mates and colleagues, Menglan, Bethany, Andrea, Emily, Zach as well as other lab members. I don't miss being far away from home and family because of them. Lastly, I thank my parents for all their sacrifices and my brother and sister-in-law for always supporting me. I love them all and they will forever be in my heart.

ABSTRACT

The proximal tubules of the kidney are target sites of injury by various toxicants. Cadmium (Cd^{2+}), an environmental nephrotoxicant can cause adverse effects and overt renal damage. To decipher the mechanisms involved in nephrotoxicity, an *in-vitro* model system is required. Mortal cultures of human proximal tubule (HPT) cells isolated from the renal cortex are used as models, but are difficult to acquire and have limited passage number. The immortalized HK-2 cell line, has served as a model but it lacks vectorial active transport and shows signs of lost epithelial features. Recently a new proximal tubule cell line, the RPTEC/TERT1, was developed. For this study we performed global gene expression analysis of this cell line in comparison to the HK-2 and HPT cells showed that the RPTEC/TERT1 cells had gene expression patterns similar to HPT cells when compared to the HK-2 cells. The HPT and the RPTEC/TERT1 cell lines showed higher expression of renal stem/progenitor like cell population, CD133+CD24+ when compared to the HK-2 cells. The level of expression of tight junctional molecules was also similar between the RPTEC/TERT1 and the HPT cells. Acute exposure to Cd^{2+} resulted in necrosis of the RPTEC/TERT1 cells whereas the HK-2 cells died by apoptosis. Thus, we verified that the RPTEC/TERT1 are similar to HPT cells and can serve as a good model system to study mechanisms involved in Cd^{2+} induced renal damage. Recent studies suggest that tubular regeneration after toxic insult may involve progenitor/ stem like cells expressing CD133 as well as CD24 markers that resides among the renal tubular cells. Our previous study shows that the RPTEC/TERT1 cells comprise of 25-30% of CD24+ cells whereas 70-75% of the CD133+CD24+ cells. To determine the response of these populations

of cells to renal insult, the two populations of cells were sorted from the RPTEC/TERT1 cells, following which they were cultured and treated with 4.5 μ M and 9 μ M Cd²⁺ for approximately 34 days. The results demonstrate that the CD133+CD24+ cells are more resistant to cadmium exposure as there was no change in the number of double positive cells in response to cadmium treatment whereas the number of CD24+ cells significantly decrease. Both populations of cells form domes in culture indicative of vectorial active transport. The CD133+CD24+ cells show faster growth rate when compared to the CD24+ cells. When injected subcutaneously into the nude mice, these cell populations form tubule structures and CD133+CD24+ cells show positive staining for the distal as well as the proximal tubule markers suggesting their heterogeneous characteristics whereas CD24+ cells show positive staining for only the proximal tubule markers. In conclusion, the data suggests that the CD133+CD24+ cells are likely the progenitor cells in the proximal tubule involved in tubular regeneration after toxic insult whereas the role of CD24+ cells is still unclear.

CHAPTER I

INTRODUCTION

The Kidney

The kidney, a pair of organ of urinary system, are located in the posterior region of the abdomen, behind the peritoneum on both sides of the vertebral column. Some of the major functions of kidney are maintaining fluid and electrolyte homeostasis; transport, absorption and elimination of various compounds and nutrients; filtration of waste products and regulation of blood pressure. The kidney is divided into three major sections known as cortex, medulla and pelvis Fig. I-1. The structural and functional unit of kidney is called nephron Fig. I-2.

Internal Kidney Anatomy

- Three regions

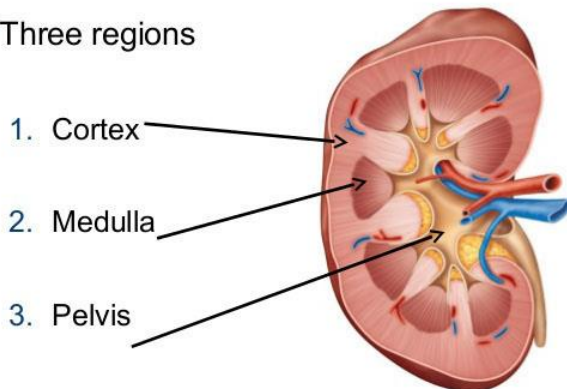


Fig I-1. Three regions of the kidney. Diagram showing three different regions of the kidney, outermost part called cortex, mid region called medulla and innermost part called pelvis.

There are millions of nephron present in the human kidney that are responsible for production of urine. Nephron consists of renal corpuscles and long renal tubule. The renal corpuscles consists of filtering unit called glomerulus which is a cluster of capillaries forming sieve-like structure

that allows passage to waste and toxic products, small biochemical metabolites and excess fluid. This ultrafiltrate passes through the renal tubule, which consists of the proximal tubule,

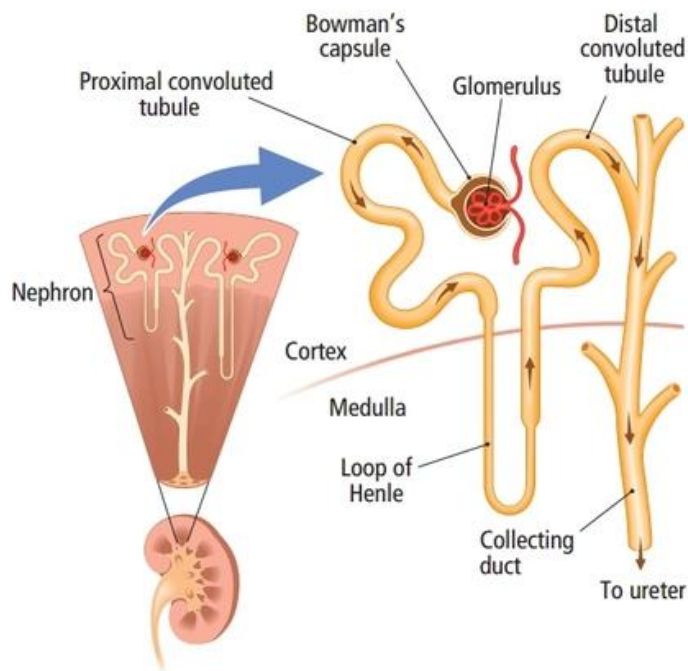


Fig I-2. Parts of the nephron. Diagram showing different cell types present in the nephron. Glomerulus, proximal and distal convoluted tubule of the nephron are present in the cortex region; loop of Henle, collecting duct of the nephron are present in the medulla region. The arrow indicates the direction of the ultra-filtrate filtered by the glomerulus and passes through different regions of the nephron and finally released to the ureter.

using these cells as a model system to study renal toxicity.

loop of Henle, distal tubule in addition, collecting duct where the kidney takes necessary actions such as absorption of essential elements like sodium and potassium, transporting them back to the blood to regulate electrolyte balance in the body. Since the primary focus of this study are the proximal tubule cells of human

kidney, the role of these cells in the human kidney is further discussed below along with the rationale of

Proximal Tubules of the Kidney, Their Function and Significance

Proximal convoluted tubules are the first cell types of the renal tubule in the nephron, whose apical surface consists of microvilli-like brush border facing the lumen and consists of the epithelial cuboidal cells adhering to the basement membrane facing the blood capillaries. The epithelial proximal tubule cells maintain cell-cell interactions that is important in maintaining of integrity of the epithelium and regulation of transepithelial permeability (Matlin K.S & Caplan M.J. 2013). Junctional adherence proteins expressed between cell to cell and cell to basement membrane play important role in signaling for maintenance of cell polarity. The proximal tubule acts as a filtration unit responsible for reabsorption of 60% of glomerular

flow through and solutes (Mandel L.J et al. 1981). To cope up with the heavy flow of glomerular ultrafiltrate, the brush borders of proximal tubules provide greater surface area for absorption of different compounds. Proximal tubule cells also consists of large quantities of mitochondria for production of energy to carry out the rapid reabsorption and transport processes. The apical as well as the basal compartments are rich in solute and ion transporters like $\text{Na}^+ \text{K}^+ \text{-ATPase}$ that are responsible for absorption and transport of different small electrolyte and nutrients in and out of the bloodstream and glomerular filtrate. In addition, the secretion of organic compound like glucose, drugs and hormones take place in proximal tubule. The gap and tight junctions of epithelial proximal tubule cells serve as barriers to avoid entrance of waste and toxic ingredients of the urine from the lumen to the blood flow (Hoppensack A et al. 2014).

Due to the physiological and structural composition of the proximal tubule cells, they are easy target of organic compounds, heavy metals, pharmaceutical metabolites and carcinogens. Factors like age, occupational exposure, pesticides, smoking and diseases like diabetes, hypertension greatly affect the toxicant accumulation and increase the risk of damage. Because of the high reabsorptive functions of the proximal tubule, kidney have high O_2 requirement, making them vulnerable to hypoxic condition particularly in high O_2 demanding absorption and circulation processes of compound and ions like glucose and sodium. In addition, longer period of toxic substances accumulation in proximal tubule cells can cause mitochondrial dysfunction resulting in production of the free radicals that can further cause DNA damage and cell death (Gilbert R.E. 2017).

Proximal tubule damage can be caused by different kidney complication like Acute Kidney Injury (AKI) defined as a rapid loss of glomerular filtration rate and its progression

towards Chronic Kidney Disease (CKD) (Molitoris B.A and Sharfuddin A; Chevalier R. L. 2016). The risk of AKI occurrence ranges from 20-50% in patients who are critically ill and suffer from diabetic nephropathy. About 30% of the AKI patients develop CKD (Tejera D et al. 2017). Prolonged injury can cause obstruction of toxicants, ischemic and hypoxic conditions of proximal tubule cells leading to cell death causing functional damages. The extent and duration of exposure to toxicants and prevailing injury induces proximal tubule cell death by apoptosis or necrosis. Histological samples from the kidney of patients with AKI, CKD and renal failure demonstrate features of necrosis, thus suggesting that during these conditions, the kidney cells die by a necrotic mode of cell death (Peres L. C et al 2012; Rosen S. & Stillman I. E. 2008). However, studies show that the proximal tubular cells after acute injury have the ability to fully regenerate and re-establish normal function. Unfortunately, severe damage causes irreversible and necrotic conditions leading to end stage renal disease (ESRD) and complete loss of kidney function.

Cadmium Toxicity

Cadmium is an environmental carcinogen and one of the major heavy metals that causes adverse health hazards and kidney problems. The major source of cadmium intake is tobacco-use like cigarettes. However, there are other sources like crops grown in cadmium rich soil, use of fertilizers, occupational exposure like mining, smelting, and nickel-cadmium batteries manufacturing companies (Satarug S & Moore M.R 2004; Prozialeck W.C and Edwards J. R. 2012). WHO in 2010 established a provisional tolerable monthly intake for cadmium as 25 µg/kg body weight. Cadmium has toxic effects on skeletal and respiratory organs but its primary target is kidney. The half-life of cadmium is about 12-30 years, and the human body cannot metabolize it, so it accumulates over time in the kidney particularly in

proximal tubule cells. In human, the effect can be dose as well as time dependent. Chronic low dose exposure to cadmium can cause proteinuria and polyuria increasing the excretion of metabolite and electrolytes like glucose, sodium and calcium leading to proximal tubule dysfunction, osteoporosis, end-stage renal disease and cancer (Järup L. 2002, Satarug S & Moore M. R. 2004). The *in-vivo* studies in animal models have shown that low level of cadmium administration over time causes adverse effect particularly in proximal tubule cells causing cell death (Prozialeck W.C. et al., 2007; Prozialeck W.C. & Edwards J.R. 2010; Chargui A. et al. 2011). Proximal tubule cells easily uptake the cadmium bound to metallothionein (Cd-MT) that is released from the liver and filtered by the glomerulus. Once inside the proximal tubule cells the lysosomes degrades the MT, freeing the cadmium. Since cadmium is not biodegradable and minimally excreted in the urine, this leads to its accumulation in proximal tubule cells over time resulting in toxic effects (Hodgson. E. 1987). The circulating cadmium can also loosely bind to sulfhydryl compounds like glutathione and cysteine or molecules like albumin, and once filtered through the glomerulus, cadmium is released due to its low binding affinity allowing the free cadmium to bind to the surface of the proximal tubules. Studies have found that free cadmium on the cell surfaces can enter the cell by the help of channels and transporters like ZIP8 that transports ions like Ca^{2+} and Zn^{2+} (He L. et al. 2009; Prozialeck W.C. 2012).

Cadmium causes injury to the proximal tubule cells by disruption of cell-cell junctional proteins, modification of intracellular signaling cascades and increase in oxidative stress eventually resulting in cell death. Studies performed with cultured cells exposed to moderate levels of cadmium for short time periods showed alteration in predominant cadherin proteins and separation of cell-cell adhesion causing cells to become round (Prozialeck W. C. &

Niewenhuis J.R. 1991). This causes loss of cell polarity and changes in predominant transporters like Na⁺K⁺-ATPase. The differential gene expression pattern in acute exposure to different levels of Cd²⁺ in primary human proximal tubule cultures showed alteration in mainly the genes involved in stress responses, cell death, cell cycle, inflammation, and cell adhesion (Garrett S.H. et al. 2011). The pathways altered by cadmium insults to proximal tubules are MAP kinase pathways, cAMP and wnt/b-catenin (Thévenod, 2009). Acute cadmium toxicity to proximal tubule cells also increases ROS production by depleting antioxidant activity, which lead to oxidative DNA damages (Bagchi et al., 1997; Waisberg et al., 2003).

Kidney Tubule Regeneration Theories

Human kidney tubules have the ability to regenerate mostly after acute toxic insult. It has been predicted that the main source of regenerating cells in kidney are the cells that reside within the kidney itself rather than any external non renal cell types (Oliver J. A & Al-Awqati Q. 2013; Duffield J.S et al 2005; Lin F et al 2005). It has been proposed that after the acute injury, the injured tubular cells shed off from the basement membrane and the surviving tubular cells undergo dedifferentiation followed by proliferation and redifferentiate into functional tubular cells to replace the space (Fig. I-3) (Bonventre J.V. 2003). The repair of tubular cells by dedifferentiation and proliferation of surviving epithelial cells hypothesis have demonstrated that most of the adult tubular epithelial cells normally have low proliferative rate and remain in G1 phase, however they readily enter the cell cycle once they encounter damaging signals (Vogetseder A et al. 2008). Another hypothesis predicts that based on *in-vivo* studies by inducing AKI to the mice, where all the cells involved in nephrogenesis were lineage labeled, the results show no evidence of any extra-tubular renal cell types entering the

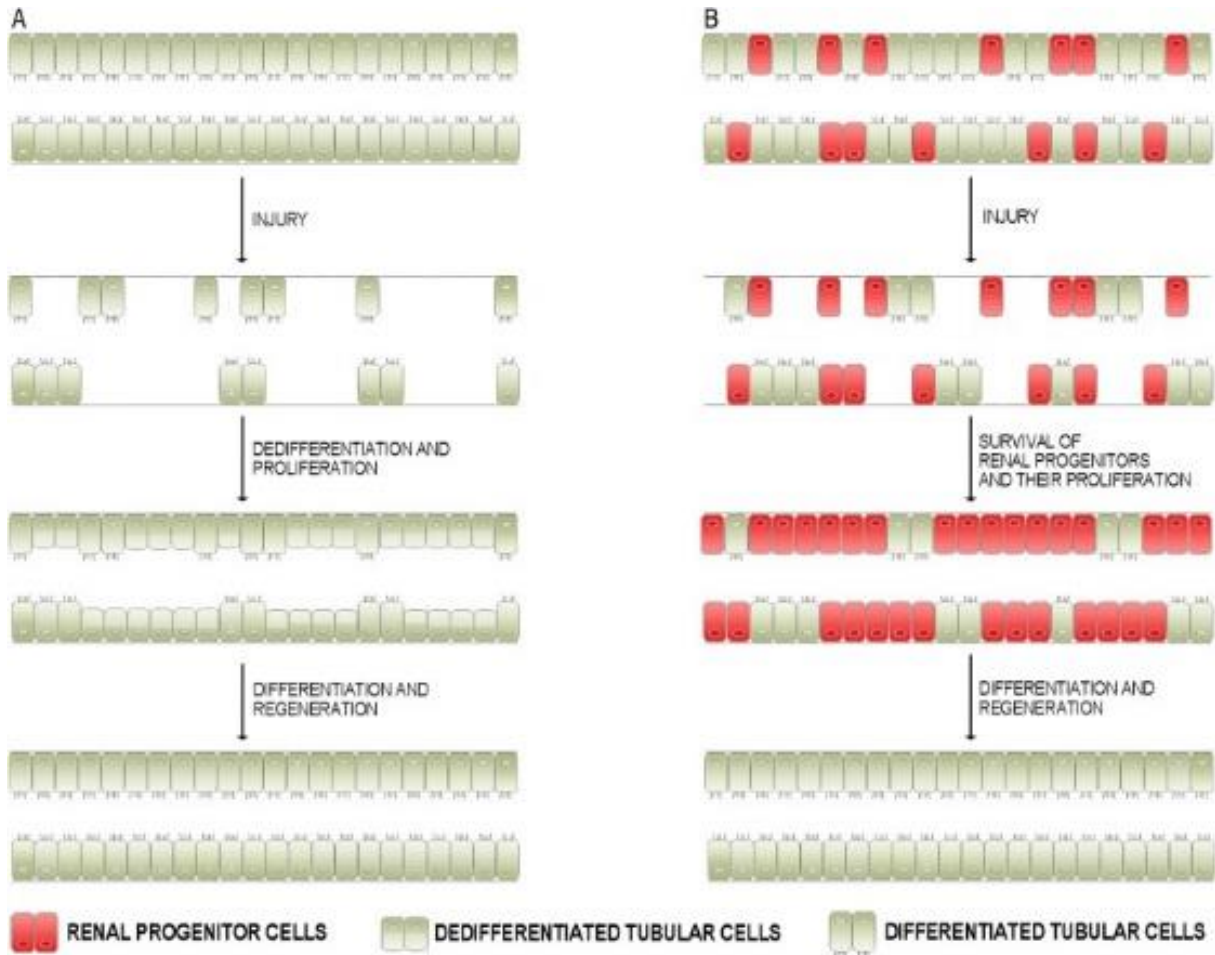


Fig I-3. Regeneration mechanism in epithelial tubular cells after injury (Lombardi D et al. 2016). A. This mechanism of regeneration state that after the injury, the differentiated tubular cells are lost and the least injured resident tubular cells dedifferentiate and proliferate into differentiated tubular cells. B. The theory shows the existence of resident renal progenitor/stem like cells in the proximal tubule, which after injury the less differentiated progenitor cells proliferate to fill up the space and restore normal function of differentiated proximal tubule cells.

tubule to help in repair processes. This proves that the source of the repair involves the group of self-renewing cells within the proximal tubule (Humphreys B. D et al. 2008). More precisely, the current evidence shows the presence of scattered stem/progenitor or epithelial stem-cell like cells residing in the proximal tubule of the kidney, which are able to proliferate and self-renew after moderate injury (Fig. I-3) (Suzuki E et al. 2016; Bussolati B et al. 2009; Lindgren D et al. 2011; Smeets B et al. 2013).

Stem/Progenitor Cells in Kidney

It has been considered that the renal tubular cells have high regenerative capabilities and particularly after moderate or acute injury level, the tubular cells undergo complete functional recovery (Lombardi D et al. 2016). A number of laboratories have predicted the presence of resident renal stem cells in the kidney, however understanding their origin, characteristics and role in repair after injury needs more research attention. Therefore based on the reports on the existence of stem/progenitor cells in renal proximal tubule and their probable contribution to repopulate the tubular epithelium, we will further explore their identification, isolation and characterization studies.

Markers of Stem/Progenitor Cells in Human Proximal Tubule Cells

Recent studies show that the human proximal tubule cells that express the markers CD24, CD133 and VIM are scattered throughout the cells of proximal tubules and act as the potential progenitor tubular cells that demonstrate the ability to form spheres and clonally expand in culture and also show epithelial differentiation after acute injury. (Lindgren D et al. 2011; Angelotti ML et al. 2012; Kim K et al. 2011; Loverre A et al. 2008; Smeets B et al. 2013). In human, both CD24 and CD133 proteins have been found to be expressed in immature cell types like the stem/progenitor cells of blood; developmental stages of intestine and neurons (Smeets B et al. 2013). Hence, the tubular epithelial cells positive for CD133 as well as CD24 are considered as progenitor cells and are associated with being co-expressed with proliferation marker like PCNA and are resistant to death after moderate injury (Kim K et al. 2011, Smeets B et al. 2013). The cells positive for CD133 as well as CD24 also show high expression of aldehyde dehydrogenase (ALDH), a universal stem cell marker. Previous work from our laboratory using flow cytometric analysis has shown that primary cultures of human proximal

tubule cells consists of approximately 55-60% cells that co-express both the CD24 and the CD133 marker, whereas about 40-45% of the cells express only the CD24 marker (Shrestha, S et al. 2017).

Studies on Isolation and characterization of Stem/Progenitor Cells from Human Proximal Tubule

The common method used to isolate the stem/progenitor cells from different cortical cell types of the nephron is to obtain the healthy cortical tissue samples from the patients, followed by dissociation method to recover the tubular suspension and prepare a single cell sample. This single cell suspension can be sorted using fluorescence activated or immunomagnetic cell sorting for obtaining cell population positive for stem/progenitor like cell-surface markers. Lindgren et al. used the fluorescence-activated cell sorting (FACS) method to isolate the cell population from the cortical tissues that are positive for the activation of the stem-cell marker ALDH. The ALDH^{high} cell population were able to form spheroid in culture, one of the characteristics of stem cell *in-vitro* and showed higher mRNA levels of CD133 gene. They also demonstrated using confocal microscopy that the ALDH^{high} cell population express CD24, moreover, some cells co-expressed both CD133 as well as CD24 and VIM (Lindgren D et al. 2011). Another group of scientists isolated the CD133+CD24+ of the glomerulus and tubular cells of human kidney section and selected CD133+CD24+CD106+ to distinguish the glomerulus cell population from the tubular population that represented CD133+CD24+CD106- population. These isolated tubular population generated clones when plated in 96-well plate; also showed higher growth rate compared to the CD133-CD24- control cells; showed higher mRNA expression of tubular-specific solute transporters like Na/K/Cl transporter; resistivity to death after exposed to Hb when compared to the control. When CD133+CD24+ cells along with CD133-CD24- cells were injected intravenously into the tail

vein of AKI induced mice, the results showed the mice injected with CD133+CD24+ cells had decreased blood urea nitrogen levels. Furthermore, to look at the regeneration ability of the CD133+CD24+ cell population *in-vivo*; they labeled the cells with a red fluorescent dye, PKH26; injected into the SCID mice and observed the generation of the new tubular cells, which was identified by expression of the red fluorescent protein. The new tubular structures were positive for both proximal as well as distal markers (Angelotti M.L et al. 2012). These *in-vivo* studies and observations based on adult human kidney tissues, confirmed that all the cells positive for CD24 are also positive for CD133 and there is no presence of CD133+ only cells in the adult human kidney tissues (Romagnani P et al. 2013). Another lab (Bussolatti B et al. 2005) isolated the CD133+ cells from the tubular suspension derived from the healthy cortex of the kidney, plated in 96-well plate for cloning and expanded the same clone as monolayer. The cells expressed epithelial markers like E-cadherin, ZO-1 and proximal tubule brush border enzyme, alkaline phosphatase and NaCl co-transporter. However, expression of CD24 was not evaluated in this study which does not exclude the probabilities of CD24 being expressed in their CD133+ cell population. The stem-cell population when plated on matrigel formed capillaries or ring like structures. The *in-vivo* subcutaneous injection of the cells led to formation of tubule like structures as seen in previous study, some of which showed staining for proximal as well as distal tubule markers such as cytokeratin7, cytokeratin 19, vimentin, Pax-2 and NaCl co-transporter (Bussolatti B. et al. 2005).

Therefore, most of the studies verify the existence of stem/progenitor like cells in the epithelial tubules of the kidney. After isolation of the stem-cell population from proximal tubule of the kidney, *in-vitro* and *in-vivo* studies are necessary to characterize this population and determine the role of these cells in regeneration after injury.

Role of Stem/Progenitor Cells in Tubular Regeneration

As discussed earlier, complications with any kidney cell types for a long period of time can cause diseases like CKD and ESRD. The prevalence of this global public health problem has been on rise and the progress on treatment has seen low success rate compromising the health quality and money invested into it by affected patients. The common effective treatment method for the CKD or ESRD is organ transplantation however, the wait for a matching donor can be very long and there is high risk of rejection (Bombelli S. et al. 2018). With the recent advancement in tissue engineering and cell reprogramming field, stem-cell and regenerative medicine show greater potential for success. Scientists have used induced pluripotent stem cells/ hematopoietic stem cells/ embryonic stem cells derived from adult cell types and attempted to program them to become renal cells. Although stem cells are said to be multipotent, use of above mentioned stem cell therapies have not shown big success in forming a functional differentiated kidney for replacement (Chou Y.H et al 2013).

Although cell-renewal capabilities of kidney is limited, the most promising source for replacement of nephron cell loss has been verified to be the renal progenitor cells that are scattered in glomerular and tubular compartments. The renal progenitor/stem like cells can be isolated and applied in kidney regeneration as evidenced previously from the *in-vivo* studies in which researchers have found that the isolated renal progenitors can repopulate the tubule to some extent by forming novel tubular structures as well as improve the condition of animals experiencing acute injuries. Recently, Bombelli S et al. developed a novel technique to analyze the regenerative abilities of the renal progenitor cells by using nephrosphere, a population of renal stem-like cells capable of forming 3-D tubular structure under renal capsule of nude mice, to repopulate the decellularized normal human kidney section obtained from patients in culture

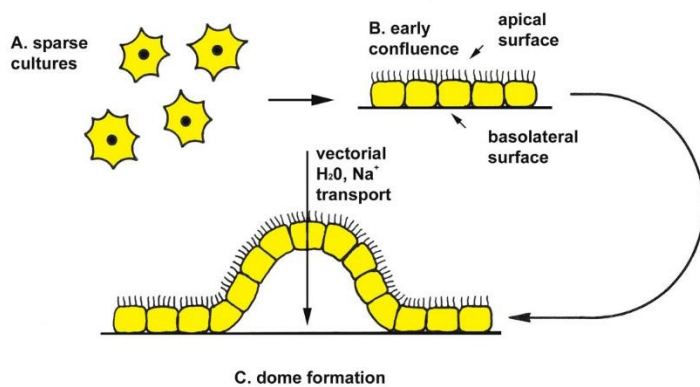
dishes. The decellularization of kidney tissue maintains the renal architecture and provides a scaffold platform for progenitor growth. They discovered that the nephrospheres cultured in decellularized human kidney section repopulated the acellular compartments and were able to differentiate into distal and proximal-tubule cell types. Current research advancement on renal stem/progenitor like population show potential that can improve some of the prevailing problems that the world is facing with kidney regenerative medicine.

Significance of *In-Vitro* Cell Culture Models

To understand and assess the mysteries of human health and risk, the use of biologically relevant conditions and sources that best represent the ongoing processes in the body is required. Cell-culture models are one of those sources that mimics *in-vivo* characteristics utilized to assess and understand the biology of any type of organ. Kidney is a complex organ that consists of heterogeneous cell types. *In-vitro* model system is a powerful tool to study the physiology, drug delivery dynamics, biochemical and mechanistic processes and also progression of diseases in the kidney specifically because it is sensitive to toxic effects of xenobiotics. As mentioned earlier, the proximal tubules perform the major component of renal reabsorption and requires extremely large amounts of energy, rendering this segment to be susceptible to a variety of injuries, both from ischemic episodes and exposure to toxic substances such as heavy metals. Therefore, *in-vitro* system is necessary to study pathophysiology of the proximal tubules (Hoppensack A. et al. 2014; Matlin K.S and Caplan M. J et. al. 2013).

Stable cell culture model is paramount in order to achieve most reliable and best replica of the *in-vivo* conditions. An ideal *in-vitro* proximal tubule model can have multi-dimensional applications in biomedical and toxicological research. Some of them are discussed below. *In-*

in vitro cell culture models are used to study the vectorial active transport activities of the proximal tubule cells. This is characterized by formation of domes in the culture flasks that represents the transport of solute in the media from the apical to the basolateral surface (Detrisac C. J. et al 1984). This has been considered as a hallmark of proximal tubule cells in culture (Fig. I-4). Epithelial polarization and measure of distribution of tight junction studies have been done by growing the cells in permeable filters supports and measuring their transepithelial resistivity (TER) (Misfeldt D.S. et al 1976). In toxicology studies, TER is indicative of the leakiness of epithelial tubular cells making it easier for molecules to enter the



cells. Structural integrity of the proximal tubule cells can be assessed by studying the distribution of various cell-cell junction and attachment proteins, extracellular matrix proteins and

Fig I-4. Schematic of dome formation. The apical cell surface is in contact with culture medium; the basolateral surface faces

various solute and ion

transporters by utilizing *in-vitro* cultures. All of these aspects can be explored after exposure to certain compounds and/or toxicants that is detrimental to proximal tubule cells. Exposure to major nephrotoxics in proximal tubule cells can lead to studies involving ROS pathway analysis; cell death and DNA damage; loss of structural integrity and function studies. Lethal doses from any particular toxicant in *in-vivo* system causes acute and chronic kidney damages. It is required to perform titration studies in *in-vitro* to understand the relevant dose and time that causes severe conditions and cell death of cultured cells after exposure to a toxicant. Using

in-vitro models and inducing them to acute and chronic doses of a toxicant, studies involving role of adult stem/progenitor cells in recovery can be assessed.

The primary *in-vitro* cell culture model is derived from the healthy cortical portion of the kidney from patients and after its dissociation and filtration; the final cell suspension sample is cultured in serum-free media with supplements necessary for normal epithelial growth. This model retains most of the physiological and structural properties of the *in-vivo* system and generates best replica of the biochemical modification happening in the human body. However, the major drawback for primary cultures is that they have limited cell division and enter replicative cell-senescence. In addition, it is difficult to obtain normal kidney tissues. For these reasons, researchers have developed immortalized *in-vitro* culture models for proximal tubule cells that pertain all the characteristic features of the primary cell cultures, can be cultured for many generations and serves as a good model for transformation and long term exposure studies. Immortalization of *in-vitro* cell culture can be performed by transduction of viral oncogenes such as SV40 and E6/7 protein of the HPV16 virus that inactivates the pRb and p53 complexes resulting in cell-cycle arrest and extending the life of the cells (Lee K. M et al. 2004). However, this method may give rise to cancer-associated changes and alter normal genetic makeup. The most promising immortalized *in-vitro* proximal tubule cells to use for experimental purpose is hTERT immortalized cells because hTERT, a catalytic unit of human telomerase enzyme, base pairs with the telomere sequence leading to its elongation and restoration of the shortening of telomere (Greider C.W 1990). Telomere shortening after every cell division ultimately leads to senescence therefore its elongation and prevention from shortening causes cells to become immortal (Lundberg A.S et al. 2000).

Cell Culture Models

Cell culture is used extensively to study the mechanisms underlying normal and disease processes that involve the renal proximal tubule. Until recently, two cell culture models of the human proximal tubule have been used in these studies. The first model is mortal cultures of human proximal tubule (HPT) cells isolated from cortical tissue of human kidneys (Detrisac C.J. et al. 1984). The second model utilizes HK-2 cells, an immortalized cell line, derived by immortalizing and cloning a cell from a primary culture of the above-described proximal tubule epithelial cells transduced with a construct containing the HPV16 E6/E7 genes (Ryan M. J et al. 1994). More recently, a third model consisting of an immortalized human proximal tubule cell line, RPTEC/TERT1, was derived by immortalizing and cloning a cell from a primary culture of the above-described proximal tubule epithelial cells transduced with a construct containing hTERT (Wieser M. et al. 2008). The HK-2 cell line, due to its immortalized property, has seen the most usage regarding studies on the proximal tubule, with over 100 citations in the previous 10 years. Primary HPT cells are utilized much less due to the need to secure human tissue and their limited lifespan, although commercial suppliers are now available. The HK-2 and HPT cell models both retain many, but not all, differentiated features of the human proximal tubule. These properties include proximal tubule markers such as alkaline phosphatase, gamma glutamyltranspeptidase, leucine aminopeptidase, acid phosphatase, and glucose-6 phosphatase (Detrisac C. J et al. 1984, Ryan M. J et al. 1994). An important marker is the enzyme glucose-6 phosphatase that is needed for gluconeogenesis and it is known that the proximal tubule is the only renal segment that can support gluconeogenesis. Functional markers of proximal tubule differentiation also retained are cAMP responsiveness to parathyroid hormone, but not antidiuretic hormone and, the ability to accumulate glycogen.

There are two major differences between the HPT and HK-2 cells that are reflected in their morphology. One major difference is that the HK-2 cells have lost the capacity for vectorial active transport as noted by the inability to form doming structures in culture (Kim D et al. 2002). The formation of domes is a hallmark of cultured renal epithelial cells that retain the *in situ* property of vectorial active transport and appear as out-of-focus areas of the cell monolayer seen upon light microscopic examination. In these raised areas, fluid is trapped underneath the monolayer owing to active transport of ions and water across the cell monolayer in an apical to basolateral direction. This in turn traps a bubble of fluid between the cell layer and the culture dish, forcing local detachment of the monolayer from the plastic surface forming a raised area with an underneath reservoir of accumulated fluid. A second major difference is that, in agreement with the absence of domes, the HK-2 cells do not develop a transepithelial resistance due to the lack of tight junctions (Kim D et al. 2002). A corresponding analysis of E- and N-cadherin expression between the cell lines demonstrated a decrease in E-cadherin and an increase in N-cadherin expression in the HK-2 cells when compared to the HPT cells (Bathula C.S. et al. 2008; Slusser A. et al. 2014). These major differences are reflected in the HPT cells having an enhanced epithelial morphology and increased polarization compared to the HK-2 cell line.

RPTEC/TERT1 are well characterized and show more similar characteristics and functional properties to the primary proximal tubule cells culture. Although not as well published, the RPTEC/TERT1 cells have been shown to retain gene expression patterns expected for the proximal tubule, as well as to form a polarized monolayer, form domes in culture, and to display a light level morphology indistinguishable from primary cultures of HPT cells (Aschauer L. et al. 2013). They also show resistivity to different nephrotoxins at

varying concentration and time points, hereby allowing long-term experimentation that most accurately predicts the scenario of mechanism of toxicity in human body (Simon B.R et al 2014). Therefore, RPTEC/TERT1 cell line has been demonstrated to serve as a model for the study of agent-induced nephrotoxicity (Crean D. et al. 2015).

Rationale/Hypothesis

As stated in the earlier sections of this introduction, the proximal tubules of the human kidney are susceptible to a variety of injuries, both from ischemic episodes and exposure to toxic substances such as heavy metals (Buser et al. 2016). The proximal tubules perform the major component of renal reabsorption and, as such, requires extremely large amounts of energy, rendering this renal segment very susceptible to exposure from nephrotoxins or the loss of nutrients and oxygen from blockage of blood flow. If severe, this result in acute tubular injury where the proximal tubule cell loses polarization followed by necrosis or apoptosis, cellular detachment and ultimately denuded basal membranes (Racusen et al. 2007). Acute tubular injury, if within defined levels of compromise, are transient and the proximal tubule cells can regenerate following such insults. The ability of proximal tubule cells to regenerate following acute injury has led to efforts to characterize the cells that can regenerate following injury.

From previous characterization studies, the RPTEC/TERT1 immortal cells is considered as an appropriate model of primary proximal tubule cultures in comparison to the HK-2 immortal cells. To establish an ideal *in-vitro* model system that mimics the nature of primary human proximal tubule cultures, the RPTEC/TERT1 cells will be utilized to study Cd²⁺ toxicity as well as to isolate the progenitor cells that may be involved in the recovery after Cd²⁺ insult. To fulfill this goal, it is necessary to study the gene expression patterns of each

cell line that will provide us with the list of differential genes. Thus, this allows comparing the differences and similarities in gene expression profiles for all cell lines. The gene expression data will further help us validate the expression levels of different markers involved in different pathways that is important for maintaining proximal tubule integrity. Validation study of the RPTEC/TERT1 cells as a good model system of the primary proximal tubule cultures will allow us to expose the cells to different concentration of cadmium and study various toxic effects occurring in the cells.

Another major challenge of this project is to identify and isolate the stem or progenitor-like cell population in the selected model system. There are many evidences that verify that both *in-vivo* as well as the primary cell lines consists of stem/progenitor cell population within the tubular cells that express CD133 as well as CD24 (Lindgren et al. 2011; Angelotti M.L et al 2012; Romagnani P et al. 2013; Bussolatti et al. 2005; Kim K. et al 2011). Therefore, RPTEC/TERT1 serve as an ideal and a stable model to isolate the stem/progenitor population that express the surface stem cell markers CD133 and CD24 by single cell sorting techniques. After obtaining a pure progenitor population, the cells will be cultured in order to characterize their morphological and biological properties. Validation studies are required to show that the isolated stem/progenitor population are able to self-renew and grow in suspension to confirm their stemness. After successful isolation of the stem/progenitor population from RPTEC/TERT1, we will test their ability to recover after damage with Cd²⁺ in acute as well as chronic conditions. The reports show that the injury caused after acute damage are recovered by proliferation of stem/progenitor cells residing in the kidney however, the chronic injury causes excessive cell loss and death causing irreversible modifications. The excessive damage of proximal tubules after insult may result in inhibition of growth of any progenitor cells.

One of the major challenges of *in-vitro* stem cell studies is to detect their abilities to grow and differentiate into organ specific structures. Recent advancement in *in-vitro* stem-cell development emphasizes on 3-D cell culture techniques to mimic the *in-vivo* nature for stem cell growth (Mckee C et al 2017). One of the 3-D cell culture techniques that this lab uses is growing spheroids in suspension in low attachment flasks. The stem cells when grown in low attachment vessels forms spheroids which shows their ability to self-renew and can form differentiated structures such as tubules. However, there are few disadvantages of spheroid culture such as inability to perform large-scale expansion limiting sample availabilities for molecular and proteomic analysis. In addition, they are extremely difficult to dissociate therefore further studies on single cell clonal differentiation and growth is difficult to perform. Alternatively, another approach taken to study the differentiation of progenitor population is subcutaneous injection of the cells with matrigel into the nude mice and tracking for any nodule formation. Matrigel consists of components of extra-cellular matrix that support growth and proliferation of progenitor cells. By harvesting the nodules, formation of tubular structures will be examined and histochemical approaches can be used to stain with various human tubule specific markers. Therefore, the ultimate aim is to obtain a well-characterized stem/progenitor cell population from tubular epithelial cells that can potentially help in regeneration after injury. Comprehensively, the hypothesis of the project is that the stem/progenitor cell population isolated from the human proximal tubules, after cadmium insult participate in regeneration by increasing their cell population and demonstrate the ability to form tubular structures when injected *in-vivo*.

CHAPTER II

METHODS

Cell Culture

Stock cultures of HPT cells which have been used previously were grown using serum-free conditions containing a 1:1 mixture of Dulbecco's modified Eagles' medium and Ham's F-12 growth medium (Detrisac et al., 1984). The culture medium was supplemented with selenium (5 ng/ml), insulin (5 µg/ml), transferrin (5 µg/ml), hydrocortisone (36 ng/ml), triiodothyronine (4 pg/ml), and epidermal growth factor (10 ng/ml) as described previously by this laboratory (Detrisac et al., 1984; Kim et al., 2002). HK-2 cells and RPTEC/TERT1 cells were obtained from American Type Culture Collection and grown using identical serum free conditions. The cells were fed fresh growth medium every 2 or 3 days, and at confluence, the cells were sub-cultured using trypsin-EDTA (ethylenediaminetetraacetic acid) (0.05-0.02 %). For use in experimental protocols, cells were cultured at a 1:4 (HK-2), 1:2 (HPT) or a 1:3 (RPTEC/TERT1) ratio, allowed to reach confluence and then used in the described experimental protocols.

RNA Isolation

Cell pellets were thawed on ice and 1ml of lysis buffer, Tri Reagent (Molecular Research Center) was added directly to the cell pellets. Once the cells were lysed in the Tri-reagent, 100 µl of 1-bromo-3-chloropropane (BCP) was added and vortexed for 30 secs and

centrifuged for 15 mins at 4 °C to separate organic phase and interphase from the topmost aqueous RNA phase. The aqueous supernatant was carefully transferred to a fresh RNase-free 1.5ml eppendorf tubes (Eppendorf) without touching the interphase; equal volume of isopropanol was added to the aqueous phase; mixed by inverting the tube couple of times and stored in -20 °C overnight. The next day, the tube was centrifuged for 10 mins at 4 °C, the supernatant was removed carefully without disturbing the pellet. The cell pellet was washed twice with 70 % alcohol by centrifugating for 10 mins and removing the supernatant. After the last wash, the cell pellet was resuspended in RNase-free water. The concentration of extracted RNA was determined using nanodrop (Thermo Scientific). Appropriate volume of RNA-free water was added to bring to required concentration to perform RT-qPCR.

Real Time PCR

The level of expression of CD133, CD24, CD44, aldehyde dehydrogenase 1 family member A1 (ALDH1A1), N-cadherin (CDH2), E-cadherin (CDH1), P-cadherin (CDH3), Ksp-cadherin (CDH16), claudin 4 (CLDN4), claudin 1 (CLDN1), occludin (OCDN), Aquaporin-1 (AQP-1) and Calbindin (CAL) genes was assessed using real-time reverse transcription PCR and commercially available primers. The primers for CD24, CD44, ALDH1A1, CDH16, CDH3 and CLDN1 were obtained from Qiagen (Qiagen Company, Valencia, CA) and the primers for CD133, CDH1, CDH2, CLDN4, OCDN, AQP-1, CAL and β -actin were obtained from Bio-Rad (Bio-Rad Laboratories, Hercules CA). Total RNA was isolated using Tri Reagent (Molecular Research Center, Inc., Cincinnati, OH) as described previously (Garrett et al., 1998). For analysis, 100ng of total RNA was used to prepare complimentary DNA (cDNA) using the iScript cDNA synthesis kit (Bio-Rad Laboratories, Hercules CA) in a total volume of 20 μ l. Real-time PCR was performed utilizing the SYBR Green kit (Bio-Rad Laboratories)

with 2 μ l of cDNA, 0.2 μ M primers in a total volume of 20 μ l in an iCycler iQ real-time detection system (Bio-Rad Laboratories). The relative levels of mRNA for each of the genes was assessed, and normalized to the change in β -actin expression.

Microarray Analysis of Global Gene Expression

Total RNA was purified from triplicate cultures of HK-2 and RPTEC/TERT1 cells and six individual cultures of human proximal tubule (HPT) cells (single sample per culture) using the RNeasy Mini kit (Qiagen, Valencia, CA). Each HPT cell isolate represents a culture from an individual patient. For global gene expression, total RNA was assessed using the Affymetrix Human Transcriptome 2.0 Array, which contains 44,699 protein coding and 22,829 non-coding transcript clusters. Fragmented biotinylated cDNA was hybridized to arrays, washed and stained using the Affymetrix Fluidics Station 450, and fluorescence intensities determined for each array using the Affymetrix GCS300 7G high-resolution confocal laser scanner. Signal intensities for all 12 arrays were normalized via the SST-RMA method in Affymetrix Expression Console (build 1.4.1.46). Expression data for 67,528 non-control transcript cluster probes, interrogating known and putative genes in the human genome, was available for gene and sample-based cluster analysis. Gene and sample-based unsupervised hierarchical cluster analysis was executed using the UPGMA algorithm based on Pearson correlation metric while cluster generation was verified via bootstrap and Euclidian distance analysis in GeneMath XT 2.0. All cluster verification was performed using greater than 10,000 permutations and clusters were verified with a cluster stability of 100.

Determination of Cell Viability by DAPI Staining

The effect of Cd⁺² on the viability and fragmentation of nuclei (apoptotic nuclei) was determined by visualization and counting of 4',6-diamidino-2-phenylindole (DAPI)- stained nuclei as described previously by this laboratory (Garrett et al., 1998; Somji et al., 2004). For this purpose, the HK-2 and RPTEC/TERT1 cells were grown to confluency following which they were treated with the appropriate concentrations of Cd⁺². At the indicated time points, wells containing the monolayers were rinsed with PBS, fixed for 15 min in 70% ethanol, rehydrated with 1 ml PBS, and stained with 10 µl DAPI (10 µg/ml in distilled water). For each time point, a minimum of 20 fields per well and 3 wells per data point were examined. The nuclear counts as well as the number of fragmented nuclei were determined for each field. The percentage of fragmented nuclei were determined for each well and the results presented as the mean ± SEM for the triplicate wells.

Western Blot

The HK-2, HPT and RPTEC/TERT1 cell pellets were lysed in an ice-cold RIPA buffer containing equal volumes of protease inhibitors, PMSF and sodium orthovanadate (Santa Cruz) and incubated 30 mins on ice by shaking. The extracts were seared using a sonicator, keeping them on ice and centrifuged for 10000g for 10 mins at 4 °C. The supernatants were transferred to a fresh, cold microfuge tubes and protein quantification was performed using BCA assay (ThermoScientific). After quantifying the samples, if required, each sample was diluted to 20 µg with RIPA; mixed with Laemmli buffer (Bio-Rad) and boiled for 5 mins at 95 °C. The samples are quickly centrifuged for 10 secs and loaded on a TGX AnyKd SDS polyacrylamide gel (Bio-Rad Laboratories) and transferred to a hybond-P Polyvinylidene difluoride membrane (Amersham Biosciences, Piscataway, NJ) overnight at 4 °C. The next day, the blots were washed 5 mins in TBST and blocked in Tris-buffered saline (TBS)

containing 0.1 % Tween-20 (TBS-T) and 5 % [wt/vol] nonfat dry milk for 1 h at room temperature. After blocking, the membranes were washed three times with TBS-T for 15 mins each and probed with the appropriate human primary antibody overnight at 4 °C in a shaker. The primary antibodies were prepared using 5 % non-fat milk or 3 % BSA in TBS-T and appropriate dilution factor was used to dilute the antibodies. The table with list of primary antibodies is shown below (Table II-1). The membranes were washed three times in TBS-T, and were incubated with the appropriate affinity purified anti-mouse or anti-rabbit antibody (1:2000) conjugated to horseradish peroxidase (HRP) (Cell Signaling) for two hrs at room temperature. The blots were visualized using the Phototope-HRP Western blot detection system (Cell Signaling Technology).

Table II-1. List of primary antibodies used for western blot.					
Antibody	Dilution	Host species	Company	Catalog #	Mol weight (kDa)
β -actin	1:1000	Mouse monoclonal	Abcam	Ab8226	42
CD133	1:100	Mouse monoclonal	Miltenyi Biotec Inc	130-090-422	95
CD24	1:500	Mouse monoclonal	Santa-Cruz Biotechnology	sc-19585	35-45
CD44	1:1000	Mouse monoclonal	Cell signaling Technology	#3570	80
ALDH1A1	1:2000	Mouse monoclonal	Santa-Cruz Biotechnology	sc-374149	56
CDH2	1:500	Mouse monoclonal	Invitrogen	MA1-2002	130

CDH1	1:250	Rabbit polyclonal	Santa-Cruz Biotechnology	sc-7870	120
CDH3	1:800	Rabbit polyclonal	Santa-Cruz Biotechnology	sc-7893	118
CDH16	1:300	Rabbit polyclonal	Abcam Inc	ab80320	90
OCDN	0.5ug/ml	Mouse monoclonal	Invitrogen	33-1500	82
CLDN4	1:500	Mouse monoclonal	Invitrogen	32-9400	22
CLDN1	1:500	Mouse monoclonal	Life Technologies	37-4900	18

Determination of LDH release

The release of lactate dehydrogenase (LDH) from Cd⁺² treated cells was determined by the Cyto Tox 967 assay kit (Promega, Madison, WI) as described previously (Somji et al., 2004). After treatment with Cd⁺² for appropriate times, 50 µl of the cell culture supernatant was transferred to a 96 well enzymatic assay plate. The reconstituted substrate mix (50 µl) was added to each well containing the sample and the enzymatic reaction was allowed to proceed for 30 min at room temperature in the dark. The assay was stopped by adding 50 µl of the stop solution (1M acetic acid) and the plate was read at 490 nm using an ELISA plate reader.

Caspase-3 Assay

The caspase-3 assay kit from R&D Systems (Minneapolis, MN) was used to determine the activity of the enzyme. The cells were grown as monolayers and after treatment with Cd⁺² for various time periods, the cells were collected by centrifugation and the pellet was lysed by the addition of the cell lysis buffer provided in the kit. The cell lysate was incubated on ice for

10 min and following centrifugation, the supernatant was transferred to a new tube and the protein concentration was determined using the bicinchoninic acid protein assay.

50 μ l of the cell lysate was transferred to a 96 well flat bottom micro plate and 50 μ l of 2X reaction buffer and 5 μ l of caspase-3 colorimetric substrate (DEVD-pNA) was added to each well. Enzyme activity was determined by enzymatic cleavage of the tetrapeptide substrate DEVD-pNA and the release of the chromophore p-nitroanilide, which was measured in a spectrophotometer at a wavelength of 405 nm. The results are plotted as absorbance units per mg total cell protein.

Florescence Activated Cell Sorting

Confluent cultures of the immortalized RPTEC/TERT1 cell line were washed two times with phosphate buffered saline (PBS); detached using Accutase (BD Biosciences, San Jose, CA) and centrifugated at 2000rpm at 4 °C for 5 mins. The cell pellet was washed once and re-suspended in BD Pharmingen™ stain buffer (BSA) (BD Biosciences). The cells were mixed with 1:10 4x trypan blue solution and counted using hemocytometer. Cells were diluted to 1×10^6 cells/ μ L with stain buffer. 5ml clear round bottom polypropylene tubes (BD Biosciences) were used to mix the cell suspension and antibodies. For every 100 μ l of cell suspension, 10 μ l of FITC conjugated CD133 (Miltenyi Biotec) and/or PE conjugated CD24 antibody (Miltenyi Biotec) was added to the tubes. The cells were incubated for 30 min on ice in the dark and then washed two times with stain buffer and re-suspended in about 1mL of stain buffer. Cells were sorted using BD FACS Aria. First, the singlet population was gated as FSC vs SSC then the selected singlet population was graphed as CD133 vs CD24 plot and four quadrants were drawn to separate double positive vs single positive cell population. Based on the compensation measurements, the threshold for positive signal was set to 1×10^3 for both

markers at x and y-axis. 1×10^5 cells were sorted for each population group. The cells were sorted directly into 5 wells of 48-well plate containing warm culture media and allowed to grow to confluency and expanded for further experiments.

For expansion of the sorted cells, the confluent wells were washed two times with PBS. Accutase (BD Biosciences) was added to all the wells containing the cells; incubated for 20 mins at 37 °C for detachment of cells and collected in a 15ml conical tube. Additional PBS was used to collect all the remaining cells in the wells and centrifuged for 5 mins at RT. The cell pellet was resuspended in about 0.5ml of warm culture media and added to 1 well of 24 well plate that contained 1ml of warm media. The cells were transferred from 48 wells to 24 wells, then to 6 wells followed by T-25 flasks and finally to T-75 flasks.

Transepithelial Resistance Measurement

RPTEC/TERT1, CD133+CD24+ and CD24+ cells were seeded at a 2:1 split ratio in triplicate onto a 0.4µm pore size, 1.1 cm² polyethylene terephthalate inserts in 12-well plate (EMD Millipore). The transepithelial resistance (TER) was measured starting on the second day of seeding until day 10 using the EVOM Epithelial Voltohmmeter (World Precision Instruments) with a STX2 electrode set according to the manufacturer's instructions. After checking and calibrating the electrodes of the voltohmmeter, the electrodes were first inserted into the well containing media only without any cells as instructed and the blank measurement was recorded. Then the electrodes were inserted into the wells containing cells according to the protocol and measurements were recorded. After the recording was complete, fresh media was supplied to the cells in the inserts and outside of the insert. For each control and sample, 3 readings were taken from three different corners of the filter giving total of 9 readings. The

calculation for total resistance = (electrical resistance measurement of the cells – electrical resistance measurement of the blank) Ω * 1.1 cm² and reported as the mean \pm S.D.

Spheroids Culture

RPTEC/TERT1, CD133+CD24+, CD24+ and HPT cells were detached using trypsin-EDTA (ethylenediaminetetraacetic acid) (0.05-0.02 %) or Accutase (BD Biosciences) and centrifuged at 2000 rpm for 5 mins. The cell pellet was resuspended in 1ml warm DMEM/F12 media. The cells were counted and diluted down to approximately 1×10^4 . In a fresh sterile tube, the cell suspension was diluted to 1:1000 with warm DMEM/F12 media and mixed gently by pipetting up and down for couple of minutes to make it a single cell suspension. The diluted cell suspension was transferred to a T-75 ultra low-attachment flask (Corning) and incubated at 37 °C with 5 % CO₂. The cells were observed for about 8-10 days for their ability to form spheroids and pictures were taken using the Zeiss light microscope.

Thick and Thin Layer Matrigel coated Cell Growth

Growth factor reduced (GFR) matrigel basement membrane matrix (BD Biosciences) was thawed overnight in 4 °C fridge keeping it on ice. Next day, to make a thin layer coat of matrigel, at least 30 mins before splitting the cells, the matrigel was added to the 2 wells of 48-well plate covering the bottom and incubated at 37 °C for at least 30 mins to let it solidify. RPTEC/TERT1 and HPT cells were trypsinized; CD133+CD24+ and CD24+ cells were detached using accutase, the obtained cell pellets were resuspended in 1:1 DMEM/F12 media and mixed well until a single cell suspension was obtained. Approximately 1.6 % of cell suspension was diluted into 1:1 DMEM/F12 media and added to the wells coated with thin layer of matrigel and placed back in the incubator. For thick gel matrigel layer, 1.6 % of cell

suspension was diluted into 1500 µl of matrigel, laid onto 2 wells of 48-well plate and placed in the incubator for 30 mins to solidify. After 30 mins, additional media was added on top of the solidified matrigel with cells and placed back in the incubator. After plating the cells with thin and thick layer of matrigel, the cell growth and changes was observed for 3 days and 14 days respectively and pictures were taken at day 4, 7, 10 and 14 days for the thick matrigel setup.

Immunofluorescence

Cells were grown on number 1.5 (0.17 mm thickness) coverslips to confluency and were fixed with 3.7% formaldehyde for 15 min, followed by permeabilization using 0.1% Triton-X 100 for 10 min. The coverslips were washed three times using PBS for 5 mins and incubated with primary antibody for 40 min in a 37 °C incubator. The primary antibodies were diluted in PBS and appropriate dilution factor was used (Table II-2). The cells were washed three times with PBS for 3 mins each. The primary antibody was detected by incubating cells with Alexa-Fluor 488 secondary antibody for 30 mins at 37 °C incubator. The cells were again washed three times with PBS for 3 mins and incubated with phalloidin for 30 mins at 37 °C incubator to stain the F-actin. The coverslips were washed three times with PBS for 3 mins and mounted upside down with Prolong Diamond Antifade Mountant with DAPI (Life Technologies). The stained cells were observed and imaged using a Leica TCS SPE, DM5500 laser scanning confocal microscope. Two coverslips per sample were set up and a minimum of 5 fields per coverslips were examined.

Table II-2. List of primary antibodies used for immunofluorescence				
Antibody	Dilution	Host species	Company	Catalog #
CD133	1:25	Mouse monoclonal	Miltenyi Biotec Inc	130-090-422
CD24	1:50	Mouse monoclonal	Santa-Cruz Biotechnology	sc-19585
AQP-1	1:100	Mouse monoclonal	Abcam	ab9566
CAL	1:1000	Rabbit polyclonal	Abcam	ab11426

MTT Growth Assay

All three cell lines were split in a 1:100 ratio into 6-well plates and The cell growth was determined by measuring the capacity of the cells to reduce MTT [3-(4,5-dimethylthiazol-2-yl)-2,5-diphenyl tetrazolium bromide] to formazan every day until day 10 after splitting them. In brief, 40 µl of the MTT reagent was added to the media containing cells in 6-well plate; incubated for 3.5 hrs in the incubator; washed 2 times with PBS; 1ml of HCl/isopropanol was added and mixed well; 200 ul of the mixture was transferred to 96-well plate and the absorbance was measured at 570 nm using the Biotek spectrophotometer.

Exposure of Cell-lines to Cd²⁺ and Determination of Cell Population

Confluent cultures of CD133+CD24+, CD24+ and RPTEC/TERT1 cells were exposed to 4.5 and 9µM Cd²⁺ for upto 34 days. The confluent cell cultures were dosed every 2 days with 4.5 and 9µM Cd²⁺ containing media and the number/percent of cells were analyzed by running the cells through SONY SH800 flow cytometer. Briefly, the cells were washed two times with phosphate buffered saline (PBS); detached using Accutase (BD Biosciences, San Jose, CA) and centrifugated at 2000rpm at 4 °C for 5 mins. The cell pellet was washed and re-suspended in BD Pharmingen™ stain buffer (BSA). The cells were counted and adjusted to a concentration of 1x10⁵ cells/mL. For every 100 µL of cell suspension, 10 µL of FITC

conjugated CD133 (Miltenyi Biotec) and/or PE conjugated CD24 antibody (Miltenyi Biotec) was added to the tubes. The cells were incubated for 30 min on ice in the dark and then washed two times with stain buffer and re-suspended in 700 μ l of stain buffer. Cells were counted with a BD LSRII and the data was analyzed using the FlowJo software. For each sample, 10,000 events were acquired. Results were gated to exclude doublets and identify the singlet population.

Subcutaneous Injection of Cell-Lines

The confluent cultures of all three cell line, RPTEC/TERT1, CD133+CD24+ and CD24+ were trypsinized and the cell pellets were obtained by centrifugation at 2000rpm at 4 °C for 5 mins. The cell pellet was resuspended in 1ml of cold PBS; mixed with an equal volume of ice-cold matrigel (Corning). All procedures were performed on ice and all the materials like pipet tips, syringes and centrifuge tubes were kept on ice to avoid polymerization of matrigel. 0.4 ml of the cell suspension mixed with matrigel was injected subcutaneously into 4 mice per cell line using a 0.2 cc syringe (BD). The nodules were harvested at day 7, 10, 13 and 16.

Immunohistochemistry

The nodules were harvested at day 7, 10, 13 and 16 from the mice; cut into appropriate size; put into tissue cassettes and routinely fixed in 10 % neutral buffered formalin for 16-18 hours. Tissue processing was performed in 10 % neutral buffered formalin and transferred to 70 % alcohol; then to 95 % alcohol; and then to 100 % alcohol followed by xylene. Tissue cassettes were removed from the processor and embedded in paraffin. Serial sections were generated by cutting the processed tissue into 3-5 μ m and mounted on a glass slide to be used for immunohistochemical staining. Paraffin was dewaxed by heating the slides at 60 °C for 15 mins. After that, the slides were immediately dipped into xylene and transferred into 100 %

alcohol followed by 95 % and 70 % alcohol and then washed in distilled water. Prior to immunostaining, sections were immersed in preheated Target Retrieval Solution (Dako, Carpinteria, CA) and heated in a steamer for 20 mins. The sections were allowed to cool to room temperature and immersed into TBS-T for 5 min. The sections were washed with the washing buffer (Dako) and then incubated 10mins with Dako Peroxidase block solution. The slides were washed and incubated with the primary antibody overnight at 4 °C. The list of primary antibodies used are shown in Table II-3. After washing the slides were incubated using DakoCytomation EnVision+ dual Link Antibody or Dako HRP-labelled antibody at room temperature for 30 min. Liquid diaminobenzidine (Dako) was used for visualization. Counter staining was performed for 8 min at room temperature using Ready-to-use Hematoxylin (Dako). Slides were rinsed with distilled water, dehydrated in graded ethanol, cleared in xylene, and cover-slipped.

Antibody	Dilution	Host species	Company	Catalog #
CD133	1:50	Rabbit polyclonal	Miltenyi Biotec Inc	ab19898
CD24	1:10	Mouse monoclonal	Invitrogen	MA5-11833
AP	1:200	Rabbit polyclonal	Abcam	ab95462
CAL	1:200	Rabbit polyclonal	Abcam	ab11426
VIM	1:100	Rabbit monoclonal	Cell signaling	5741S
CK AE1&3	1:200	Mouse monoclonal	Dako	M351501
CK7	1:200	Mouse monoclonal	Dako	M7018
CK19	1:100	Rabbit polyclonal	Abcam	ab155118
PAX-2	1:50	Rabbit monoclonal	Abcam	ab150391

Statistical Analysis

All experiments were done in triplicates and the data was analyzed using ANOVA with Tukey *post-hoc* testing performed by Graphpad PRISM 4. The data is plotted as the mean \pm SEM of triplicate determinations.

CHAPTER III

RESULTS

Global Gene Expression Pattern of HK-2, HPT and RPTEC/TERT1 Cells

The gene expression profiles were obtained using total RNA from triplicate samples of HK-2 cells and RPTEC/TERT1 cells and six isolates of HPT cells. To determine if the global expression profile of all non-control transcript clusters could distinguish all three groups of cells, sample-based clustering analysis was performed using the entire 67,528 non-control transcript cluster expression profile without any statistical filtering. The results (Fig. III-1) demonstrated that the triplicate samples of HK-2 cells clustered together with 100% accuracy while the HPT and RPTEC/TERT1 cells clustered together with 66% accuracy, respectively. Specifically, four of the six HPT cell samples segregated into a cluster with one sample from the RPTEC/TERT1 cell line while two of the six HPT cell samples segregated into another cluster with two samples from the RPTEC/TERT1 cell line. Sample-based clustering demonstrates three main clusters that segregate the samples from the HPT, RPTEC/TERT1 and HK-2 cell lines. Cluster verification, using bootstrapping, of sample-based clusters revealed all clusters had exceptionally high stability, all equaling 100, indicating the clusters (and segregation of the HK-2 cell line from HPT/ RPTEC/TERT1 cells) are representative of authentic structures in the data set. This analysis convincingly indicate that the gene expression profile of the HK-2 cells was distinct from that of either the HPT or the

RPTEC/TERT1 cells. The cluster analysis also suggest that the gene expression of the HPT and RPTEC/TERT1 cells may be similar because the UPGMA clustering algorithm did not

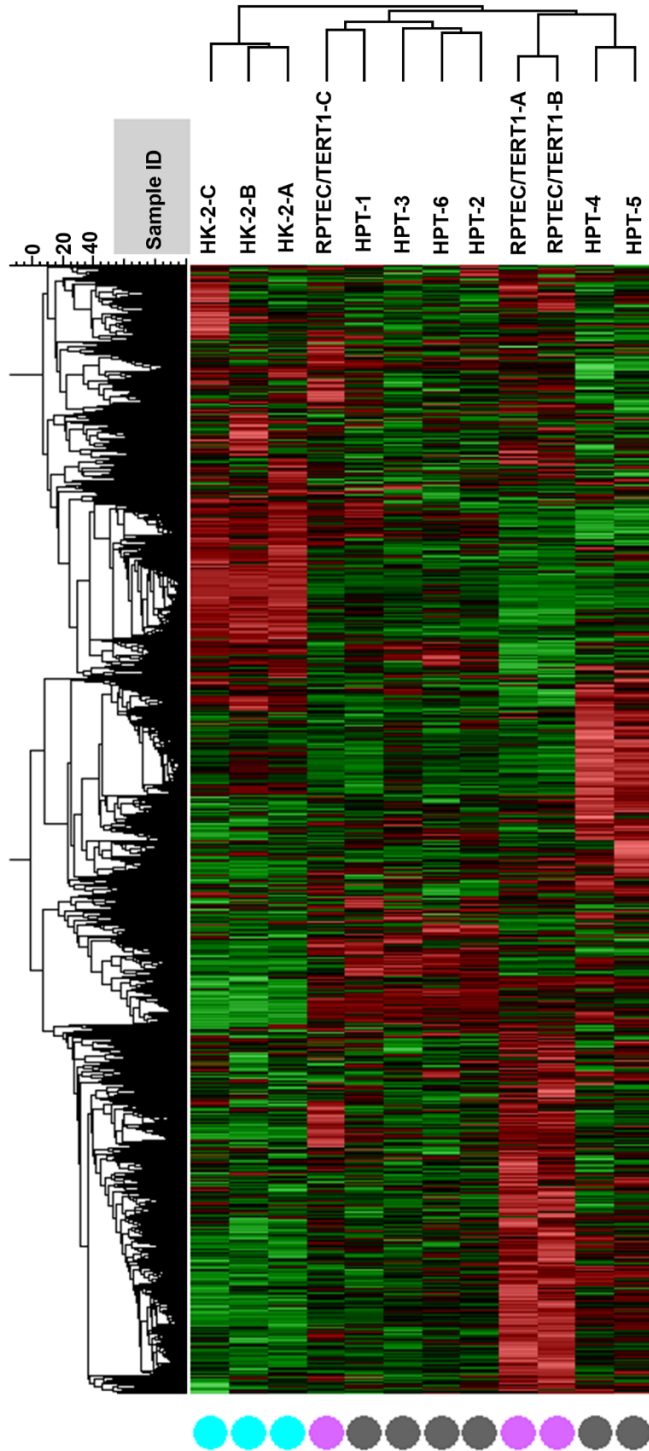


Fig. III-1. Hierarchical clustering of various proximal tubule cell transcriptomes. All transcript clusters from the HTA 2.0 array (67,528) were subjected to hierarchical clustering using the UPGMA algorithm based on Pearson correlation metric without any statistical filtering of transcript clusters. Samples include triplicate RNA samples from three parallel cultures of HK-2 (HK-2-A, -B, and -C), RPTEC/TERT1 (RPTEC/TERT1-A, -B, and -C) and single RNA samples from six independent isolates of human proximal tubule cells (HPT-1, -2, -3, -4, -5 and -6).

succeed in separating the two groups of cells into distinct clusters. Principal component analysis on the 67,529 non-control transcript clusters confirmed the findings of the cluster analysis (Fig. III-2). In terms of separation of samples by component, HK-2 samples separated from HPT/ RPTEC/TERT1 samples across the x-component (first component, 36% of variance in the dataset) while HPT and RPTEC/TERT1 samples were slightly separated across the z-component (third component, 14.7% of variance in the dataset).

An increase in the diversity of gene expression profiles from the HPT cells was anticipated due to each culture being derived from an independent patient sample. This is the reason six isolates were used in the current study. As predicted, the samples from the six independent isolates of HPT cells showed the most diversity in gene expression. The samples from the HPT cells segregated with the samples from the RPTEC/TERT1 cell line into two clusters. One cluster was composed of samples from four HPT cell isolates and from one sample from the RPTEC/TERT1 cell line (5.3% similarity). The second cluster was composed of samples from two HPT cell isolates and samples from two RPTEC/TERT1 cell lines (-8.6% similarity). For this second cluster, the sample from the RPTEC/TERT1 cell line segregated under one sub-cluster (60.5% similarity) and the samples from the HPT cells segregated under another sub-cluster (45.8% similarity).

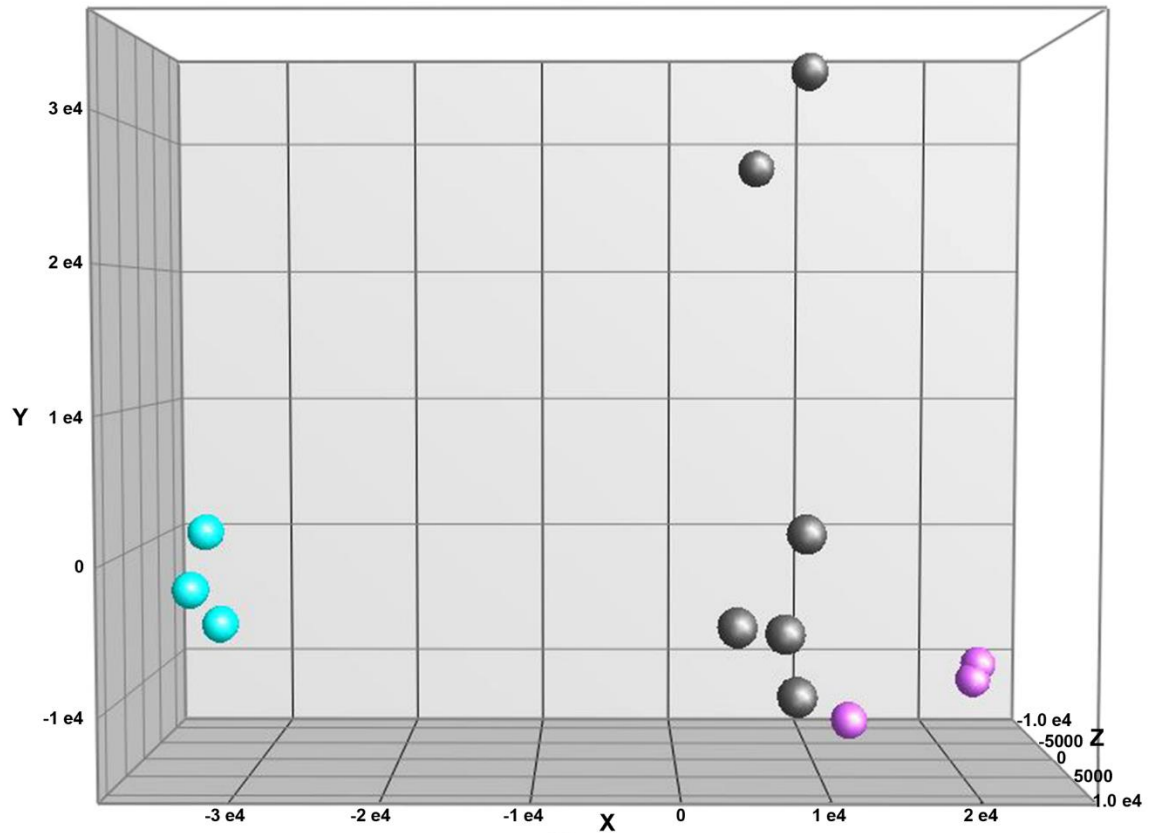


Fig. III-2. Principal component analysis using all 67,528 non-control transcript clusters. Turquoise dots represents HK-2 cells; grey dots represents HPT isolates, and pink dot represents RPTEC/TERT1 cells. The two outliers of the HPT group are HPT-4 and HPT-5. The X-component accounts for 73% of the variance between groups, and the Y-component represents 26.7% variance between groups.

The gene expression patterns from the three groups of cells were subjected to pairwise analysis using parametric methods of differentially expressed genes using an FDR-adjusted p-value of ≤ 0.05 or ≤ 0.01 . Employing a p-value of ≤ 0.05 demonstrated 1,427 transcript clusters were induced and 694 were repressed in HK-2 cells compared to HPT cells with 65,407 being of similar expression (Fig. III-3A). An identical analysis of samples from the RPTEC/TERT1 cells showed 77 transcript clusters induced and 30 repressed with 67,421 having similar expression when compared to the HPT cells (Fig. III-3B).

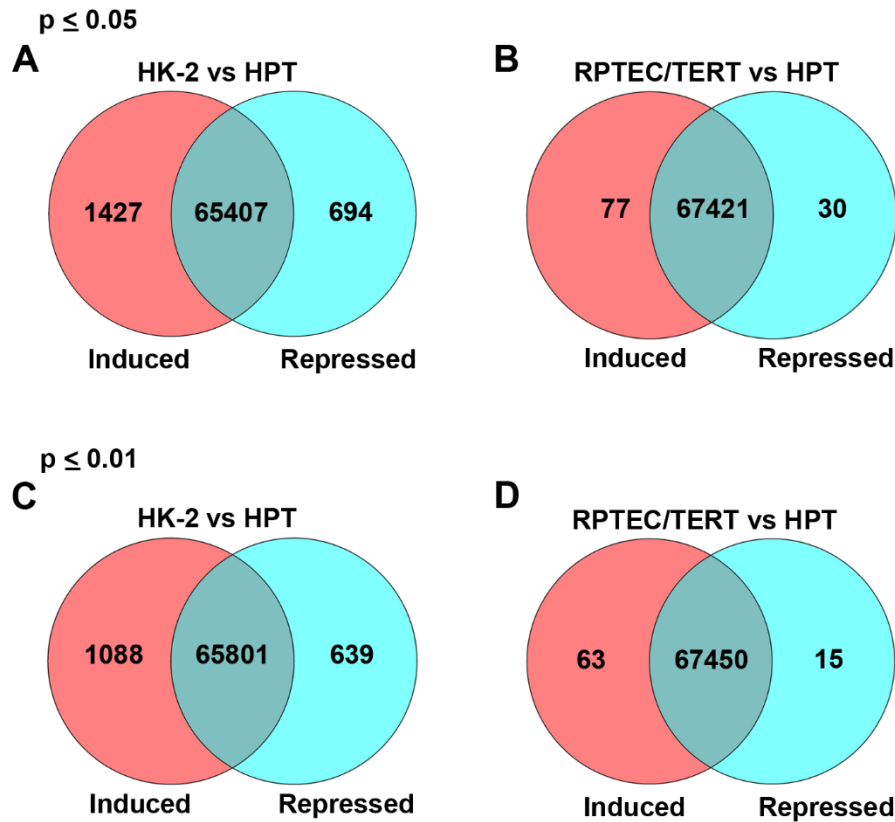


Fig. III-3. Venn diagram showing differentially expressed genes in HK-2 cells and RPTEC/TERT1 cells in comparison to mortal human proximal tubule cell (HPT) isolates. Pairwise analysis was used to compare the number of differentially expressed genes from HK-2 in comparison to six isolates of HPTs or RPTEC/TERT1 cells in comparison to HPT cells. A differentially expressed gene is defined as one that is an absolute fold change ≥ 2 or ≤ 0.5 , and an FDR-adjusted ANOVA and T-test p-value of ≤ 0.05 or ≤ 0.01 . (A). Differentially expressed genes in HK-2 vs HPT cells at $p \leq 0.05$. (B). Differentially expressed genes in RPTEC/TERT1 vs HPT cells at $p \leq 0.05$. (C) Differentially expressed genes in HK-2 vs HPT cells at $p \leq 0.01$. (D). Differentially expressed genes in RPTEC/TERT1 vs HPT cells at $p \leq 0.01$.

Employing a p-value of ≤ 0.01 demonstrated 1,088 transcript clusters induced and 639 repressed with 65,801 being similarly expressed for the HK-2 cell line compared to HPT cells. For the RPTEC/TERT1 cell line, only 63 transcript clusters were induced and 15 were repressed with 67,450 transcript clusters being similarly expressed between the RPTEC/TERT1 cell line and the HPT cells. This analysis shows that the HK-2 cell line has a

much greater divergent global gene expression pattern from HPT cell cultures than that of the RPTEC/TERT1 cell line.

The segregation of the gene expression profiles from the three cell culture groups were also subjected to a transposed principal component analysis view after performing discriminant analysis of pre-defined groups (Fig. III-4). The results of this analysis shows

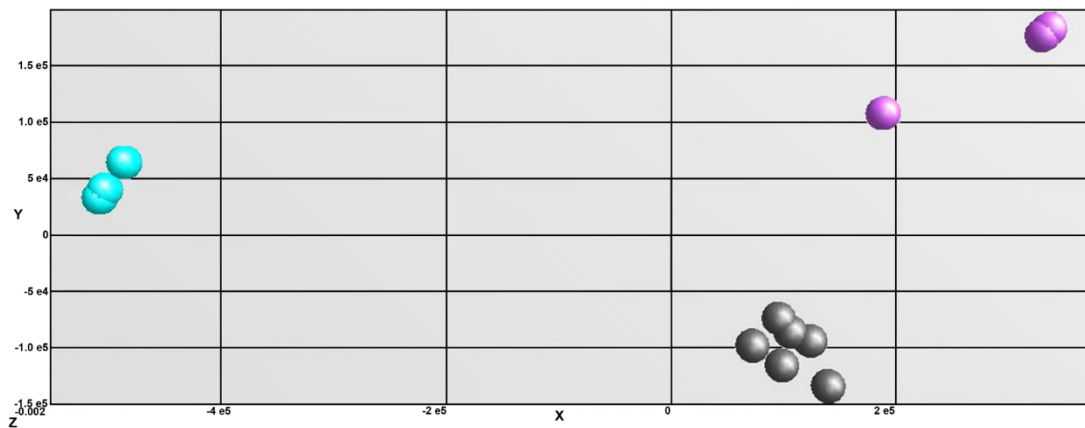


Fig. III-4. Transposed principal component analysis after performing discriminant analysis of pre-defined groups. Discriminant Principal Component Analysis, selecting for the top 0.015% of discriminating genes that discriminates between groups with 100% accuracy following sample-based clustering by UPGMA. Turquoise dots represents HK-2 cells; grey dots represent HPT isolates, and pink dots represent RPTEC/TERT1 cells.

that the X-component separates the samples from the HPT and RPTEC/TERT1 cells to one side of the axis and the samples from the HK-2 cells to the other side of the axis. This X-component accounts for 73.3% of the variance between the two groups. The Y-component separates the samples of the HPT and RPTEC/TERT1 cells on either side of the axis, while samples from the HK-2 cells are borderline on the Y-axis. The Y-component accounts for the remaining 26.7% of the variance between groups. The fact that the X-component accounts for 73.3% of the variance indicates that the majority of differences in the dataset arise from a

comparison of the HK-2 cells to the HPT and RPTEC/TERT1 cells. The differences between the HPT and RPTEC/TERT1 cells are marginal when compared to the HK-2 cells.

To identify differences in gene expression between the HPT, RPTEC/TERT1 and HK-2 cell culture groups, clustering analysis was performed by the UPGMA Algorithm based on Pearson correlation metric. To identify a maximum expression profile distinguishing groups, transcript clusters with FDR-adjusted ANOVA p-value ≤ 0.01 were subjected to sample and gene-based clustering analysis (Fig. III-5). The clustering accuracy of the individual groups, HK-2, RPTEC/TERT1 and HPT, segregated into 4 distinct sub-clusters with 100% accuracy. Gene-based clustering analysis identified 6 groups (Cluster ID) of genes with distinct expression profiles (Group A - F, Table 1, Supplemental Materials). Group A contains the vast majority of genes, with a majority being repressed in RPTEC/TERT1 and HPT cells but induced in HK-2 cells. Group B represent genes repressed in RPTEC/TERT1 cells and induced in HK-2 and HPT cells. Group C represent genes repressed in HK-2 and RPTEC/TERT1 cells and induced in HPT cells. Group D represent genes repressed in HK-2 cells, while genes in HPT and RPTEC/TERT1 cells are induced. Group E represent genes induced in RPTEC/TERT1 cells and repressed in HPT and HK-2 cells. Group F genes represent genes repressed in HPT cells, induced in RPTEC/TERT1 cells, with no change expression in HK-2 cells.

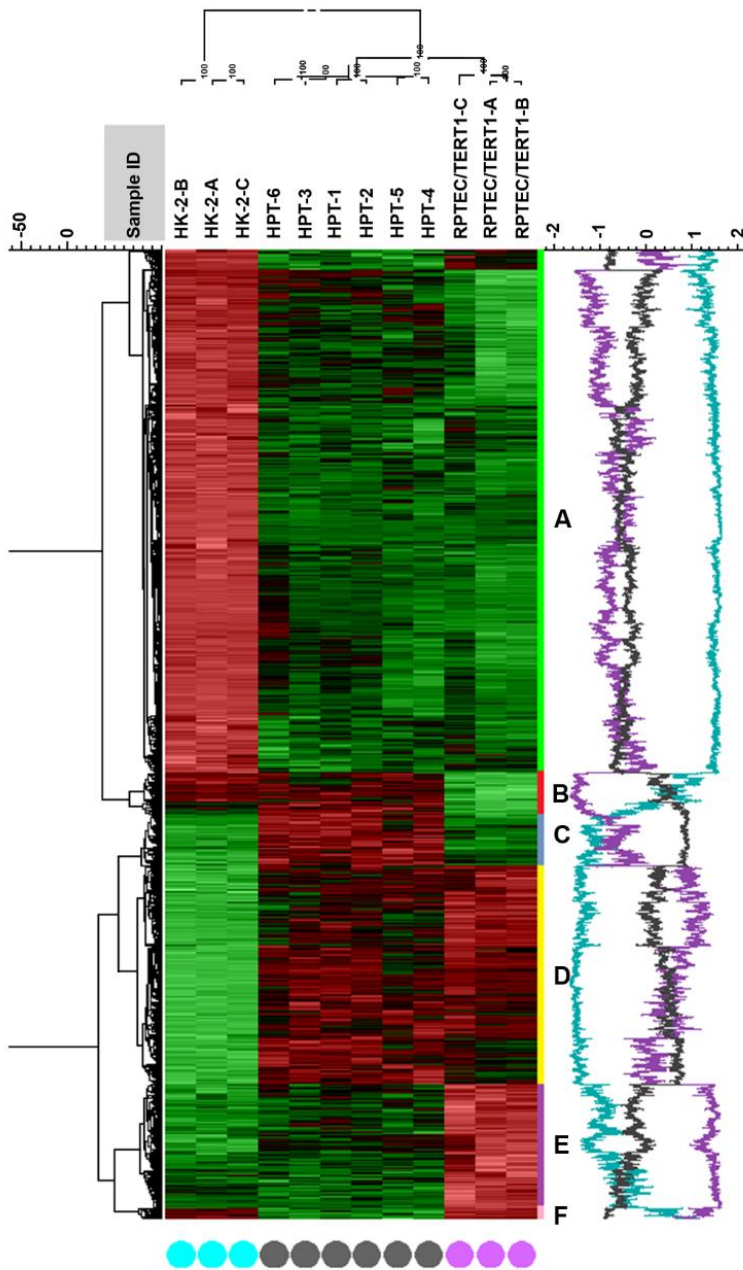


Fig. III-5. Hierarchical clustering of transcript cluster expression after statistical filtering. All 67,528 non-control transcript clusters were filtered to meet an FDR-adjusted ANOVA p-value ≤ 0.01 , which gave 5,604 transcript clusters. These were subjected to unsupervised hierarchical clustering using the UPGMA algorithm based on Pearson correlation metric. Samples form three clusters, with the HK-2 triplicate samples forming a separate cluster, the RPTEC/TERT1 triplicate samples, and six HPT samples forming two separate sub-clusters. The relative level of expression of each cluster is color-coded and is shown on the right. On the right side of the heat map is designated the gene groupings (A – F) and is listed in Table 1 (Supplementary file).

Expression of CD24 and CD133 in the HK-2, HPT and RPTEC/TERT1 Cells

The second goal of this study was to determine if the 3-cell culture models contained a population of cells displaying progenitor /stem cell markers. For this purpose, the co-expression of CD24 and CD133 was determined on all 3-cell culture models using flow cytometry (Fig. III-6A-D). The results of this analysis demonstrated that CD24 and CD133 molecules were co-expressed in approximately 20% of the HK-2 cells (Fig. III-6A). In contrast, 62% of the HPT cells and 79% of the RPTEC/TERT1 cells co-expressed CD24 and CD133 (Fig. III-6B and C). Thus, the CD24/CD133 population was significantly increased in both the HPT and RPTEC/TERT1 cells when compared to the HK-2 cells (Fig. III-6D). The CD24/CD133 population was also significantly different between the HPT and RPTEC/TERT1 cells (Fig. III-6D) with the RPTEC/TERT1 cell culture having a significantly higher percent of cells co-expressing CD24 and C133. The expression of CD24 and CD133 mRNA and protein was also determined for each of the cell isolates (Fig. III-7 A-B). The results showed that CD133 mRNA and protein was increased in the RPTEC/TERT1 cells and HPT cells when compared to the HK-2 cells (Fig. III-7A). The levels of CD24 mRNA and protein was increased in the RPTEC/TERT1 cells when compared to both the HPT and HK-2 cells (Fig. III-7B). For the HPT cells, there was an increase in expression in 2 of the isolates, whereas the third isolate had expression levels similar to the HK-2 cells (Fig. III-7B). The expression of two additional genes, aldehyde dehydrogenase 1A1 (ALDH1A1) and CD44 that are associated with stem/progenitor cells in other organs, were also assessed in the HPT, HK-2 and RPTEC/TERT1 cells (Fig. III-7C and D). As seen in Fig. III-7C, the expression of CD44 was increased in the HK-2 cells when compared to both the HPT and RPTEC/TERT1 cells (Fig. III-7C), however the expression levels were similar between the RPTEC/TERT1 and the

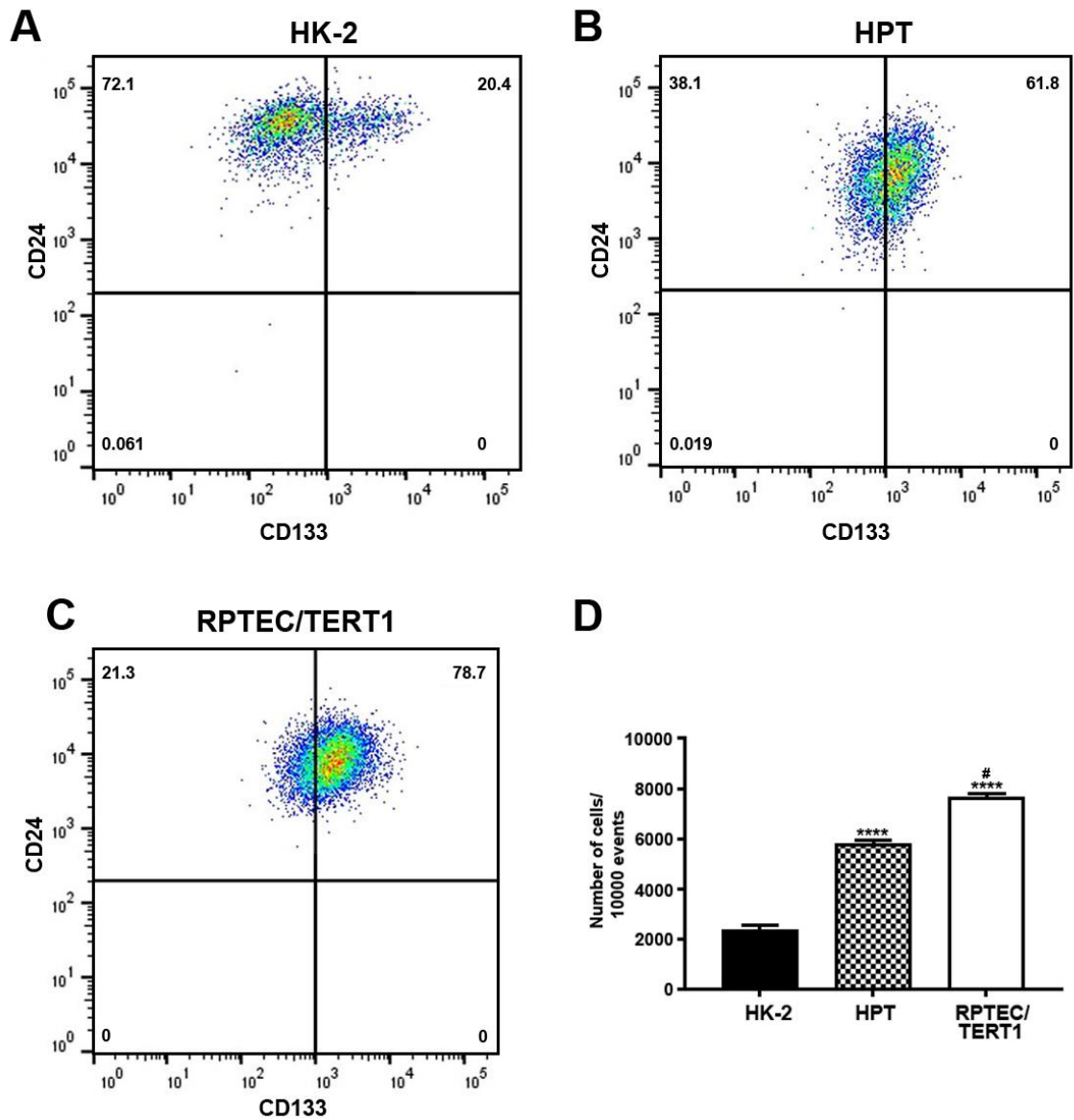


Fig. III-6. Flow cytometry analysis of CD24 and CD133 populations in proximal tubule cells. Analysis of CD24 and CD133 and CD24/CD133 populations in HK-2 (A), HPT (B) and RPTEC/TERT1 (C) cell cultures. (D). Graphical representation of the number of CD24/CD133 co-expressing cells in the three groups of cell cultures. **** indicates significantly different in the RPTEC/TERT1 cells and HPT cells when compared to the HK-2 cells at p-value of ≤ 0.0001 . # indicates significantly different in the RPTEC/TERT1 cells when compared to the HPT cells at p-value of ≤ 0.01 .

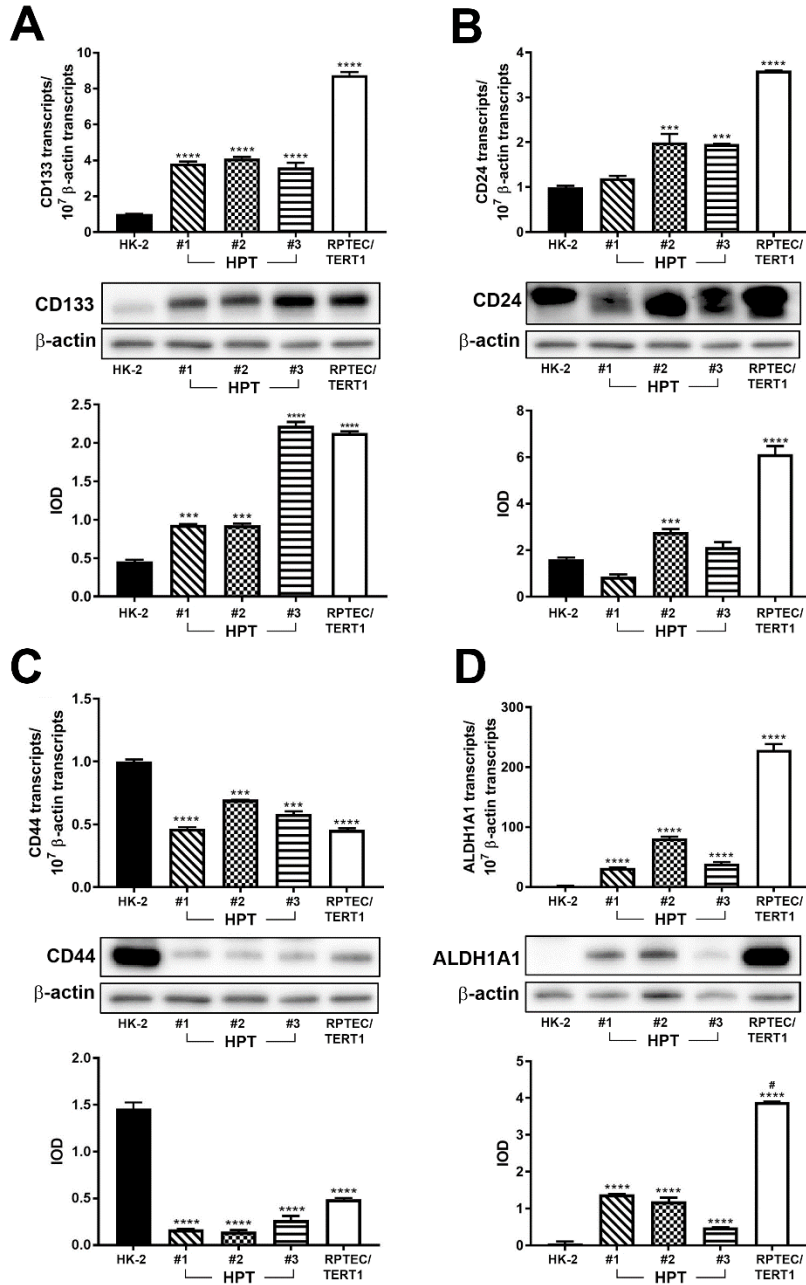


Fig. III-7. Expression of stem cell markers in cultures of human proximal tubule cells. (A). Expression of CD133 in HK-2 cells, HPT cells and RPTEC/TERT1 cells. (B). Expression of CD24 in HK-2 cells, HPT cells and RPTEC/TERT1 cells. (C). Expression of CD44 in HK-2 cells, HPT cells and RPTEC/TERT1 cells. (D). Expression of ALDH1A1 in HK-2 cells, HPT cells and RPTEC/TERT1 cells. **** indicates significantly different in the RPTEC/TERT1 cells and HPT cells when compared to the HK-2 cells at p-value of ≤ 0.0001 . *** indicates significantly different in HPT cells when compared to HK-2 cells at p-value of ≤ 0.001 . # indicates significantly different in the RPTEC/TERT1 cells when compared to the HPT cells at p-value of ≤ 0.01 .

HPT cells. The expression of ALDH1A1 was increased in the RPTEC/TERT1 cells when compared to both the HK-2 cells and HPT cells (Fig. III-7D). The HPT isolates had significantly higher levels of ALDH1A1 expression when compared to the HK-2 cells (Fig. III-7 D).

Expression of Cadherins, Claudins and Occludin in the HK-2, HPT and RPTEC/TERT1 Cell Isolates

The expression of E-, N-, P- and Ksp-cadherins, occludin (OCDN), claudin 1 (CLDN1) and claudin 4 (CLDN4) genes were determined in the HK-2, HPT, and RPTEC/TERT1 cells. These genes were analyzed since they showed an alteration in expression on the global gene expression array and they are known to be associated with the epithelial to mesenchymal transition (EMT) of cells. The results showed that expression of E-cadherin was elevated in both the HPT and RPTEC/TERT1 cells when compared to the HK-2 cells (Fig. III-8A). The level of E-cadherin expression in HK-2 cells was at or near the level of detection, in contrast, the expression of N-cadherin was elevated in the HK-2 cells when compared to the HPT or RPTEC/TERT1 cells (Fig. III-8B). The level of N-cadherin expression in the RPTEC/TERT1 cells was close to the level of detection. The expression of P-cadherin was increased in the HPT and RPTEC/TERT1 cells when compared to the HK-2 cells (Fig. III-8C). The expression of Ksp-cadherin was highest in the RPTEC/TERT1 cells when compared to the HPT and HK-2 cells (Fig. III-8D). The expression of OCDN was higher in the RPTEC/TERT1 cells compared to the HPT and HK-2 cells (Fig. III-9A). However, when the expression levels were compared between the HPT and the RPTEC/TERT1 cells, it was

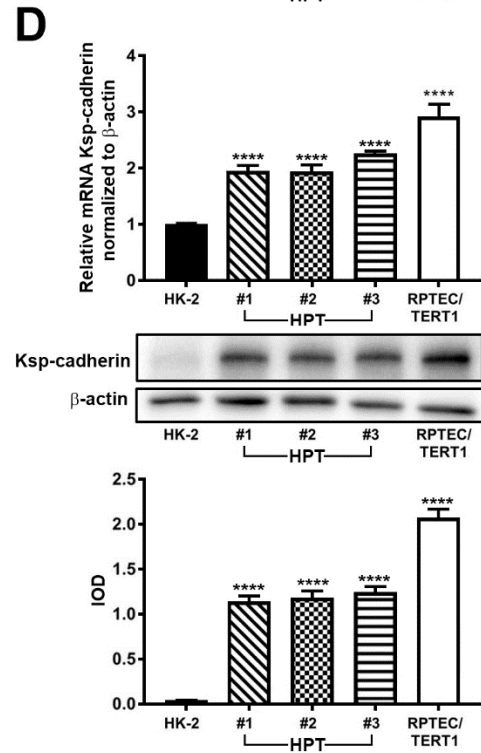
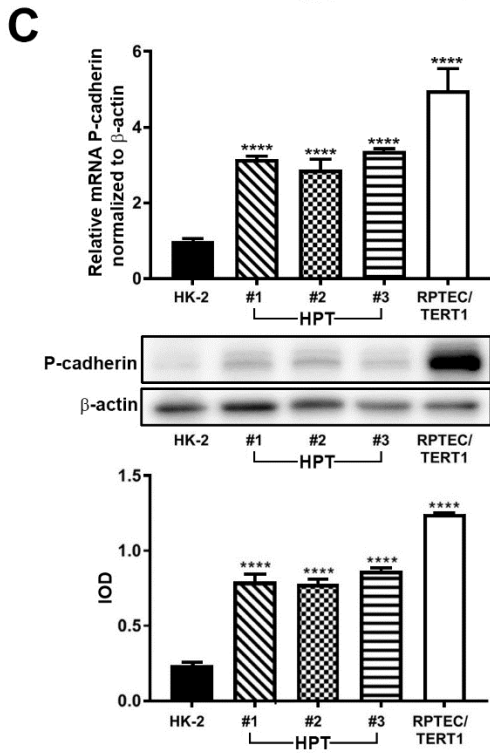
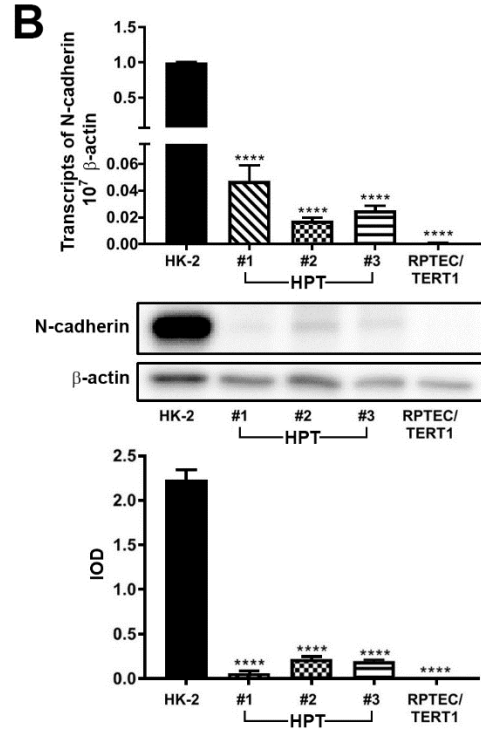
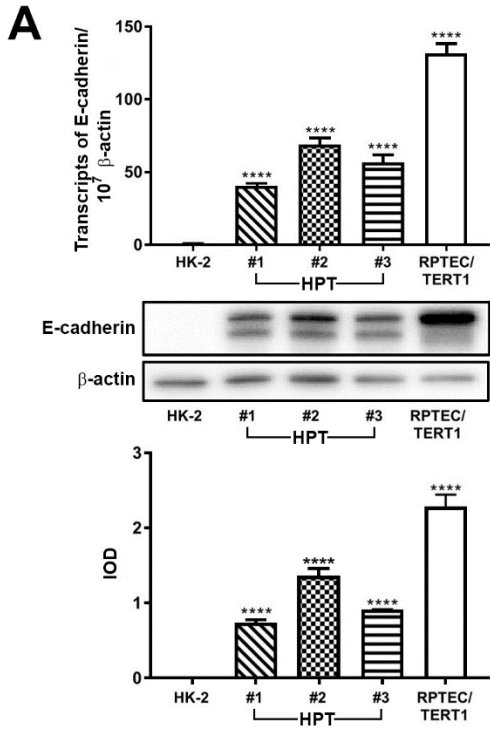


Fig. III-8. Expression of cadherins in cultures of human proximal tubule cells. (A). Expression of E-cadherin in HK-2, HPT and RPTEC/TERT1 cells. (B). Expression of N-cadherin in HK-2, HPT and RPTEC/TERT1 cells. (C). Expression of P-cadherin in HK-2, HPT and RPTEC/TERT1 cells. (D). Expression of Ksp-cadherin in HK-2, HPT and RPTEC/TERT1 cells. **** indicates significantly different in the RPTEC/TERT1 cells and HPT cells when compared to the HK-2 cells at p-value of ≤ 0.0001 .

shown that the RPTEC/TERT1 cells had higher expression of OCN when compared to the HPT cell. The expression of CLDN1 was elevated in the HK-2 cells when compared to both the HPT and RPTEC/TERT1 cells (Fig. III-9B), whereas the levels of expression were similar between the HPT and the RPTEC/TERT1 cells. The expression of CLDN4 was opposite to that of CLDN1, with the HPT and RPTEC/TERT1 cells expressing higher levels when compared to the HK-2 cells (Fig. III-9C).

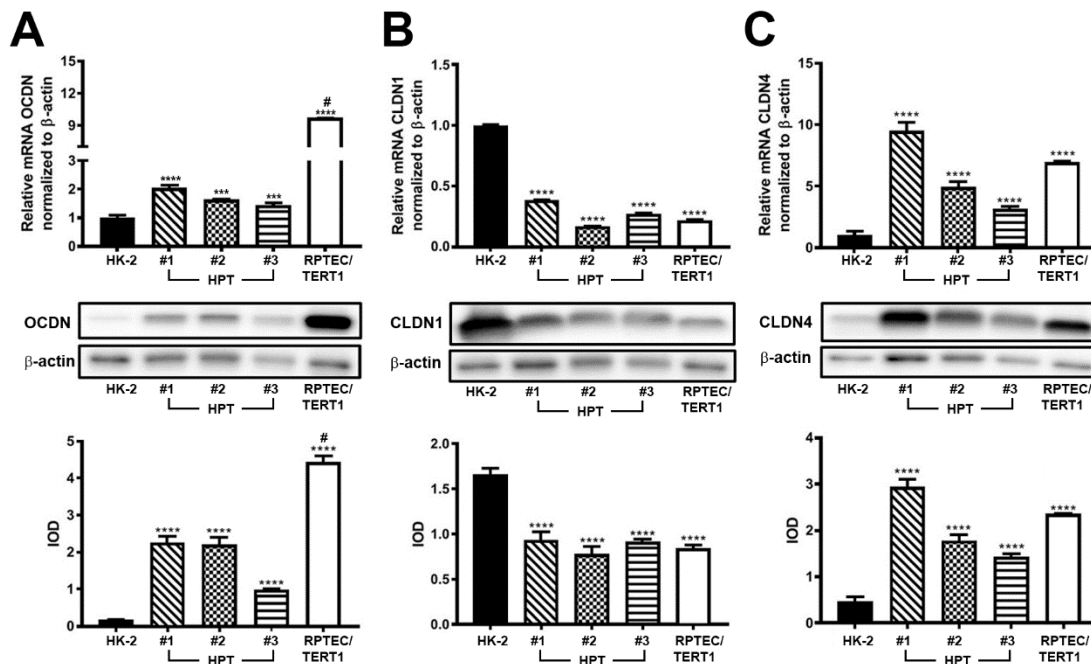


Fig. III-9. Expression of tight junction proteins in cultures of human proximal tubule cells. (A). Expression of occludin (OCN) in HK-2, HPT and RPTEC/TERT1 cells. (B).

Expression of claudin 1 (CLDN1) in HK-2, HPT and RPTEC/TERT1 cells. (C). Expression of claudin 4 (CLDN4) in HK-2, HPT and RPTEC/TERT1 cells. **** indicates significantly different in the RPTEC/TERT1 cells and HPT cells when compared to the HK-2 cells at p-value of ≤ 0.0001 . *** indicates significantly different in HPT cells when compared to HK-2 cells at p-value of ≤ 0.001 . # indicates significantly different in the RPTEC/TERT1 cells when compared to the HK-2 cells at p-value of ≤ 0.01 .

Mode of Cell Death in RPTEC/TERT1 Cells in Response to Cd²⁺ - Induced Toxicity

This laboratory has previously shown that HPT cells undergo necrotic cell death when exposed to Cd²⁺ while HK-2 cells undergo cell death by apoptosis (Somji et al. 2004). A similar study was performed to determine the mode of cell death in RPTEC/TERT1 cells following acute exposure to Cd²⁺ (Fig. III-10 A-D). The results of this analysis showed that the RPTEC/TERT1 cells were more resistant to Cd²⁺ when compared to the HK-2 cells

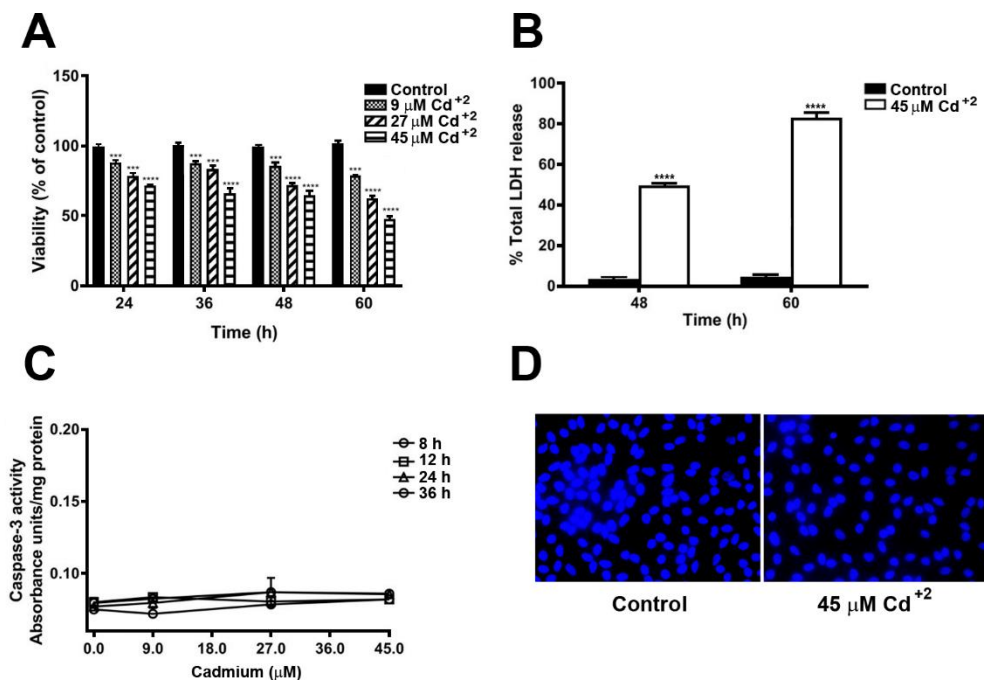


Fig. III-10. Effect of Cd²⁺ on RPTEC/TERT1 cells. (A). Effect of Cd²⁺ on the viability RPTEC/TERT1 cells exposed to 9, 27 and 45 μM Cd²⁺ for 24, 36, 48 and 60 h. Viability was determined by counting the DAPI stained nuclei and is expressed as percent of control. (B). LDH release by Cd²⁺ treated cells. RPTEC/TERT1 cells were exposed to 45 μM Cd²⁺ for 48 and 60 h. The release of LDH by the cells was quantified spectrophotometrically at a

wavelength of 490 nm and is expressed as percent of total LDH release. (C). Caspase-3 activation in Cd²⁺ treated cells. RPTEC/TERT1 cells were exposed to 9, 18, 27, 36 or 45 μM Cd²⁺ for 8, 12, 24 and 36 h. Caspase-3 activity was determined by the release of the chromophore, p-nitroanilide, which was quantitated spectrophotometrically at a wavelength of 405 nm. (D). DAPI staining of RPTEC/TERT1 cells exposed to 45 μM Cd²⁺ for 48 h. **** indicates significantly different in Cd²⁺ exposed cells when compared to untreated controls at p-value of ≤ 0.0001. *** indicates significantly different in Cd²⁺ exposed cells when compared to untreated controls at p-value of ≤ 0.001.

(Fig. III-10A vs Fig. III-11A). Upon treatment with Cd²⁺, there was a high level of release of LDH into the growth media (Fig. III-10B). Furthermore, there was no increase in the activity of the enzyme caspase-3 (Fig. III-10C), and nuclear fragmentation a marker for cells undergoing apoptosis was not observed in DAPI stained nuclei (Fig. III-10D). Treatment of

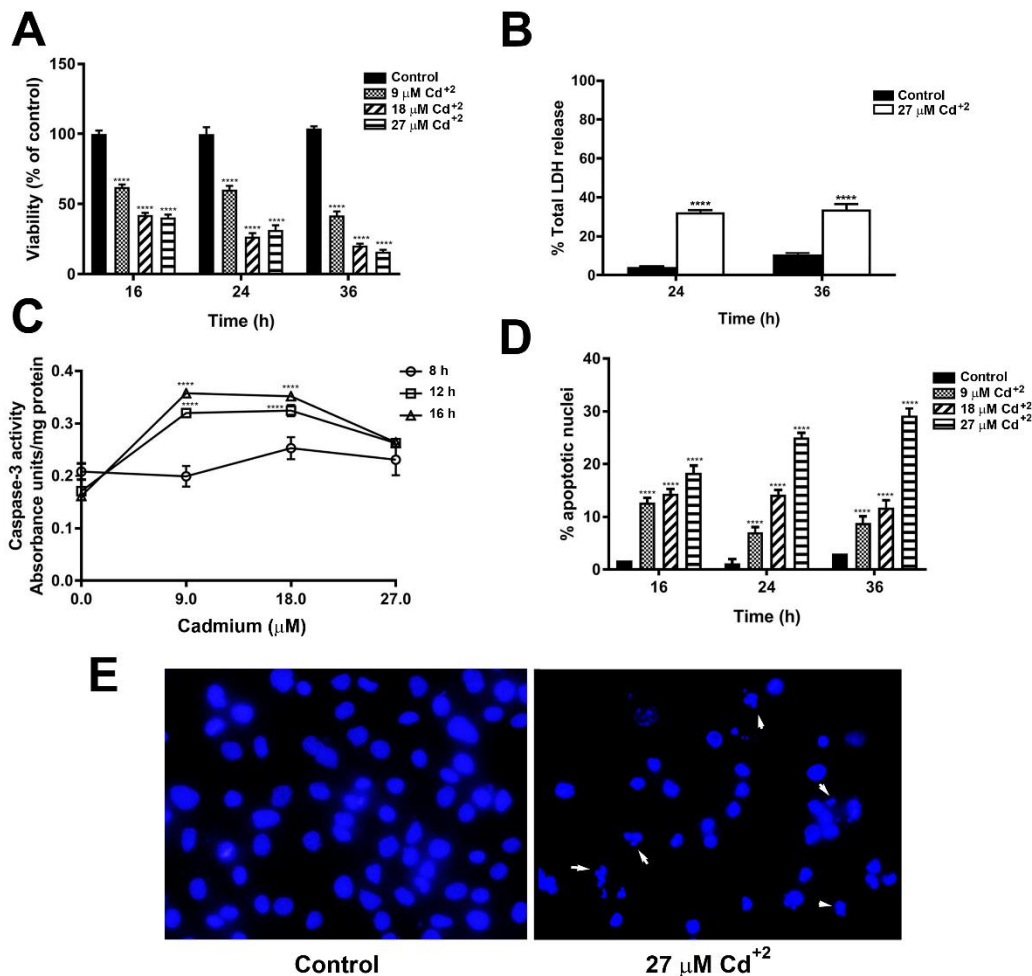


Fig. III-11. Effect of Cd²⁺ on HK-2 cells. (A). Effect of Cd²⁺ on the viability HK-2 cells exposed to 9, 18 and 27 Cd²⁺ for 16, 24 and 36 h. Viability was determined by counting the DAPI stained nuclei and is expressed as percent of control. (B). LDH release by Cd²⁺ treated cells. HK-2 cells were exposed to 27µM Cd²⁺ for 24 and 36 h. The release of LDH by the cells was quantified spectrophotometrically at a wavelength of 490 nm and is expressed as percent of total LDH release. (C). Caspase-3 activation in Cd²⁺ treated cells. RPTEC/TERT1 cells were exposed to 9, 18 and 27 µM Cd²⁺ for 8, 12 and 16 h. Caspase-3 activity was determined by the release of the chromophore, p-nitroanilide, which was quantitated spectrophotometrically at a wavelength of 405 nm. (D). Quantification of nuclear fragmentation for control and cadmium treated cells. The percent of apoptotic nuclei was determined after exposure to 9, 18 and 27 µM Cd²⁺ for 16, 24 and 36 h. Results are expressed as percent of apoptotic nuclei. (E). DAPI staining of HK-2 cells exposed to 27 Cd²⁺ µM for 48 h. Arrows indicate fragmented nuclei. **** indicates significantly different in Cd²⁺ exposed cells when compared to untreated controls at p-value of ≤ 0.0001.

HK-2 cells with Cd²⁺ under similar conditions showed changes consistent with cells undergoing apoptosis. The cells were more sensitive to Cd²⁺ (Fig. III-11A) when compared to the RPTEC/TERT1 cells (Fig. III-10A), and there was lower release of LDH (Fig. III-11B) as published previously for HK-2 cells (Somji et al. 2004). In addition, there was an increase in caspase-3 activity (Fig. III-11C), with significant numbers of DAPI stained fragmented nuclei visible microscopically (Fig. III-11D and E).

Isolation of CD133+CD24+ and CD24+ Cell Population from RPTEC/TERT1 Cell Cultures

RPTEC/TERT1 cells consists of about 79 % of the CD133+CD24+ and about 20 % of CD24+ cell population (Fig. III-6C). The data was analyzed using the fluorescence compensation parameters that were set for CD133 and CD24 markers to avoid any spectral overlap. 10,000 events were recorded and plotted as dot plot in FSC vs SSC graph and the singlet population was selected using a polygon. The singlet population was plotted as dot plot in CD133 vs CD24 graph to count the percent of positive events that occurred in four different

quadrants: CD133-CD24- (double negative), CD133+CD24- (CD133-positive), CD133+CD24+ (double positive) or CD133-CD24+ (CD24-positive). The graph obtained represents that out of all the singlet population, RPTEC/TERT1 consists of an average of about 76 % of CD133+CD24+ and about 24 % of CD133-CD24+ when performed in triplicate (Fig. III-12 A-D). In order to isolate these two cell populations from the RPTEC/TERT1, single cell suspension was prepared and ran through the BD FACS Aria IIu (BD Biosciences). Gates were drawn to select the specific cell population to be sorted and 100,000 cells were sorted into 5

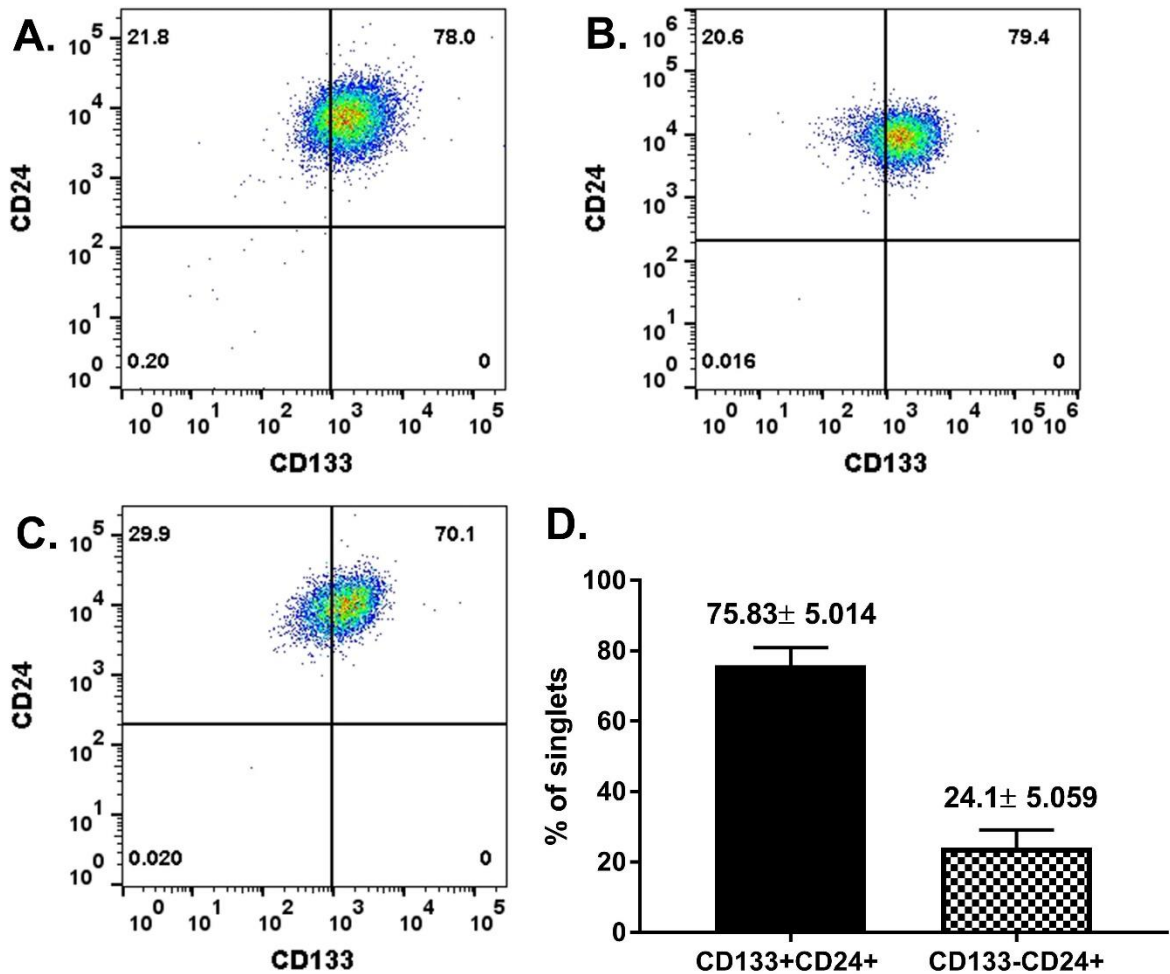


Fig III-12. Flow cytometry analysis of CD133+CD24+ and CD24+ populations in RPTEC/TERT1 cells ran in triplicate (A-C). (D). Graphical representation showing the

average percent of CD133+CD24+ and CD24+ (CD133-CD24+) cell population in RPTEC/TERT1 cells, the value is shown as the % of cell population \pm S.D.

wells of the 48 well plate. At confluency, the cells were detached and transferred into a 24 well plate and subsequently expanded to 6-wells, T-25 flasks and T-75 flasks for future use and further experiments. During this process before plating the cell suspension into the 24 well plate from 48 well plate, approximately 100 μ l of cell suspension was removed from the stock and run through the flow cytometer to check for the purity level for both the CD133+CD24+ and CD24+ cell population. The graph shows the % of CD133+CD24+ cells (Fig. III-13 A-G) and % of CD24+ cells (Fig. III-14 A-F) obtained at each split point while the cells were being expanded from a smaller surface area to a larger surface area culture plates and flasks.

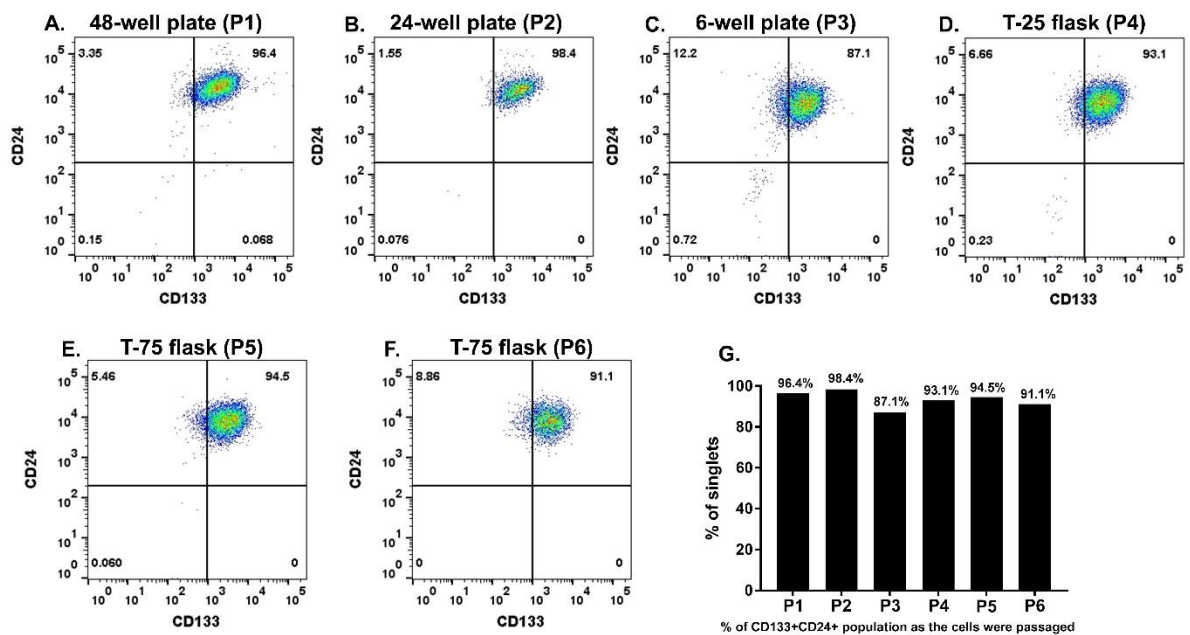


Fig III-13. Flow cytometry analysis of CD133+CD24+ cells to test purity at each passage number. 10⁵ no. of CD133+CD24+ cells were sorted from the RPTEC/TERT1 and plated in 48-well plate and after confluency transferred to bigger area. At each split point the cells were analyzed for their purity percent by running flow with CD133 and CD24 markers. The cells were analyzed when they were plated in 48-well plate (A) and then seeded into 24-well plate

(B); after confluency they were seeded into 6-well plate (C) then into the T-25 flask (D) and finally into T-75 flasks (E, F). (G) Graphical representation of % of CD133+CD24+ cells within singlet population at every passage.

The first group of the sorted double positives cells that were plated on the 24 well plate from 48 well plate showed 96.4 % of CD133+CD24+ population (fig. III-13A), which were split into 6 wells. The double positive cell population in the 6-well plate maintained the purity and stability by expressing 98.4 % of CD133+CD24+ population (fig. III-13B). The percent of double positive events decreased when cells were in T-25 flask showing 87.1 % of CD133+CD24+ population (fig. III-13C), however, the double positive events gradually increased to 93.1 %; 94.5 % and 91.1 % in CD133+CD24+ cell population (fig. III-13 D-F) as they were split into the T-75 flasks. The cells were expanded and cryopreserved when they expressed >90 % of double positive events. Similarly, the CD24+ cell population were also

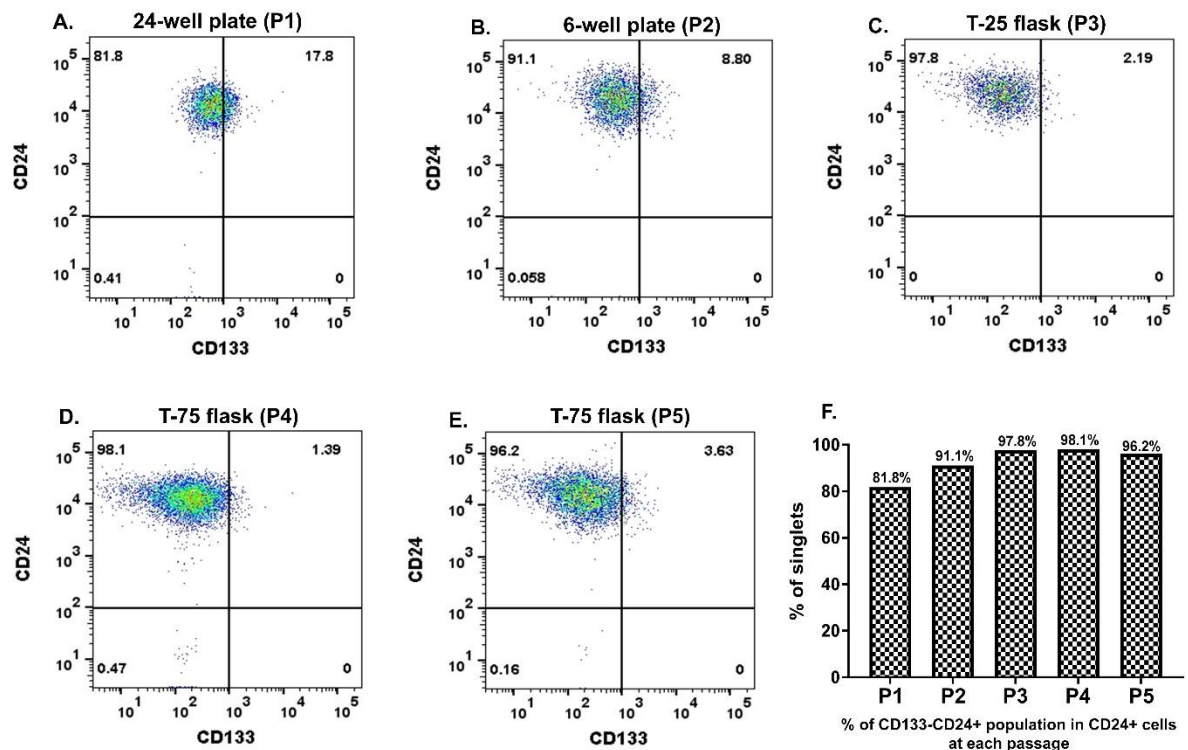


Fig III-14. Flow cytometry analysis of CD24+ cells to test purity at each passage number. 10^5 no. of CD24+ cells were sorted from the RPTEC/TERT1, plated in 48-well plate, and after confluency transferred to bigger area. At each split point, the cells were analyzed for their purity percent by running flow with CD133 and CD24 markers. The cells were analyzed when they were plated in 48-well plate (A) and then seeded into 24-well plate (B); after confluency they were seeded into 6-well plate (C) then into the T-25 flask (D) and finally into T-75 flask (E). (F) Graphical representation of % of CD24+ cells within singlet population at every passage.

analyzed to determine the purity and stability of cells to express the CD24 marker exclusively, 24 well plate showed 81.8% of CD24+CD133- population (fig. III-14A). The cells grown in 6-well plate showed significant increase in percent of CD24+ expression that was recorded to be 91.1% of CD24+CD133- population (fig. III-14B). The CD24+ events increased to 97.8% when cells were grown in T-25 flasks (fig. III-14C). The cells split into subsequent T-75 flasks showed 98.1% and 96.2% of CD24+CD133- population (fig. III-14D, E). The cells were expanded and cryopreserved when they expressed >95% of CD24+ events.

Expression of CD133 and CD24 Markers in RPTEC/TERT1, CD133+CD24+ and CD24+ Cells Cultures

In order to validate that both the sorted cell lines, CD133+CD24+ cells contained high expression of CD133 as well as CD24 stem/progenitor cell markers and CD24+ cells expressed exclusively CD24 but no CD133, RT-qPCR and immunofluorescence staining was performed to detect the expression levels of CD133 and CD24 in RPTEC/TERT1, CD133+CD24+ and CD24+ cells. The expression of the CD133 gene was high in RPTEC/TERT1 and CD133+CD24+ cells while in CD24+ cells the expression of CD133 was significantly decreased and almost close to level of detection (Fig. III-15A). The confocal staining results showed that the expression of CD133 was completely abolished in

the CD24+ cells (Fig. III-15C). RPTEC/TERT1 showed positive staining of CD133 which was observed to be higher on the cell surfaces (Fig. III-15C). The CD133+CD24+ cells showed CD133 staining on the cell surfaces as well as in the intracellular compartments (Fig. III-15C).

The mRNA expression of CD24 gene was significantly higher in the CD133+CD24+ as well as CD24+ cells when compared to RPTEC/TERT1 (Fig. III-15B). All three cell lines showed positive staining for CD24 protein. RPTEC/TERT1 cells showed positive staining on the cell surface (Fig. III-15C) while both CD133+CD24+ and CD24+ cells showed positive

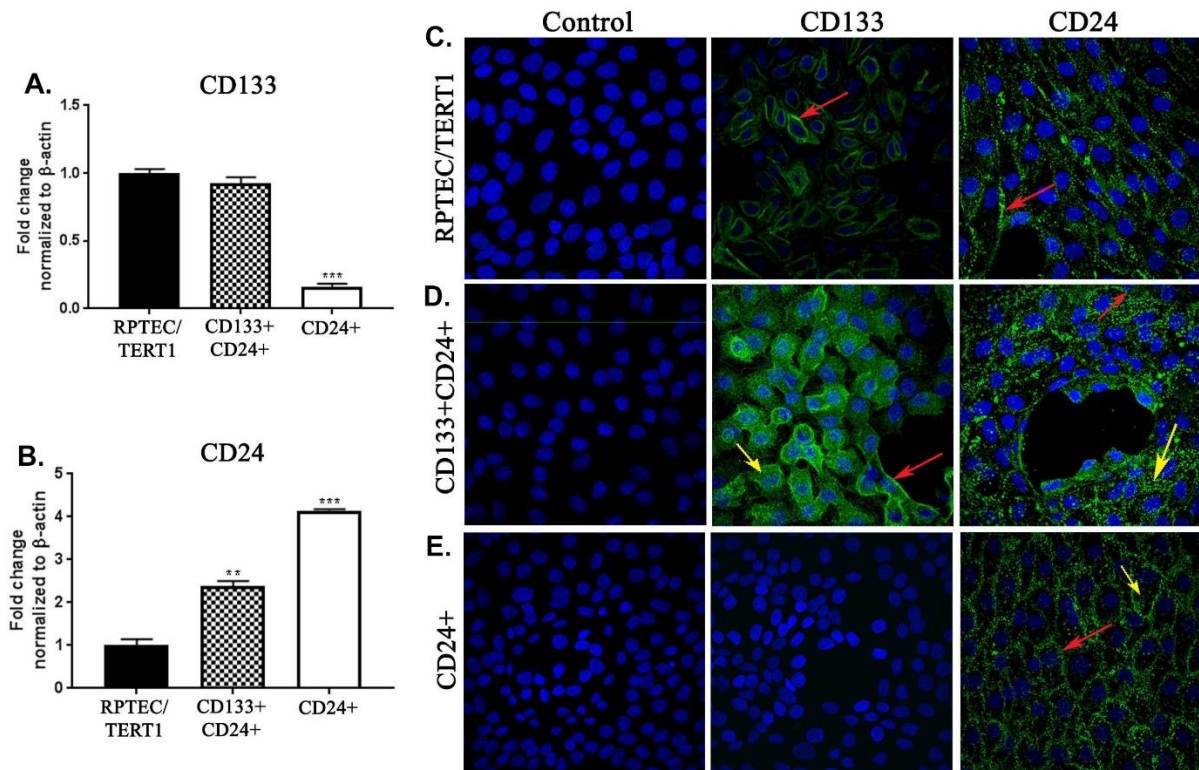


Fig III-15. Expression of CD133 and CD24 in various populations of renal tubular cells. A and B. Real time PCR analysis of the expression level of CD133 (A) and CD24 (B) in the RPTEC/TERT1 cells, the sorted CD133+CD24+ and the CD24+ cells. ** indicates p-value of ≤ 0.01 ; *** indicates p-value of ≤ 0.05 . C-E. Immunofluorescent staining showing the localization of CD133 and CD24 in various populations of renal tubular cells. C. Localization of CD133 and CD24 in the RPTEC/TERT1 cell line. D. Localization of CD133

and CD24 in the double positive CD133+CD24+ cells. E. Localization of CD133 and CD24 in the CD24+ cells. The red arrow shows cell surface staining whereas the yellow arrow indicates intracellular staining. Nuclei are stained with DAPI.

staining on the cell surfaces as well as intracellular compartments (Fig. III-15C). These results validated that the sorted CD133+CD24+ and CD24+ cells are pure populations as CD133+CD24+ showed expression of CD133 as well as CD24 and CD24+ cells showed expression of CD24 but not CD133 markers.

Morphology, Transepithelial Resistance and Growth Rate Determination of RPTEC/TERT1, CD133+CD24+ and CD24+ Cells

CD133+CD24+ or double positive cells and CD24+ were grown in culture after sorting them from the RPTEC/TERT1 cells. The cells were maintained by feeding them every other day with serum-free DMEM/F-12 media. The morphology of the CD133+CD24+ cells is identical to the RPTEC/TERT1 cells and grow as a monolayer comprised of flat cuboidal epithelial cells. Morphologically, the CD24+ cells look very similar to the RPTEC/TERT1 however; some of the areas consist of small round shaped cells and asymmetrical growth (Fig. III-16C). These type of small rounded cells are not found in the RPTEC/TERT1 or the CD133+CD24+ cells and at present, the identity of CD24+ cells is not

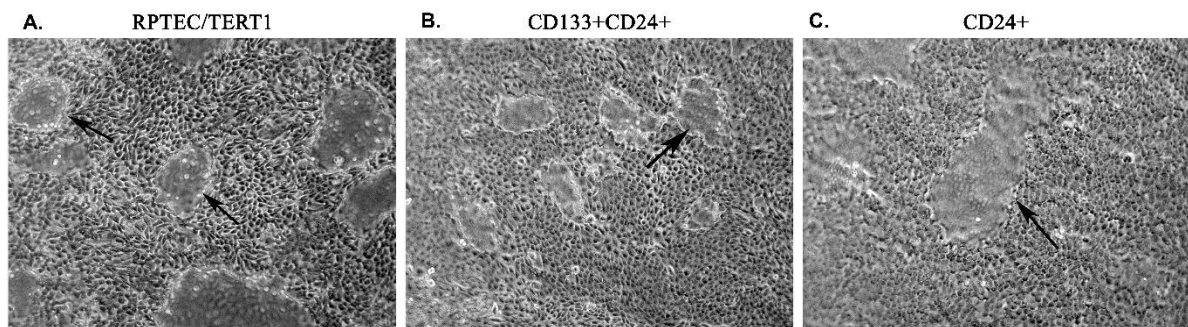


Fig III-16. Light level microscopy of different proximal tubular cell cultures after sorting. Light level microscopy of RPTEC/TERT1 cells (A), CD133+CD24+ cells (B) and CD24+ cells (C). Arrows indicate the presence of domes, which are indicative of vectorial active transport.

known. Both of the CD133+CD24+ and the CD24+ cells form dome at confluency (Fig. III-16 A-C). This indicates that both these cell population demonstrate vectorial active transport properties of the differentiated epithelial proximal tubular cells.

Transepithelial resistance (TER) of RPTEC/TERT1, CD133+CD24+ and CD24+ cells was evaluated. TER measurement determines the integrity of the tight junction in cell culture models and this is important to know in order to design therapeutical drugs for targeted delivery to cells and tissues (Srinivasan B et al. 2015). The one-way anova multiple comparison analysis shows that the TER of CD133+CD24+ cells, calculated as an average of $378.8\Omega\text{cm}^{2+}$ is significantly higher than RPTEC/TERT1 and CD24+ cells, calculated as an average of $299.8\Omega\text{cm}^{2+}$ and $294.1\Omega\text{cm}^{2+}$ respectively (Fig III-17).

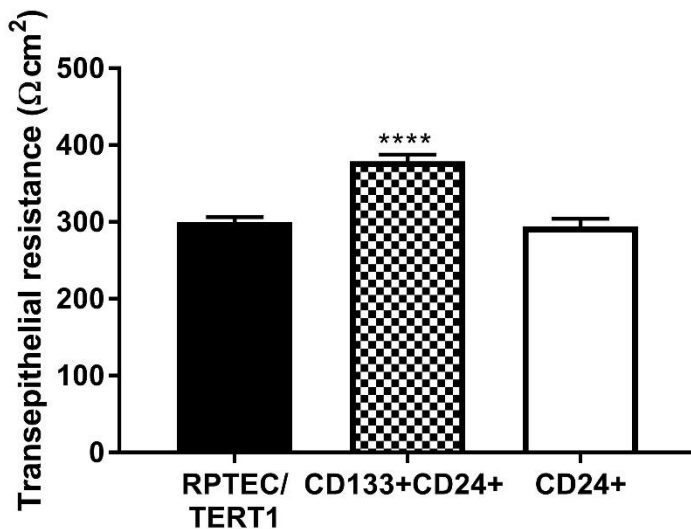


Fig III-17. Transepithelial resistance measurement of RPTEC/TERT1, CD133+CD24+ and CD24+ cells. Cells were grown in 1.1cm^2 polyethylene terephthalate inserts in 12-well

plate at 2:1 split ratio and TER was measured using EVOM voltammeter starting next day after seeding until day 10. Transepithelial resistance measurement of RPTEC/TERT1 was $299.8 \pm 6.4 \Omega\text{cm}^{2+}$; CD133+CD24+ was $378.8 \pm 9.1 \Omega\text{cm}^{2+}$ and CD24+ cell was $294.1 \pm 10.3 \Omega\text{cm}^{2+}$. **** indicates CD133+CD24+ cells value is significantly different compared to RPTEC/TERT1 and CD24+ cells at p-value of ≤ 0.0001 .

The growth rate was analyzed using MTT assay to determine the population doubling time. The results showed that CD24+ cells grew slower than the CD133+CD24+ cells. The doubling time of RPTEC/TERT1 and CD133+CD24+ cells was determined to be 76.8 ± 0.006 days and 79.2 ± 0.03 days respectively (Fig. III-18 A & B). CD133+CD24+ showed similar doubling time period as RPTEC/TERT1 however, the doubling time of CD24+ cells was significantly higher than RPTEC/TERT1 and CD133+CD24+ and calculated to be 108 ± 0.031 days (Fig. III-18C).

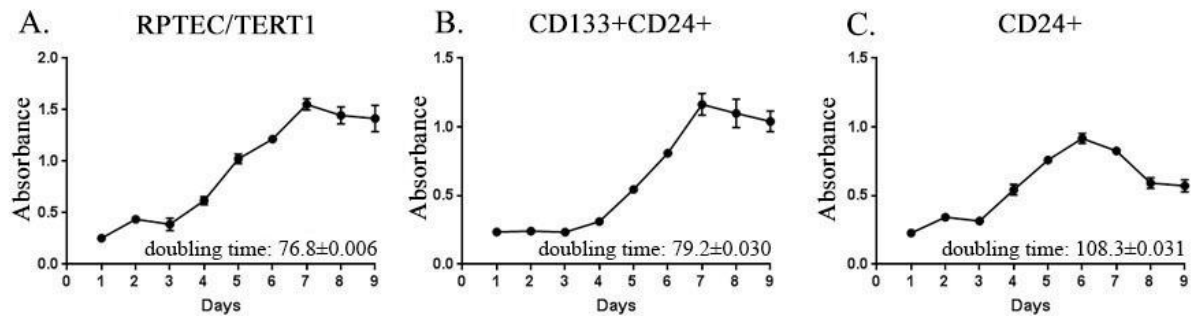


Fig III-18. Determination of growth rates of various populations of renal tubular cells. A-C. Determination of the growth rate of (A) RPTEC/TERT1 cells, (B) CD133+CD24+ cells and (C) CD24+ cells using the MTT assay. The doubling time for each cell line indicated in the figure.

Ki67 Expression in RPTEC/TERT1, CD133+CD24+ and CD24+ Cells

In order to study the growth cycle of RPTEC/TERT1, CD133+CD24+ and CD24+ cells, all three cell lines were fixed, permeabilized and stained with proliferation marker, Ki67

and the expression was detected using flow cytometry. Ki67 is present in the nuclei during the cell cycle phases G1, S and G2 however, it is absent during the G0 phase (Scholzen T et al. 2000), thus, its expression indicates cell division and proliferation. The flow cytometric analysis showed that 34.6 % of RPTEC/TERT1 cells expressed Ki67 (Fig. III-19 D), 22.5 % of CD133+CD24+ cells expressed Ki67 (Fig. III-19 E) whereas only 10.1% of CD24+ cells were positive for Ki67 protein (Fig. III-19 F). For all three cell lines, the unstained sample was used as control which showed no expression of Ki67. The cut-off value for positive and negative signal in Ki67 stained samples was determined based on the value where negative signal was collected from the unstained control (Fig. III-19A-C). The

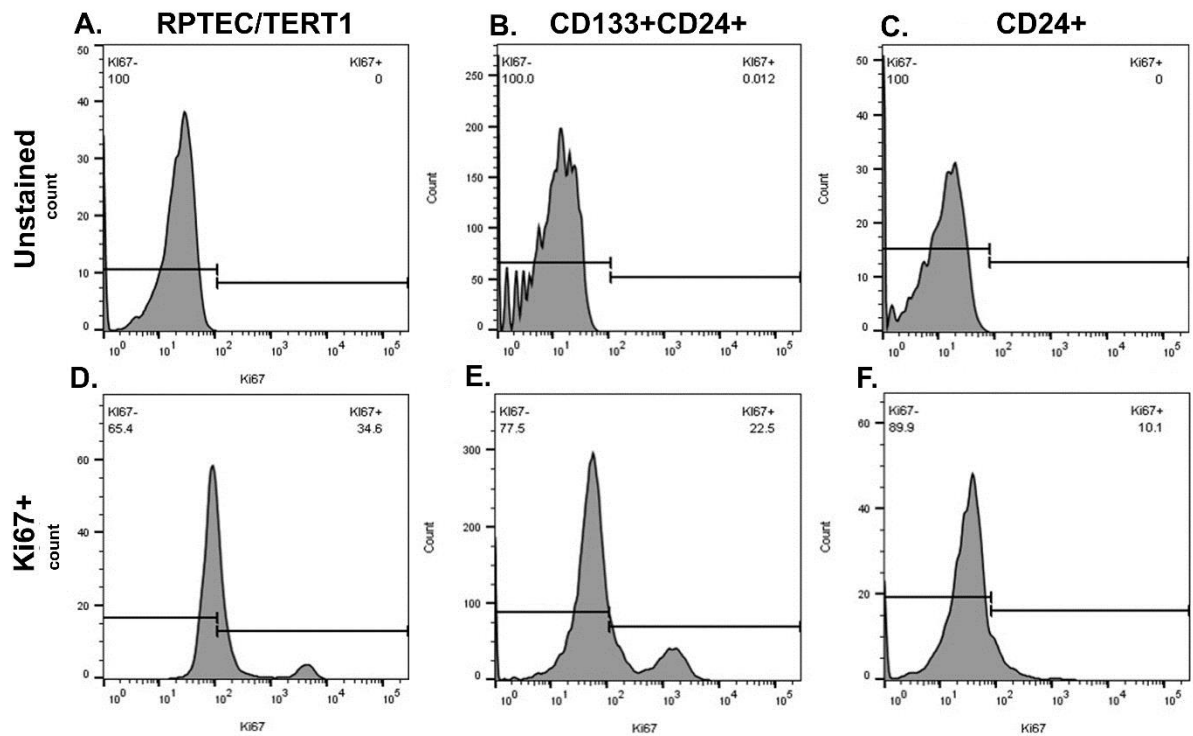


Fig III-19. Flow cytometric analysis of number of cells stained positive for Ki67 in fully confluent cultures RPTEC/TERT1, CD133+CD24+ and CD24+ cells. For all three cell lines, unstained samples were run as control (A) unstained RPTEC/TERT1 cells; (B) unstained CD133+CD24+ cells; (C) unstained CD24+ cells. Percent of cells stained positive for Ki67 in (D) RPTEC/TERT1 cells; (E) CD133+CD24+ cells and (F) CD24+ cells. The histogram is plotted as the relative intensity of Ki67 in log scale vs number of event or cell count.

higher expression of Ki67 in CD133+CD24+ cells when compared to CD24+ cells shows that CD133+CD24+ cells may have greater proliferation capacity.

Expression of AQP-1 and CAL Markers in RPTEC/TERT1, CD133+CD24+ and CD24+ Cells

RT-qPCR and immunofluorescence staining was performed on the RPTEC/TERT1, CD133+CD24+ and CD24+ cells to analyze the expression of the proximal tubule marker aquaporin-1, AQP-1 and the distal tubule marker calbindin, CAL. The expression of AQP-1 and CAL was evaluated to determine if these cells have proximal tubule like features and if they possess the ability to form other differentiated cell types of the kidney. The mRNA results showed significantly higher expression of the AQP-1 in CD133+CD24+ and CD24+ cells when compared to the RPTEC/TERT1 (Fig. III-20 A). Immunofluorescence of AQP-1 showed positive staining on the cell surfaces of all three cell lines (Fig. III-20 C).

The mRNA expression results showed significantly higher expression of CAL in CD133+CD24+ cell line when compared to RPTEC/TERT1 cells while in the CD24+ cells the expression level was low and similar to that of the RPTEC/TERT1 cells (Fig. III-20 B). The confocal imaging showed strong intracellular expression of CAL in the CD133+CD24+ cells while the RPTEC/TERT1 and CD24+ cells did not show any staining for the CAL protein (Fig. III-20 C). These results indicate that CD133+CD24+ cells express both proximal as well as distal tubule markers and may have multipotent characteristics, thus being able to give rise to various cell types of the kidney.

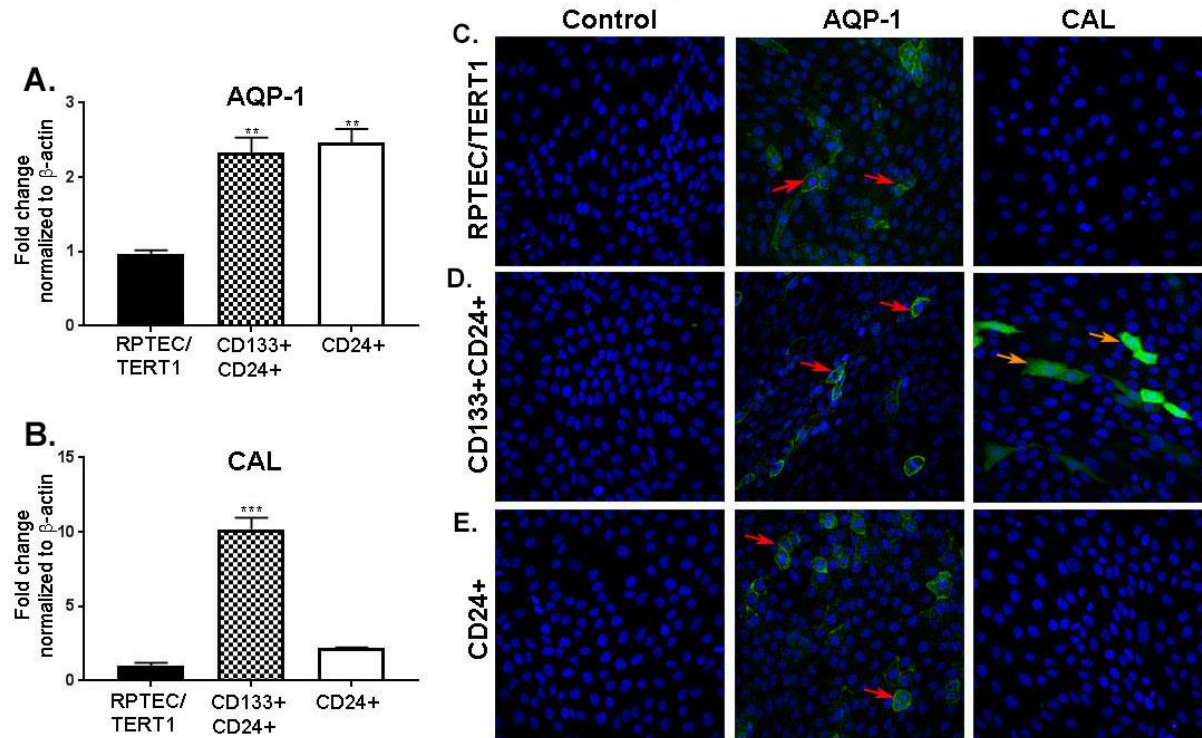


Fig III-20. Expression of aquaporin-1 (AQP-1) and calbindin (CAL) in various populations of renal tubular cells. A and B. Real-time PCR analysis of the expression (A) AQP-1 (proximal tubular marker) and (B) calbindin (distal tubular marker). ** indicates p-value of ≤ 0.01 ; *** indicates p-value of ≤ 0.05 . C-E. Immunofluorescence staining showing the localization of AQP-1 and CAL in RPTEC/TERT1 (C) cells, CD133+CD24+ cells (D) and CD24+ cells (E). The red arrow shows AQP-1 staining on the surface of the cells while the yellow arrow shows intracellular CAL staining. The nuclei are DAPI stained.

Ability of RPTEC/TERT1, CD133+CD24+ and CD24+ Cells to Form Spheroids

Spheroid formation is one of the in-built characteristics of the stem cells grown *in-vitro*. The stem cells when cultured in suspension with minimal adherent support is able to divide and form a ball that consists of many cells hence called spheroids (Buzhor E et al. 2011; Bombelli S et al. 2018). After validating that the sorted population is stable and pure, their ability to form spheres was determined by growing single cell suspension in ultra-low attachment flasks. 1:100 -1:1000 cells were seeded in an ultra-low attachment flask, allowed to grow for about 7 to 10 days and then the pictures were taken using Zeiss light microscope

at 10x magnification (Fig. III-21 A-C) and 20x magnification (Fig. III-21 D-F). RPTEC/TERT1 and CD133+CD24+ cells were able to form 3-4 spheroids per field after 7 days as shown in fig. III-21 A & B when observed at 10x magnification. Both cell lines were also capable of forming small tubule like structures shown in images taken at 20x magnification fig. III-21 D&E. However, the CD24+ cells were unable to form spheres except for very few cysts like structures shown in the image taken at 20x magnification (Fig. III-21F). Majority of CD24+ cells remained as single cells in the ultra-low attachment flasks until day 9 of post seeding observed at 10x magnification (Fig. III-21C).

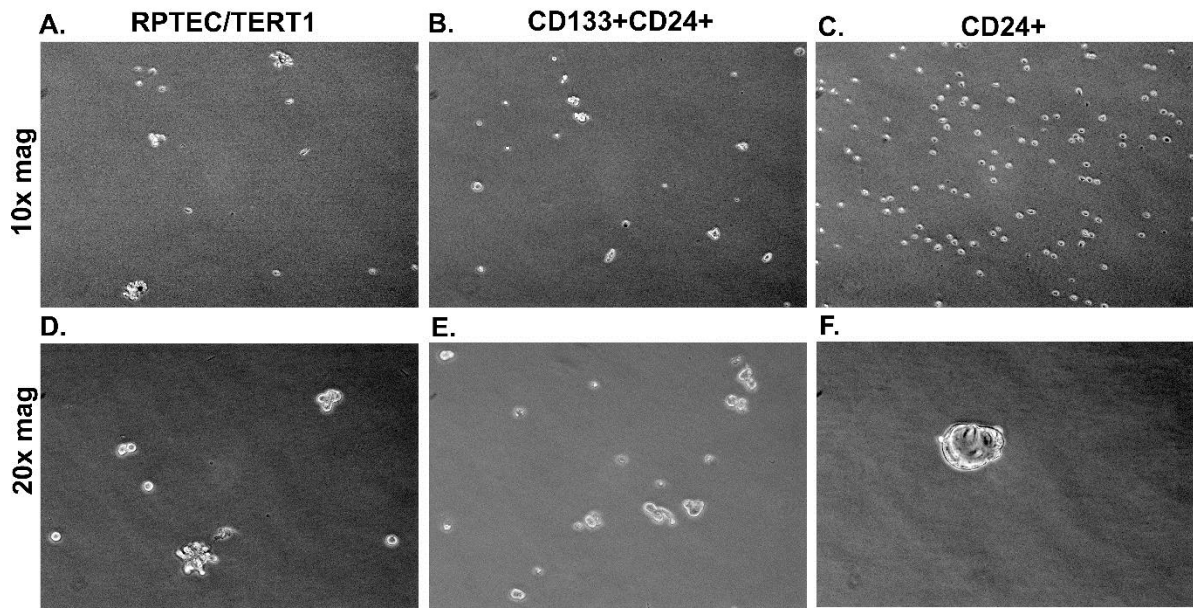


Fig III-21. Light level microscopy of spheroids generated from RPTEC/TERT1, CD133+CD24+, CD24+ cells. The top panel is the spheroid images taken at 10x magnification generated from (A) RPTEC/TERT1 cells; (B) CD133+CD24+ cells; (C) CD24+ cells. The bottom panel is the spheroids taken at 20x magnification generated from (D) RPTEC/TERT1 cells; (E) CD133+CD24+ cells; and (F) CD24+ cells. All the images were taken after 10 days of seeding in the ultra-low attachment flasks.

Change in CD133+CD24+ and CD24+ Cell Population after Exposure to Cd²⁺ for 34 Days

RPTEC/TERT1 cells were exposed to 0, 4.5, 9, 13.5, 18, 27 and 45 μM Cd²⁺ for 16 days and their viability was determined by DAPI staining (fig. III-22). Based on the viability results obtained by exposing RPTEC/TERT1 cells to various concentration of Cd²⁺, CD133+CD24+ and CD24+ cells were exposed to 0, 4.5, 9, 27 and 45 μM Cd²⁺ for 34 days and the effect of cadmium was determined by observing the morphology of the cells after exposure to cadmium using the light microscope. At present, the DAPI viability test for CD133+CD24+ and CD24+ cells after exposure to different concentration of Cd²⁺ has not been completed. Fig. III-23(A-F) are the pictures taken with Zeiss light microscope of

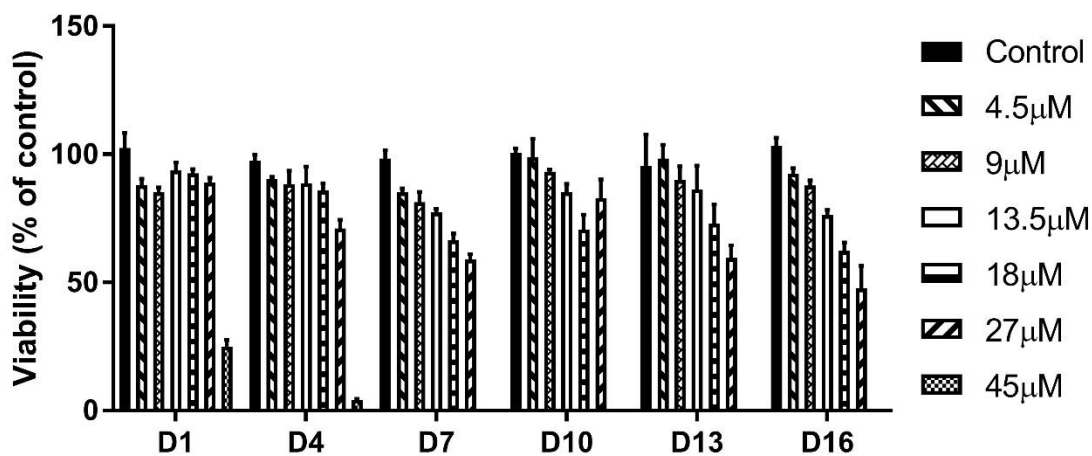


Fig III-22. Effect of Cd²⁺ on the viability RPTEC/TERT1 cells exposed to 0, 4.5, 9, 13.5, 18, 27 and 45 μM Cd²⁺ for 16 days. Viability was determined by counting the DAPI stained nuclei every 3 days after exposing to the above mentioned cadmium concentration and is expressed as percent of control.

the CD133+CD24+ cells treated with 0, 4.5 and 9 μM Cd²⁺ for 34 days. Dome formation was not affected by any of the dose upto 34 days and minimal cell death was observed compared

to the control (0 μM). Fig. III-24 (A-F) shows the images of CD24+ cells

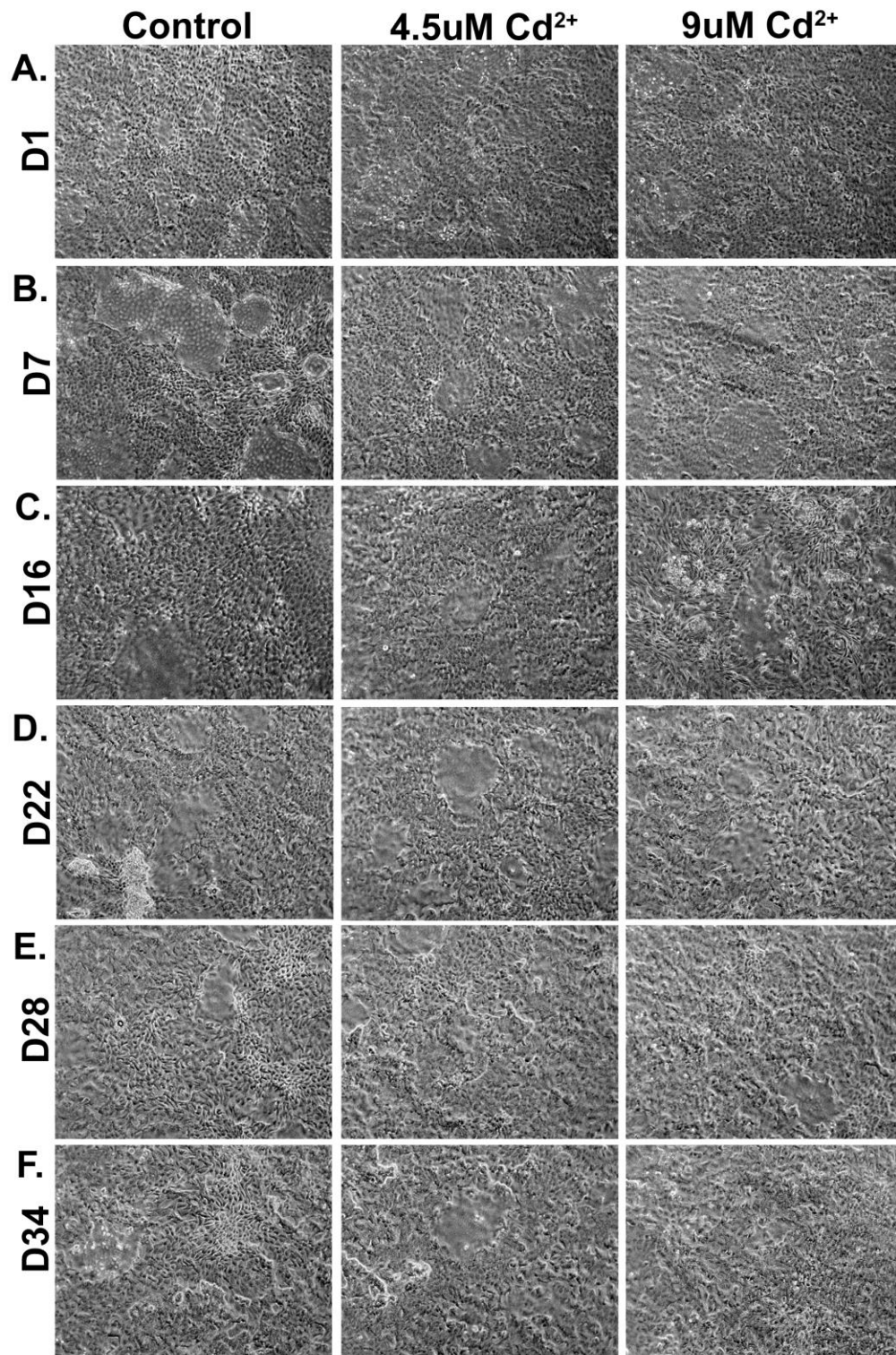


Fig III-23. Light level microscopy of CD133+CD24+ cells treated with 4.5 and 9 μM Cd²⁺ for 34

days. Each panel from left to right shows images of CD133+CD24+ cells treated with 0 μ M (control), 4.5 μ M and 9 μ M Cd²⁺ on (A) day 1; (B) day 7; (C) day 16; (D) day 22; (E) day 28 and (F) day 34. Dome formation was observed at each dose and exposure time. All images were taken at 20x magnification.

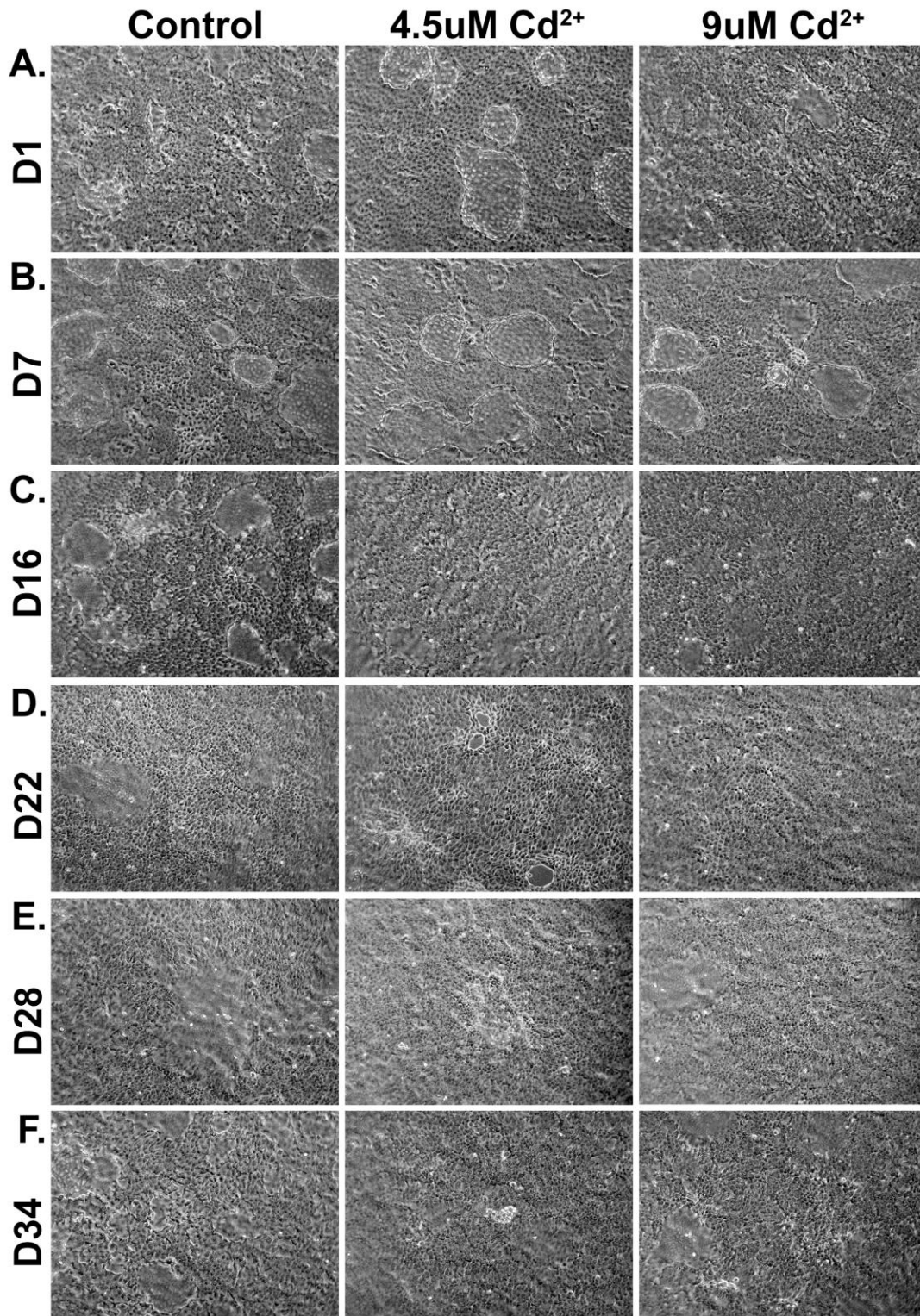


Fig III-24. Light level microscopy of CD24+ cells treated with 4.5 and 9 μM Cd^{2+} for 34 days. Every panel from left to right shows images of CD24+ cells treated with 0 μM (control), 4.5 μM and 9 μM Cd^{2+} on (A) day 1; (B) day 7; (C) day 16; (D) day 22; (E) day 28 and (F) day 34. Cell loss caused holes in the monolayer shown by arrows with 4.5 μM Cd^{2+} in addition, domes were abolished with both 4.5 & 9 μM Cd^{2+} on day 22, however the holes were filled and dome formation were resumed by day 28. All images were taken at 20x magnification.

treated with 4.5 and 9 μM Cd^{2+} for 34 days. At day 22, cell death was observed to be higher with 4.5 as well as 9 μM Cd^{2+} causing small spaces in the monolayer, however regrowth of cells was observed that filled up the spaces by day 28 (Fig. III-24 D, 4.5 μM Cd^{2+}). Approximately during the same time period, day 22, domes were not formed in CD24+ cells exposed to 4.5 & 9 μM Cd^{2+} , however the cells again started to form domes by day 28 (Fig. III-24 D, 4.5 & 9 μM Cd^{2+}). CD24+ cells showed higher cell death at higher concentration of Cd^{2+} when compared to RPTEC/TERT1 and CD133+CD24+ cells. Based on the viability study performed on RPTEC/TERT1 and the observation made on cell death and morphology of CD133+CD24+ and CD24+ cells treated with different concentration of cadmium, 4.5 and 9 μM Cd^{2+} was chosen to be the ideal concentrations to study the changes in cell population number after Cd^{2+} exposure (Fig. III-23, III-24 & III-25). The viability study showed that the change in cell population was not because of cell death due to Cd^{2+} toxicity but an actual effect on proliferation or suppression on growth of the cells after exposure.

To look at the extended effect of Cd^{2+} in all three cell lines, the cells were exposed to 4.5 and 9 μM Cd^{2+} for 34 days and were dosed every 2 days. The result shows the change in percentage of cell population compared to the untreated control in RPTEC/TERT1, CD133+CD24+ and CD24+ cells treated with 4.5 & 9 μM Cd^{2+} at day 7, 16, 22, 28 and 34 with 4.5 and 9 (Fig. III-26). The calculation was done as a percentage value of no. of singlet cell population recorded for the treated sample divided by the no. of singlet cell population

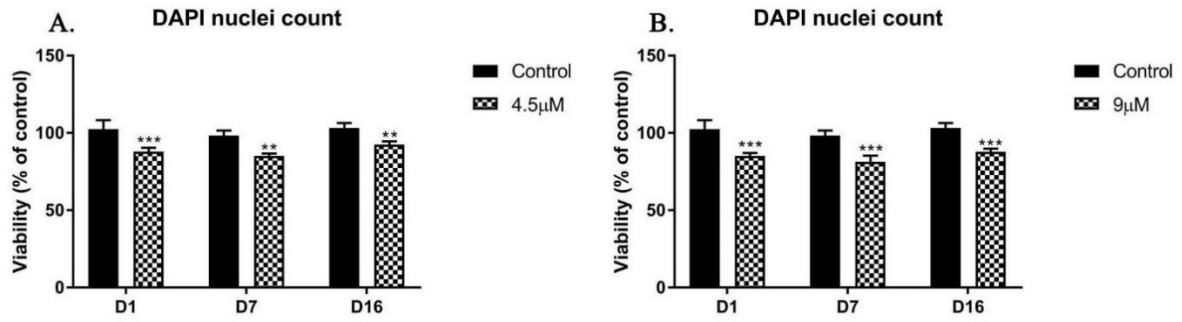


Fig. III-25. Effect of cadmium on the viability RPTEC/TERT1 cells. The RPTEC/TERT1 cells were treated with (A) 4.5 μM Cd^{2+} and (B) 9 μM Cd^{2+} up to 16 days. Cell viability determined by counting the DAPI stained nuclei. The data is represented as percent of control. ** indicates p-value of ≤ 0.01 ; *** indicates p-value of ≤ 0.05 .

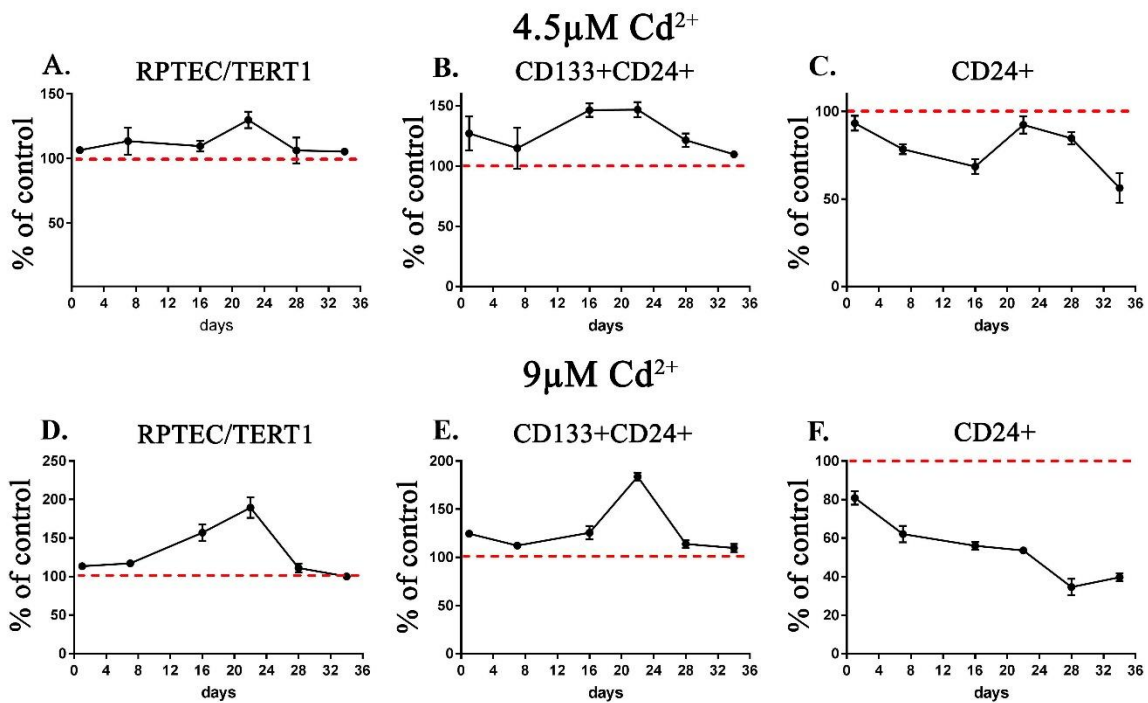


Fig III-26. Effect of cadmium on the viability of various populations of renal tubular cells. RPTEC/TERT1, CD133+CD24+ and CD24+ cells treated with (A-C) 4.5 and (D-F) 9 μM Cd^{2+} for 34 days and the viable number of cells were determined by flow cytometric analysis. The data is represented as % of control (untreated cells).

recorded for the untreated sample and represented as % of control. The RPTEC/TERT1 (Fig. III-26 A & D) and CD133+CD24+ (Fig. III-26 B & E) cells when exposed to 4.5 as well as 9 μM Cd^{2+} for 34 days showed either no change or increase in number of cells when compared to the control (Fig. III-26 A&B; D&E). However, CD24+ cells treated with 4.5 as well as 9 μM Cd^{2+} for 34 days showed decrease in the number of cells when compared to the control (Fig. III-26 C & E).

Growth of RPTEC/TERT1, CD133+CD24+, CD24+ and HPT cells with matrigel in culture plates.

To determine if RPTEC/TERT1, CD133+CD24+, CD24+ and HPT cells could form tubular structures when allowed to grow on matrigel coated plates, each of the cell lines were plated as single cells in matrigel coated (thin matrigel coat protocol) as well as after mixing with matrigel (thick matrigel protocol) and allowed to grow until 14 days. The matrigel consists of extracellular proteins that support growth and differentiation of cells. The stem cells tend to grow as a cyst in the matrigel. The cells were mixed with matrigel in order to analyze formation of any differentiated tubular structures. Single suspension of cells were mixed with the matrigel and plated onto 2 wells of 48-well plate and observed for 14days.

At day 4, the RPTEC/TERT1 cells appeared as single cells (Fig. III-27 A) that formed a hollow ball by day 7 (Fig. III-27 B-D) and grew in size by day 14. There were quite a few

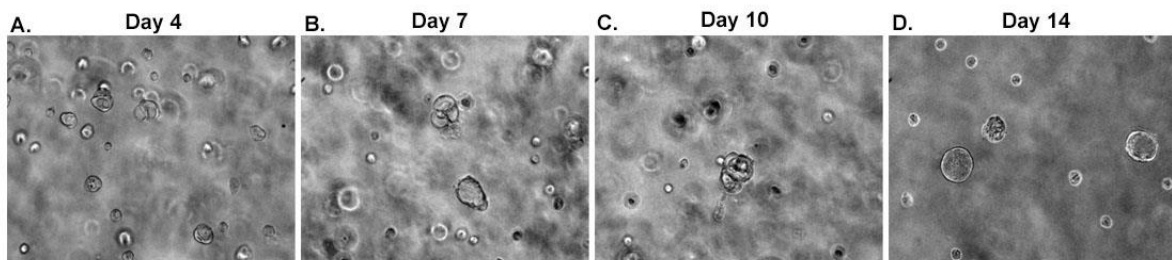


Fig III-27. Light level microscopy of RPTEC/TERT1 cells plated with matrigel in a 48-well plate. Single cell suspension of RPTEC/TERT1 cells mixed with matrigel to form thick coat of cells and matrigel mix in a 48-well plates. Light level microscopy images of cells in matrigel were taken at (A) day 4; (B) day 7; (C) day 10 and (D) day 14. All images taken at 20x magnification.

cells that did not form structures and remained as single cells throughout the time course. CD133+CD24+ cells formed tubule like structures at day 4 (Fig. III-28A) and formed larger cysts like structures by day 7 and day 10 (Fig. III-28 B & C). At day 10, some of CD133+CD24+ cells appeared as hollow balls consisting of multiple cells (Fig. III-28C). At day 14, the cells appeared to be smaller (Fig. III-28D). The CD24+ cells mostly remained as single cells at day 4 and day 7 with a few of them forming small clusters or spheroids,

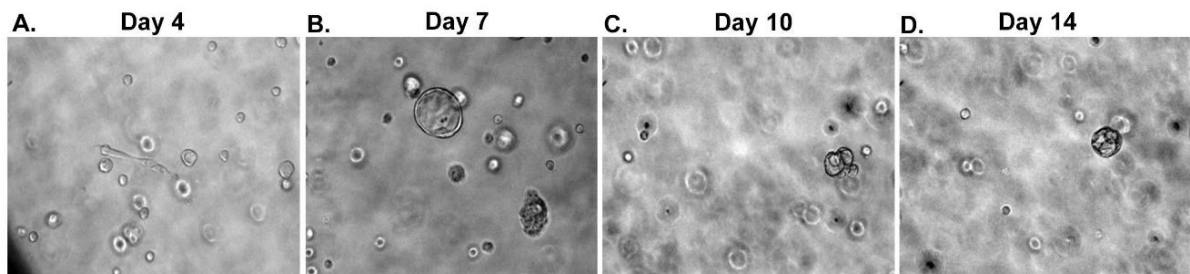


Fig III-28. Light level microscopy of CD133+CD24+ cells plated with matrigel in a 48-well plate. Single cell suspension of CD133+CD24+ cells mixed with matrigel to form thick coat of cells and matrigel mix in a 48-well plates. Light level microscopy images of cells in matrigel were taken at (A) day 4; (B) day 7; (C) day 10 and (D) day 14. All images taken at 20x magnification.

however by day 14, large multi-cellular structures were seen (Fig. III-29 C). The HPT cells

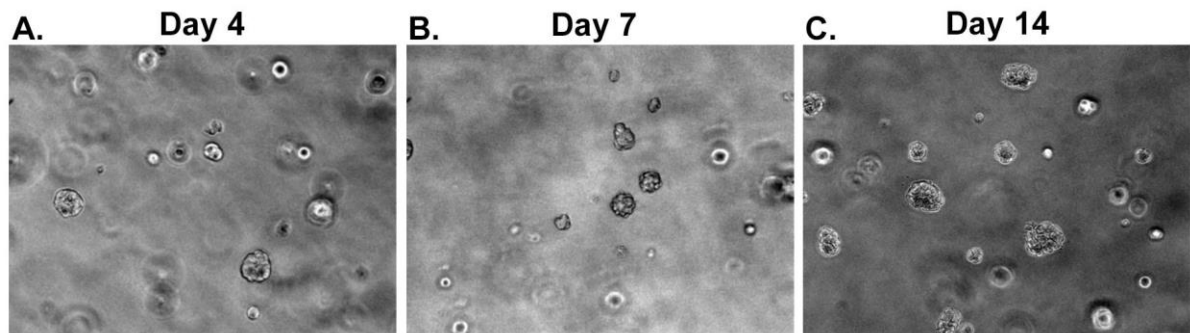


Fig III-29. Light level microscopy of CD24+ cells plated with matrigel in a 48-well plate. Single cell suspension of CD24+ cells mixed with with matrigel to form thick coat of cells and matrigel mix in a 48-well plates. Light level microscopy images of cells in matrigel were taken at (A) day 4; (B) day 7 and (C) day 14. All images were taken at 20x magnification.

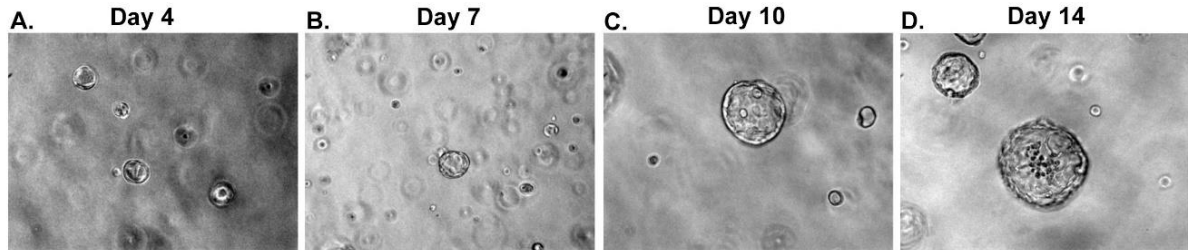


Fig III-30. Light level microscopy of HPT cells plated with matrigel in a 48-well plate. Single cell suspension of HPT cells mixed with with matrigel to form thick coat of cells and matrigel mix in a 48-well plates. Light level microscopy images of cells in matrigel were taken at (A) day 4; (B) day 7; (C) day 10 and (D) day 14. All images were taken at 20x magnification.

formed hollow structures at day 4 and 7 (Fig. III-30 A & B) that were larger at day 10 and 14 and most of these structures appeared to be multicellular (Fig. III-30 C & D).

RPTEC/TERT1, CD133+CD24+, CD24+ and HPT cells were plated as single cell in wells coated with thin layer of matrigel and allowed to grow for approximately 10 days. RPTEC/TERT1 and CD133+CD24+ cells form mesh-like long stretches (Fig. III-31 A&B) while CD24+ and HPT cells did not form mesh like structure but formed clumps of cells with some cell death (Fig. III- 31 C & D).

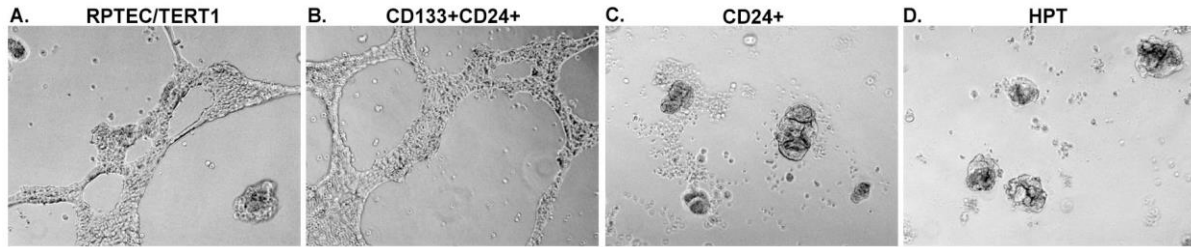


Fig III-31. Light level microscopy of RPTEC/TERT1, CD133+CD24+ and CD24+ cells plated on the surface of thin matrigel coated 48-well plate. Single cell suspension of RPTEC/TERT1, CD133+CD24+, CD24+ and HPT cells plated in wells coated with thin layer of matrigel. Light level microscopy images of cells (A) RPTEC/TERT1; (B) CD133+CD24+; (C) CD24+ and (D) HPT growing on the surface of the matrigel coat. All images taken at 20x magnification.

Histology and Immunohistochemical staining of tubular structures formed by various populations of RPTEC/TERT1 cells

To determine if RPTEC/TERT1, CD133+CD24+ and CD24+ cells could form tubular structures when injected with matrigel in immune compromised mice, the monolayer cultures of RPTEC/TERT1, CD133CD24 and CD24+ cell lines were trypsinized and the obtained pellet was mixed with equal volume of matrigel. The cell suspension was injected subcutaneously into the immune compromised mice and the formation of a nodule at the injection site was monitored for 16 days. Each cell line was injected into 4 nude mice and the nodules were harvested at 7, 10, 13 and 16 days. The nodules were paraffin embedded, cut into sections and stained for with hematoxylin and eosin (H&E) for histological observations. The nodules harvested at day 13 were used for immunohistochemical studies since nodules harvested at day 7 and 10 were small and those harvested at day 16 showed cystic changes. H&E staining of RPTEC/TERT1, CD133+CD24+ and CD24+ showed formation of tubule like structures of different sizes along with some single epithelial cells in the matrigel. Some spindle shaped stromal cells were also visible. Figure III-32 panel A shows the histology of the tubules stained

with H&E. The normal human kidney was used as a control (Fig. III-32, first image in panel A, B and C). Immunohistochemical staining with CD133 showed positive staining for most of the cell types in the kidney including filtration membrane of the glomerulus, the proximal tubule cells and their brush borders as well as the distal tubule cells of the normal human kidney as shown by black arrows (Fig. III-32B, human kidney). Many of the tubules formed by RPTEC/TERT1 and CD133+CD24+ cells stained for CD133, whereas the tubules formed by CD24+ cells were negative for CD133. (Fig. III-32B, left to right). The dark staining in the center of the tubules formed by CD133+CD24+ as well as CD24+ cells is non-specific and

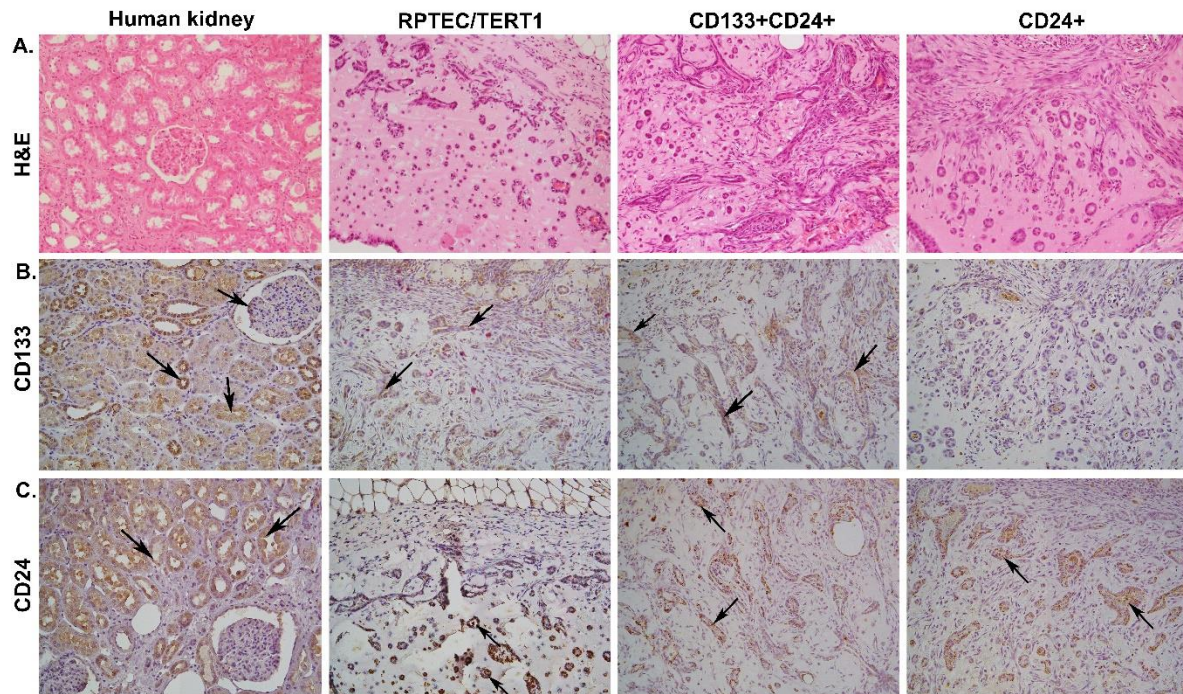


Fig III-32. Immunohistochemical analysis of proximal tubule stem cell markers in subcutaneous nodules formed in immuno-compromised mice. RPTEC/TERT1 cells, CD133+CD24+ cells and CD24+ cells were mixed with matrigel and injected subcutaneously into mice. After 7 days, the nodules were harvested to determine if the cells formed tubular structures and stained to determine the expression of proximal as well as distal tubular markers. A. H&E staining of the normal human kidney and the subcutaneous nodules. Expression of CD24 (B) and CD133 (C). The arrows indicate positive staining as indicated by the brown color.

observed in most of the matrigel sections stained with other antibodies as well. CD24 stained mostly the proximal tubules of the normal human kidney shown by the arrows (Fig. III-32C, human kidney). Most of the cells of the RPTEC/TERT1, CD133+CD24+ and CD24+ tubules stained with CD24 that are shown by the arrows (Fig. III-32 C, left to right).

The normal human kidney and the tubules from all three cell lines were stained with the proximal tubule brush border protein alkaline phosphatase (ALP) and the distal tubule marker calbindin (CAL) (Fig. III-33 A & B). The proximal tubules brush border of the normal kidney showed strong staining for ALP (Fig. III-33 A). The tubules formed by RPTEC/TERT1 and CD24+ cells were strongly stained with ALP whereas the tubules formed by CD133+CD24+ cells stained weakly for ALP (Fig. III-33A). Most of the distal tubules of the normal human kidney showed strong staining for CAL (Fig. III-33B). Most of

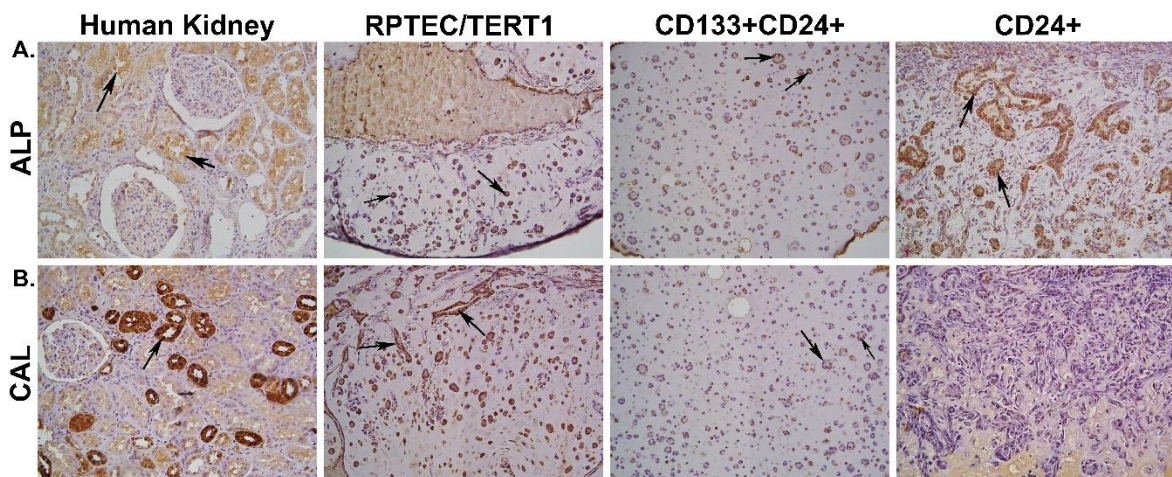


Fig III-33. Immunohistochemical analysis of tubular markers in subcutaneous nodules formed in immuno-compromised mice. Expression of alkaline phosphatase (ALP) (A) and calbindin (CAL) (B) in normal kidney, RPTEC/TERT1, CD133+CD24+ and CD24+ cells (Left to right). The arrows indicate positive staining as indicated by the brown color.

the tubules formed by RPTEC/TERT1 cells showed strong staining for CAL (Fig. III-33B), whereas the tubules formed by CD133+CD24+ cells showed weak staining for CAL. There was no staining for CAL in any of the tubules formed by CD24+ cells except for some non-specific staining seen in the center of the tubules (Fig. III-33B).

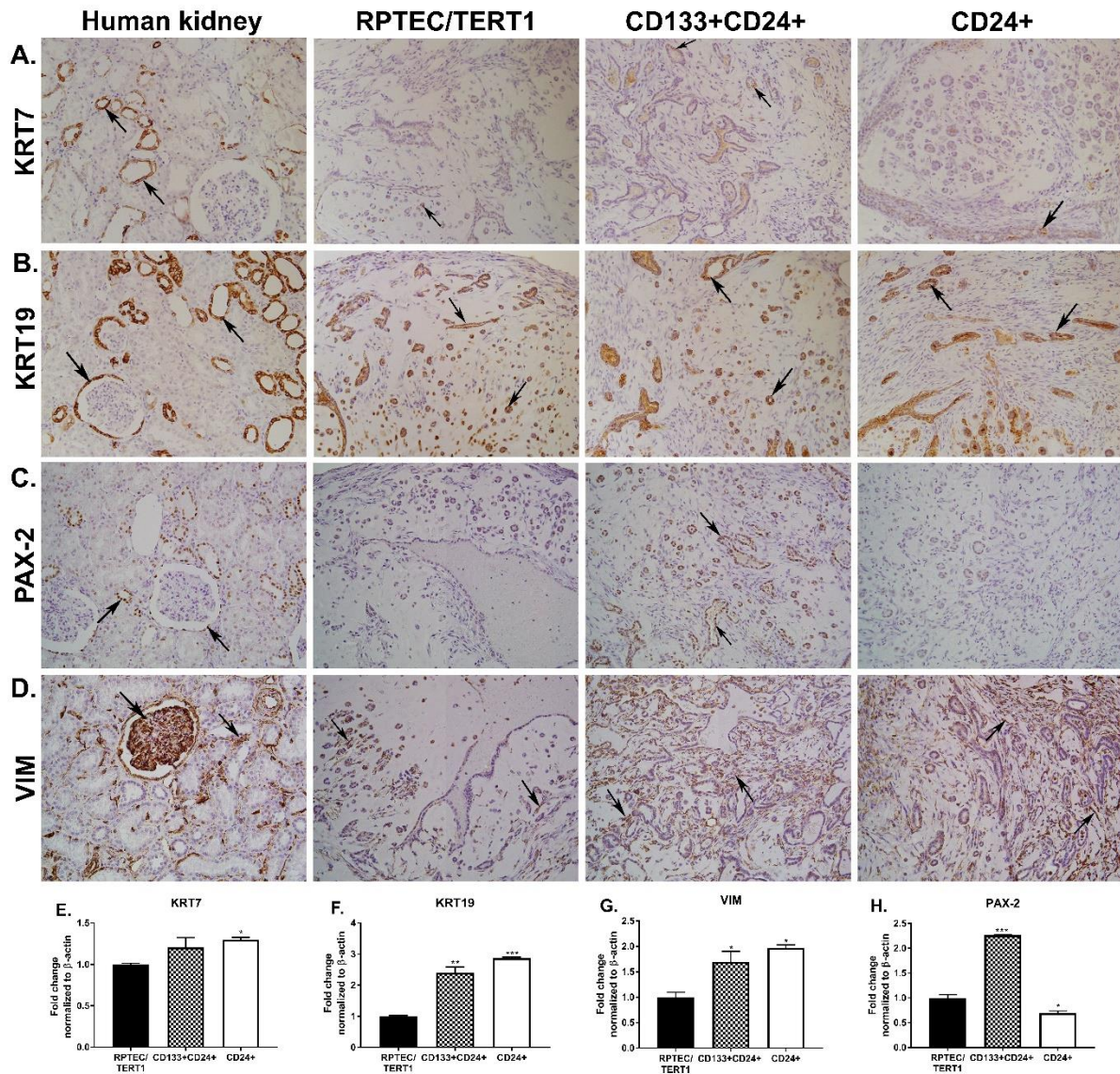


Fig III-34. Immunohistochemical analysis of keratin proteins, filament protein and nephron development marker in subcutaneous nodules formed in immuno-compromised mice. Expression of cytokeratin 7 (KRT7) (A); cytokeratin 19 (KRT19) (B); vimentin (VIM) (C) and paired box-2 (PAX-2) in normal kidney, RPTEC/TERT1, CD133+CD24+ and CD24+ cells (Left to right). The arrows indicate positive staining as indicated by the brown color. Real

time PCR analysis of the expression level of KRT7 (E); KRT19 (F); VIM (G) and PAX-2 (H) in the RPTEC/TERT1 cells, the sorted CD133+CD24+ and the CD24+ cells.

The tubules and the normal human kidney were also stained with epithelial markers cytokeratin proteins 7 & 19 (KRT7 & KRT19), filament protein marker vimentin (VIM) and nephron developmental marker paired box-2 (PAX-2) (Fig. III-34 A-D). mRNA expression levels were also analyzed for each of the genes on RPTEC/TERT1, CD133+CD24+ and CD24+ cell lines (Fig. 34 E-H). Most of the distal as well as some of the proximal tubules of the normal human kidney showed positive staining of KRT7 (Fig III-34 A, human kidney). Few tubules of RPTEC/TERT1, CD133+CD24+ and CD24+ cells showed weak staining for KRT7 (Fig III-34 A). Non-specific staining was observed in the center of the tubular structures formed by CD133+CD24+ cells and CD24+ cells (Fig. III-34A, CD133+CD24+ & CD24+).

There was strong immunostaining for KRT19 in the proximal and distal tubules as well as the bowman's capsule of the human kidney (Fig. III-34 B). The tubules formed by RPTEC/TERT1 cells as well as the CD133+CD24+ and the CD24+ cells showed strong staining for KRT19 (Fig. III-34B, left to right). There was strong staining for PAX2 in the cells of the proximal as well as the distal tubules and the cells of the bowman's capsule of the human kidney (Fig. III-34 C). The tubules formed by the CD133+CD24+ cells showed strong staining for PAX2, whereas the tubules formed by the RPTEC/TERT1 cells and the CD24+ cells showed weak or no staining for PAX2 (Fig. III-34 C). Staining for VIM was mostly seen in the glomeruli, wall of the blood vessels and stroma around the renal tubules (Fig. III-34 D). The tubules formed by RPTEC/TERT1, CD133+CD24+ and CD24+ cells did not show any staining for VIM, however the staining was strong in the spindle shaped cells surrounding the tubules (Fig. III-34 D, left to right). The mRNA levels for KRT7, KRT19, VIM and PAX2

were also determined in RPTEC/TERT1 and CD133+CD24+ and CD24+ cells by real-time PCR and the data is shown in Fig. III-34 E-H. As seen in the Figure III-34 E, the expression of KRT7 was the highest in the CD24+ cells when compared to the CD133+CD24+ cells and the RPTEC/TERT1 cells. The expression of KRT19 was the highest in the CD24+ cells when compared to the RPTEC/TERT1 cells and the CD133+CD24+ cells. The expression of KRT19 was high in the CD133+CD24+ cells when compared to the RPTEC/TERT1 cells, but was lower than the levels seen in the CD24+ cells (Fig. III-34 F). The expression of PAX2 was the highest in the CD133+CD24+ cells when compared to the RPTEC/TERT1 cells, whereas the expression in the CD24+ cells was the lowest when compared to the RPTEC/TERT1 cells and the CD133+CD24+ cells (Fig. III-34 G). The expression of VIM was the highest in the CD24+ cells when compared to the RPTEC/TERT1 cells and the CD133+CD24+ cells (Fig. III-34 H).

CHAPTER IV

DISCUSSION

Characteristic Features of *In-Vitro* Human Proximal Epithelial Cell Culture

Primary cultures of human-derived renal epithelial cells were first isolated and characterized in the middle to late 1980s (Detrisac et al. 1984; Trifillis et al. 1985; Wilson et al. 1985; States et al. 1986; Kempson et al. 1989). The isolation of these cultures from human renal cortical tissue relied on the use of serum-free, hormone-defined cell culture media. This growth media that was developed supports the growth of animal derived immortal cell lines, such as MDCK and LLC-PK1 cells, as well as primary cultures from animal kidneys (Taub et al. 1979; Taub and Sato, 1979, 1980; Chuman et al. 1982; Chung et al. 1982). The human renal cell cultures so derived from these early animal studies were mortal and displayed a limited life span in cell culture of 10 to 20 generations before senescence. During the time these human renal cell cultures were developed, there was an expectation that the site of origin be identified within the human nephron for the studies to undergo publication. This expectation resulted in most of the reports on the isolation of human renal epithelial cells from human cortical tissue to be identified as retaining differentiated features of the human proximal tubule. Many of these observations were consistent among laboratories and included: epithelial morphology; cell polarization; vectorial active transport; enzyme profiles for markers associated with known in situ properties of proximal tubule cells; an increase in cAMP and short circuit current when cells are exposed to parathyroid hormone (PTH) but not

arginine vasopressin (VP); the presence of gap and tight junctions; and, the generation of a transepithelial resistance associated with a “leaky epithelium”. There are also features of these cells that are not consistent with an origin and recapitulation of the properties of the proximal tubule. The major feature of the in situ proximal tubule not recapitulated in any of the reports on human renal cell cultures is a fully developed brush border, a hallmark of the human proximal tubule (Blackburn et al. 1988). While the putative HPT cell cultures do show increased polarity and apical microvilli when grown on permeable supports, there is no evidence of a brush border approaching that found in vivo (Blackburn et al. 1988). Other features of the cultured renal cells not in agreement with in situ properties is an increase in the transepithelial resistance of the cultured cells over that noted for the proximal tubule (Blackburn et al. 1984; Todd et al. 1993). While the transepithelial resistance of the cultured cells is still characteristic of a “leaky epithelium”, it is many fold higher than that measured in situ for the proximal tubule. Last, the expression of E-cadherin in the cultured cells appears to be elevated and N-cadherin reduced compared to that noted for the in situ proximal tubule (Nouwen et al. 1993; Prozialeck et al. 2004; Bathula et al. 2008; Nurnberger et al. 2010; Slusser et al. 2015). Thus, primary cultures derived as described above from human renal cortex retain some, but not all, features of proximal tubule differentiation and will likely continue to be referred to as cultured HPT cells.

The primary cultures of HPT cells are difficult to use as an experimental model to study proximal tubule structure and function. For many laboratories, human cortical tissue is difficult to obtain, and even for those with tissue resources, the tissue is in limited supply. There is also substantial expertise and cost involved in cell isolation and growth. There is also considerable expense in obtaining these cells from commercial sources. These limitations have

led to the wide use of the immortalized HK-2 cell line in research related to defining mechanisms related to human proximal tubule function in health and disease. The HK-2 cell line was derived from a primary HPT cell culture and immortalized by a construct containing HPV16 E6/E7 genes (Ryan et al. 1994). As detailed in the introduction, a major difference between the HK-2 cells and HPT cells is the absence of tight junctions, loss of vectorial transport, and a more mesenchymal morphology compared to the HPT cells. These differences may be important for studies that employ HK-2 cells to study EMT following renal injury (Bathula et al. 2008; Slusser et al. 2014). A second cell line has recently been characterized that is derived from a primary culture of HPT cells and immortalized using a construct containing hTERT (Wieser et al 2008). The morphology of these cultures and the ability to form domes is similar, if not identical to that shown previously for the primary HPT cells (Wieser et al 2008).

Immortalized RPTEC/TERT1 Cells as a Model System to Study Human Proximal Tubule Cells

One of the goals of the present study was to determine how closely related the HK-2 cell line and the RPTEC/TERT1 cell line are to the primary HPT cell culture that was the original source of cells used for immortalization. The results from an analysis of global gene expression patterns clearly demonstrated that the primary HPT cell cultures and the RPTEC/TERT1 cell line are closely related, while the HK-2 cell line was substantially different from both the HPT and RPTEC/TERT1 cells. The number of differentially expressed genes in the HK-2 (in comparison to the HPT cells) was about twenty-fold greater than that of the RPTEC/TERT1 cell line. Six independent isolates, each from a different patient, were used in the current study to cover for possible individual variation in culture properties, both

phenotypic and genetic, and represent the normal variation in gene expression of this cell type in culture. While there is a clear spectrum of gene expression within this group as seen in the principal component as well as the hierarchical clustering, the RPTEC/TERT1 cell line, while very similar in its overall gene expression, was clearly distinct from the HPT cell group, suggesting that there are fundamental gene expression changes in this cell line that sets it apart from cultures of normal HPT cells.

The array data can further be interpreted in the context of the co-expression of CD24 and CD133 being a marker of a human renal progenitor/stem cell for tubule regeneration following injury (Romagnani and Remuzzi 2014; Smeets et al. 2013; Romagnani et al. 2013; Angelotti et al. 2012; Lindgren et al. 2011; Sallustio et al. 2013; Ronconi et al. 2009). If such is true, then the RPTEC/TERT1 cell line presents as a valuable, easy to use, cell culture system that models the cellular component of the renal epithelium that is capable of renal cell regeneration. The fact that approximately 80% of the RPTEC/TERT1 cell population co-expresses CD24 and CD133 is convincing that it can serve to explore the underlying mechanisms involved in this cells ability to regenerate tubular epithelium. The remaining 20% of the RPTEC/TERT1 cells that do not co-express CD24 and CD133 have likely undergone differentiation to another cell lineage. While speculation, this might indicate that cell culture conditions could be identified to differentiate these CD24 and CD133 co-expressing cell into specific cell types. The HK-2 cells demonstrated a very different pattern of CD24 and CD133 expression and only limited identity with both the HPT and RPTEC/TERT1 cell lines. The lower percentage of HK-2 cells co-expressing CD24 and CD133 (21%) may indicate that these are the cells driving proliferation of the culture with the remaining cells having undergone differentiation into another cell lineage. All the HK-2 cells not co-expressing CD24 and CD133

do express CD24. Precisely what tubule type is modeled by the HK-2 cells has not been resolved by this study. The differences between the two cell lines, HK-2 and RPTEC/TERT1, may simply represent what clonal cell was isolated and immortalized from the primary culture of HPT cells. It would have been informative to compare the global gene expression profiles of the 3 cell cultures to that of the in vivo human proximal tubule; however, the authors could not identify the existence of such a study.

One of the main features of the RPTEC/TERT1 cell line that is absent from the HK-2 cells, is the presence of vectorial active transport and the formation of dome structures, a common feature consistently observed in HPT cells. This feature requires the presence of adherens and tight junctions, cell structures that require the expression of cadherins, claudins and occludin proteins. Particularly important is the formation of the tight junction because this structure forms the boundary of two-dimensional diffusion of the apical and basal-lateral plasma membrane, which enables the polar distribution of uptake and efflux transporters (Cao et al., 2012). The current study assessed the expression of many members of these three classes of proteins. Occludin, a mandatory component of the tight junction showed very low levels of expression in the HK-2 cells when compared to the HPT and the RPTEC/TERT1 cells. The adherens junction cadherins (E-, P- and Ksp-cadherin) were either absent or expressed at a very low level in the HK-2 cells when compared to the HPT and the RPTEC/TERT1 cells. This data is in accord with a previous assessment of these proteins and the development of transepithelial resistance in HK-2 and HPT cells (Slusser et al., 2015 and Bathula et al., 2008). In addition to lacking E-cadherin, the HK-2 line highly expressed N-cadherin, a pattern commonly found in cells that have undergone a transition to a more mesenchymal morphology, also known as EMT. This is also reflected in the loss of vectorial

active transport, loss of cell junctions and less polarity. As such, this may render the HK-2 cell line as an appropriate model system for a cell that has undergone part of the process associated with EMT.

Mode of Cell Death after Cadmium Insult in RPTEC/TERT1 Cells

The RPTEC/TERT1 cell line was shown in the current study to exhibit a primarily necrotic mode of cell death in response to lethal levels of Cd^{+2} , whereas the HK-2 cell line exhibited extensive apoptosis during lethal exposures of this metal. Cultures of HPT cells respond primarily via a necrotic mechanism as previously reported by this laboratory (Somji et al., 2004 & 2006). Cd^{+2} is a well-known nephrotoxin and a member of a well-known class of nephrotoxicants that cause acute tubular necrosis (Alpers and Chang, 2015). Many of the early studies of Cd^{+2} -induced nephrotoxicity both in animal models (Cha 1987; Itokawa et al. 1974; Kawamura et al. 1978; Kotsonis and Klaassen 1978; Prigge 1978) and in case reports (Beton et al., 1966; Chugh et al., 1994), describe necrosis as the morphologically discernable form of cell death (ATSDR 2012). The literature has been replete with studies characterizing the apoptotic mode of cell death in Cd^{+2} -induced nephrotoxicity (Fujiwara et al, 2012, Prozialek et al., 2012), but clearly, necrosis is the predominant mode of cell death during acute exposure and this is similar to that of many acutely toxic nephrotoxins (Sharfuddin et al, 2016) with apoptosis being a contributing component. It is noteworthy that at lower doses of Cd^{+2} that cause low amounts of proximal tubule cell death, apoptosis can predominate (Prozialek et al., 2009, Templeton and Liu, 2010). With the new advancements in the area of programmed cell death, particularly necroptosis, the current study underscores the need for the proper application of an in vitro model system to investigate the mechanism of the different modes of cell death.

Overall, the present study provides evidence that the RPTEC/TERT1 cell line could be a valuable model system to determine the effects that nephrotoxins might have on the regenerative capability of tubular epithelium.

Expression of CD133 and CD24 Markers in Primary Human Proximal Tubule Cultures

The recent studies defining the progenitor/stem cells of the human kidney impacts on the understanding of the origins of these primary cultures of HPT cells. As detailed in the introduction, in the human kidney the renal epithelial cells capable of regeneration following renal injury are sparsely scattered throughout the kidney cortex and are characterized by the co-expression of CD24 and CD133. The finding that approximately 62 percent of HPT cells co-express CD24 and CD133 suggests that the origin of the majority of these cells are ones that are capable of regenerating the renal tubule cells. The data also showed that the cells not co-expressing CD24 and CD133 do continue to express CD24, in line with studies showing that CD133+ cells are a subset of CD24 expressing renal epithelial cells (Romagnani and Remuzzi, 2014). Taken together, these observations would suggest that the HPT cells that co-express CD24 and CD133 are those cells in the culture that are capable of sustaining growth of the cell culture. If the CD24+CD133+ are the cells sustaining growth of the cell culture, then it is likely that the CD24 expressing cells that do not express CD133 have undergone senescence or have undergone differentiation.

Characterization of CD133+CD24+ and CD24+ Cells isolated from RPTEC/TERT1 Cells

CD133+CD24+ as well as CD24+ cell population isolated from RPTEC/TERT1 show high stability and purity upon sub-culture. Real time PCR and confocal staining analysis for CD133 and CD24 markers in CD133+CD24+ and CD24+ cells confirmed our observation that

the CD24+ cells did not express CD133. Morphologically, both of the cell population show dome formation in culture indicating vectorial active transport functions. Transepithelial electrical resistance (TEER) is the measurement of the electrical resistance across a cellular monolayer and is a sensitive method to confirm the integrity and permeability of the cellular membrane. These measurements were performed on the RPTEC/TERT1 cells as well as the double positive CD133CD24 cells and the single positive CD24 cells, and it was found that the resistance of the CD133+CD24+ cells was higher than the CD24+ cells and the RPTEC/TERT1 cells, but was in the range of values seen for proximal tubule cells in culture. The doubling time for the various cell lines were also determined and the results showed that the CD133+CD24+ cells grow significantly faster compared to the CD24+ cells. In addition, the expression of Ki67, a proliferation and cell cycle marker was evaluated in all three cell lines and the results showed higher Ki67 expression in CD133+CD24+ cells compared to CD24+. Thus the data shows that the CD133+CD24+ cells grow and self-renew at a faster rate compared to the CD24+ cells. One of the characteristics of the stemness of stem/progenitor cells is the ability to grow in an anchorage independent condition and form spheroids in suspension. When the sorted CD133+CD24+ and CD24+ cells were tested to evaluate their capability to form spheroids in low attachment flasks, the CD133+CD24+ formed spheroids from single cells however CD24+ were found to remain as single cells. The ability of CD133+CD24+ to form spheroids confirms its ability to self-renew. Previous studies have shown that the spheroids grown from human kidney epithelial cells that are positive for proximal tubule markers like LTA and AQP-1, expressed higher levels of CD133, CD24, CD44 and ALDH (Buzhor et al. 2011). Thus, our data suggests that the CD133+CD24+ cells

have stem cell characteristics whereas the CD24+ cells are the differentiated cells that may not have the ability to self-renew itself.

Proximal tubule marker, AQP-1 and distal tubule marker, CAL expression was assessed with using qPCR and confocal analysis in RPTEC/TERT1, CD133+CD24+ and CD24+ cells. The results showed that AQP-1 was expressed in all three cell lines however CAL was strongly expressed only in CD133+CD24+ cells, which suggest that the CD133+CD24+ cell population is capable of generating heterogeneous cell types of the kidney. In the current study, we only assessed the expression of AQP-1 and CAL, which are markers for the proximal and distal tubules respectively and markers for other cell types of the kidney such as glomerulus and collecting duct were not assessed. Previous studies performed on frozen human kidney sections (Angelotti M.L et al. 2012) have shown that the majority of the cells that co-express CD133 and CD24 and are localized in the proximal tubules also express AQP-1, suggesting that these cells eventually give rise to the differentiated cells of the proximal tubules.

Exposure to Cadmium decreases CD24+ Cell Population while increases CD133+CD24+ Cell Population

The effect of Cd²⁺ on the proliferative and regeneration ability of RPTEC/TERT1, CD133+CD24+ and CD24+ cells was also determined. The obtained results showed that CD133+CD24+ cells increased their cell number after they were exposed to 4.5 and 9.0 µM Cd²⁺ at each exposure time-period. However, the number of CD24+ cells decreased after exposure to 4.5 and 9.0 µM Cd²⁺. Since none of the doses of Cd²⁺ caused toxicity to the various cell types, the decrease in the number of CD24+ cells could be due to loss in proliferative capacity. CD133+CD24+ cells are considered as putative stem/progenitor cells which have the

ability to proliferate and regenerate, whereas CD24⁺ cells are considered the differentiated cell type that lacks regenerative capacity. Thus in our model system, CD133⁺CD24⁺ cells isolated from RPTEC/TERT1 cell line display stem like features. Previous studies done by Bussolati et al. have shown that CD133⁺ cells isolated from the adult human kidney, when injected intravenously into mice suffering from acute renal injury could home to the injured kidney and give rise to proximal as well as distal tubule cells. Thus, this study supports our results which suggest that CD133⁺CD24⁺ cells have progenitor/ stem cell like characteristics with proliferative and regenerative capability.

Higher susceptible of CD24⁺ to cell loss after cadmium treatment in CD24⁺ cells and resistance of CD133⁺CD24⁺ cells to toxic effects of cadmium may also indicate the possibility of role of cadmium binding metals proteins such as metallothioneins in susceptibility of cells to cadmium toxicity. As mentioned earlier cadmium targets and is accumulated primarily in kidney as well as liver. Previous studies have shown that Cd²⁺ binds to sulfhydryl groups in metallothionein proteins and helps in lowering the concentration of free cadmium ions resulting in resistance to cadmium toxicity in kidney (Faroon O. et al. 2012). Our laboratory has previously shown that the in situ proximal tubule as well as HPT cultures have high basal levels of MT-3 RNA (Kim D. et al. 2002). Thus it is possible that RPTEC/TERT1 cells also express high basal levels of MT-3 and the levels of metallothioneins in CD133⁺CD24⁺ cells are higher than CD24⁺ cells, thus rendering them more resistant to the toxic effects of Cd²⁺ thus increasing their proliferative capacity in presence of a toxic agent. Thus, in the future studies need to be performed to determine the levels of various metallothionein isoforms in the various cell populations isolated from RPTEC/TERT1 cells to determine if metallothioneins have a role on providing resistance to the cells.

Ki67 Expression in Cultured RPTEC/TERT1 after Cadmium Insult

Ki67 is a nuclear protein that is present in mid G1, S, G2 and the entire M phase of the cell cycle, and serves as a marker for cell proliferation and is used to determine cell growth. In this study, the levels of Ki67 were determined in RPTEC/TERT1 cells after exposure to various concentrations of cadmium. The data obtained did not show a change in the levels of the Ki67 protein when compared to the untreated control samples. Since these experiments were performed at confluency, it is possible that the cells were contact inhibited and were not growing and proliferating, therefore there was no change in the levels of Ki67. Previous studies performed by Smeets et al. have shown that CD24+ which co-express CD133 and vimentin are the major proliferating cells found in the human kidney. In their study, the normal human kidney sections showed that CD24+ cells in proximal tubule were less differentiated, showed less cytoplasm, fewer mitochondria, lack of basolateral invagination and lack of mature brush borders (B. Smeets et al. 2013). The study also suggested that CD24+ cells that co-express CD133 and vimentin are the major proliferating cells that may be involved in regeneration of the injured tubular cells. The study came to this conclusion by evaluating the expression of proliferation marker, Ki67 in the patient biopsies with acute kidney injury (B. Smeets et al. 2013). Future studies will need to be performed to determine the proliferative capacity of RPTEC/TERT1, CD133+CD24+ and CD24+ cells when exposed to toxic insult such as cadmium.

Demonstration of the ability of various populations of cells to form tubular structures in-vitro and in-vivo

Surface markers are one of the powerful biological molecules that can be utilized to identify and isolate adult stem/progenitor cells. However, it is important to evaluate the functional properties of stem cells such as self-renewal and ability to differentiate into different cell types. Formation of spheroids from single cells is one of the methods to assess the self-renewal capabilities; however, it is also required to know if the spheres formed can be propagated for multiple passages after dissociating individual cells that form the spheroids. RPTEC/TERT1, CD133+CD24+ and HPT cells were able to form spheroids when cultured in low adherence conditions. Dissociation of cells forming the spheroids is challenging and depends upon the cell types used in the study. In our study, we were unable to dissociate the spheroids using multiple dissociating reagents such as trypsin, accutase and the chelating agents like EDTA. However, we were able to sub-culture the spheroids three times suggesting that they do have self-renewing capabilities.

Another major characteristic feature of a committed adult stem/progenitor cell is to differentiate into different cell types present in an organ or a tissue from which they were isolated. Therefore, in order to examine this property, the stem cells can be grown in extracellular matrix proteins like collagen and matrigel to monitor growth of three-dimensional structures. By culturing cells in thin matrigel coated wells, RPTEC/TERT1 and CD133+CD24+ cells formed spherical and cylindrical structures whereas the HPT cells and the CD24+ cells were unable to form these structures. Previous studies performed by Bussolati et al. have shown that CD133+ cells isolated from the cortex of human kidney could form similar structures. In a study done by Bombelli et al., epithelial cells isolated from the dissociated kidney tissue could form nephrospheres. In order to isolate and identify the stem cells within the nephrospheres, Bombelli et al. labelled the epithelial cells with the fluorescent

dye PKH26. This dye binds to the phospholipid membrane and is diluted as the cells divide. The authors found that within the nephrospheres, very few cells retained the epifluorescence suggesting that within the nephrospheres there are very few quiescent cells that possess stem cell properties and are needed to maintain the nephrosphere culture.

They found that the PKH^{high} nephrospheres contain cells that were quiescent/ slow-replicating cells and sorted based on spheres that expressed high PKH fluorescence height. They also showed that PKH^{high} cells express both CD133 as well as CD24 markers. PKH^{high}CD133+CD24+ spheres were sorted and assessed for their capabilities to differentiate along multiple lineage. Those spheres that were cultured as a monolayer were reported to stain with proximal tubule marker, CD13 as well as distal tubule marker, CAL. In addition, PKH^{high} spheres were assessed for their ability to generate 3-D structures by culturing in matrigel. The spheres were observed to form spherical and tubular like structures in the matrigel set up and stained positive for proximal tubule markers, CD10 and CK7. Thus these studies, similar to what has been observed in our studies suggest that the CD133+CD24+ cells can give rise to different cell types present in the kidney.

In this study, the expression of tubular markers was determined in all the three cell lines grown *in-vitro* as well as *in-vivo*. The RPTEC/TERT1 cells only expressed AQP-1, whereas the CD133+CD24+ cells expressed both AQP-1 as well as CAL, thus suggesting that this cell type could give rise to both the proximal as well as the distal tubules. The CD24+ cells only expressed AQP-1 suggesting that they may be the differentiated proximal tubule cells. In addition, we also evaluated the ability of RPTEC/TERT1, CD133+CD24+ and CD24+ cells to form tubular structures *in-vivo* when injected with matrigel subcutaneously into immune compromised mice. Furthermore, the expression of various tubular markers was assessed by

immunohistochemistry. All the three isolates were able to form tubular structures of various sizes 6 days post-injection. The tubular structures formed by all the three cell lines stained for cytokeratins using the CK AE1/AE3 antibody that recognizes keratins belonging to the acidic as well as basic family thus confirming their epithelial origin. The lack of staining by VIM in the tubular structures reinforced the epithelial origin of the tubular structures. The staining of the tubules formed by CD133+CD24+ cells for ALP (a proximal tubule brush border enzyme) and CAL (a distal tubule marker) further confirms that these double positive cells can give rise to different cell types of the kidney. The tubules formed by the CD24+ cells only stained for ALP suggesting that they may have proximal tubule characteristics. The expression of PAX2, a nephron development marker was only seen in the tubules formed by CD133+CD24+ cells. PAX2, a transcription factor is important for kidney development but is also found in the medulla and collecting ducts of the adult, but its expression is low in the cortex (Cai Q et al. 2005).

From the study performed by Bombelli S. et al., the nephrospheres generated from the primary renal tubular epithelial cells when implanted in the renal capsule of the kidney was capable of generating tubular-like structures that stained positive for cytokeratin 18 and E cadherin proteins. In this current study, spheroid cultures obtained from the CD133+CD24+ cells have not yet been characterized and analyzed for expression of tubular, epithelial/mesenchymal or stem/progenitor like markers. Renal capsule implantation or subcutaneous injection of spheroid into the nude mice using CD133+CD24+ spheroids have also not yet been assessed. Further investigation is anticipated to characterize the spheroid cultures formed from RPTEC/TERT1, CD133+CD24+ and CD24+ cells which will give deeper insights on the proliferative and multipotent nature of the spheroids. Bussolati et al.

performed a similar study where they injected CD133+ cells mixed with matrigel into nude mice. The tubular structures that were formed stained for both proximal as well as distal tubular markers conforming the stem/progenitor characteristics of CD133+ cells. Therefore based on the data published by other groups and the current data produced in this study, CD133+CD24+ cells possess stem/progenitor like features which is characterized by their ability to form self renewing spheroids cells and generate differentiated tubular like structures capable of producing distal as well as proximal cell types of the kidney. Further investigation is required to study the possibilities of these cells to differentiate into tubular structures when transplanted under the renal capsule of the nude mice, which would provide further evidence of their multipotent nature thus giving rise to various cell types of the kidney.

REFERENCES

- Akesson, A., Lundh, T., Vahter, M., Bjellerup, P., Lidfeldt, J., Nerbrand, C., Samsioe, G., Stromberg, U., Skerfving, S. 2005. Tubular and glomerular kidney effects in Swedish women with low environmental cadmium exposure. *Environ. Health. Perspect.* 113(11), 627-631.
- Alpers, C.E., Chang, A. 2015. The Kidney, in: Kumar, V., Abbas, Abul K., Aster, Jon C. (Eds), *Robbins & Cotran Pathologic Basis of Disease.* Elsevier, Philadelphia, PA, pp. 897-957
- Angelotti ML, et al. (2012) Characterization of renal progenitors committed toward tubular lineage and their regenerative potential in renal tubular injury. *Stem Cells* 30(8):1714–1725.
- Aschauer L, Gruber LN, Pfaller W, Limonciel A, Athersuch TJ, Cavill R, Khan A, Gstraunthaler G, Grillari J, Grillari R, Hewitt P, Leonard MO, Wilmes A, Jennings P. Delineation of the key aspects in the regulation of epithelial monolayer formation. *Mol Cell Biol.* 2013 Jul;33(13):2535-50.
- ATSDR. Agency for Toxic Substances and Disease Registry. 2012. Toxicological Profile for Cadmium. US Department of Health and Human Services, Public Health Services.
- Bathula CS, Garrett SH, Zhou XD, Sens MA, Sens DA, Somji S. Cadmium, vectorial active transport, and MT-3-dependent regulation of cadherin expression in human proximal tubular cells. *Toxicol Sci.* 2008 Apr;102(2):310-8.
- Beton, D.C., Andrews, G.S., Davies, H.J., Howells, L., Smith, G.F. 1966. Acute Cadmium Fume Poisoning: Five Cases with one Death from Renal Necrosis. *Br. J. Ind. Med.* 23(4), 293-301.
- Blackburn, J.G., Hazen-Martin, D.J., Detrisac, C.J., Sens, D.A. 1988. Electrophysiology and ultrastructure of cultured human proximal tubule cells. *Kidney. Int.* 33(2), 508-516.
- Bombelli S, Meregalli C, Scalia C, Bovo G, Torsello B, De Marco S, Cadamuro M, Viganò P, Strada G, Cattoretti G, Bianchi C, Perego RA. Nephrosphere-Derived Cells Are Induced to Multilineage Differentiation when Cultured on Human Decellularized Kidney Scaffolds. *Am J Pathol.* 2018 Jan;188(1):184-195.
- Bonventre JV. Dedifferentiation and proliferation of surviving epithelial cells in acute renal failure. *J Am Soc Nephrol.* 2003 Jun;14 Suppl 1:S55-61.

Buser MC, Ingber SZ, Raines N, Fowler DA, Scinicariello F. Urinary and blood cadmium and lead and kidney function: NHANES 2007-2012. *Int J Hyg Environ Health*. 2016 May;219(3):261-7.

Bussolati B, Hauser PV, Carvalhosa R, Camussi G. Contribution of stem cells to kidney repair. *Curr Stem Cell Res Ther*. 2009 Jan;4(1):2-8.

Bussolati, B., Bruno, S., Grange, C., Buttiglieri, S., Deregibus, M. C., Cantino, D., & Camussi, G. (2005). Isolation of Renal Progenitor Cells from Adult Human Kidney. *The American Journal of Pathology*, 166(2), 545–555.

Buzhor E, Harari-Steinberg O, Omer D, Metsuyanin S, Jacob-Hirsch J, Noiman T, Dotan Z, Goldstein RS, Dekel B. Kidney spheroids recapitulate tubular organoids leading to enhanced tubulogenic potency of human kidney-derived cells. *Tissue Eng Part A*. 2011 Sep;17(17-18):2305-1hargui A, Zekri S, Jacquillet G, Rubera I, Ilie M, Belaid A, Duranton C, Tauc M, Hofman P, Poujeol P, El May MV, Mograbi B. Cadmium-induced autophagy in rat kidney: an early biomarker of subtoxic exposure. *Toxicol Sci*. 2011 May;121(1):31-42.

Cai Q, Dmitrieva NI, Ferraris JD, Brooks HL, van Balkom BW, Burg M. Pax2 expression occurs in renal medullary epithelial cells in vivo and in cell culture, is osmoregulated, and promotes osmotic tolerance. *Proc Natl Acad Sci U S A*. 2005 Jan 11;102(2):503-8.

Cao, X., Yang, Q., Qin, J., Zhao, S., Li, X., Fan, J., Chen, W., Zhou, Y., Mao, H., Yu, X. 2012. V-ATPase promotes transforming growth factor- β -induced epithelial-mesenchymal transition of rat proximal tubular epithelial cells. *Am. J. Physiol. Renal Physiol*. 302(9), F1121-F1132.

Cha, C.W. 1987. A study on the effect of garlic to the heavy metal poisoning of rat. *J. Korean. Med. Sci*. 2, 213-224.

Chevalier RL. The proximal tubule is the primary target of injury and progression of kidney disease: role of the glomerulotubular junction. *Am J Physiol Renal Physiol*. 2016 Jul 1;311(1):F145-61.

Chou YH, Pan SY, Yang CH, Lin SL. Stem cells and kidney regeneration. *J Formos Med Assoc*. 2014 Apr;113(4):201-9.

Chugh, K.S., Jha, V., Sakhuja, V., Joshi, K. 1994. Acute renal cortical necrosis-a study of 113 patients. *Ren. Fail*. 16(1), 23-47.

Chuman, L., Fine, L.G., Cohen, A.H., Saier, M.H. Jr. 1982. Continuous growth of proximal tubular kidney epithelial cells in hormone-supplemented serum-free medium. *J. Cell. Biol*. 94(3), 506-510.

Chung, S.D., Alavi, N., Livingston, D., Hiller, S., Taub, M. 1982. Characterization of primary rabbit kidney cultures that express proximal tubule functions in a hormonally defined medium. *J. Cell. Biol*. 95(1), 118-126.

Contribution of stem cells to kidney repair. Bussolati B1, Hauser PV, Carvalhosa R, Camussi G. *Curr Stem Cell Res Ther*. 2009 Jan;4(1):2-8.

Crean D, Bellwon P, Aschauer L, Limonciel A, Moenks K, Hewitt P, Schmidt T, Herrgen K, Dekant W, Lukas A, Bois F, Wilmes A, Jennings P, Leonard MO. Development of an in vitro renal epithelial disease state model for xenobiotic toxicity testing. *Toxicol In Vitro*. 2015 Dec 25;30(1 Pt A):128-37.

Detrisac CJ, Sens MA, Garvin AJ, Spicer SS, Sens DA. Tissue culture of human kidney epithelial cells of proximal tubule origin. *Kidney Int*. 1984 Feb;25(2):383-90.

Duffield JS, Park KM, Hsiao LL, Kelley VR, Scadden DT, Ichimura T, Bonventre JV. Restoration of tubular epithelial cells during repair of the postischemic kidney occurs independently of bone marrow-derived stem cells. *J Clin Invest*. 2005 Jul;115(7):1743-55.

Faroon O, Ashizawa A, Wright S, Tucker P, Jenkins K, Ingerman L, Rudisill C. Toxicological Profile for Cadmium. Atlanta (GA): Agency for Toxic Substances and Disease Registry (US); 2012 Sep. PubMed PMID: 24049863.

Ferraro, P.M., Costanzi, S., Naticchia, A., Sturniolo, A., Gambaro, G. 2010. Low level exposure to cadmium increases the risk of chronic kidney disease: analysis of the NHANES 1999-2006. *BMC Public Health*. 10, 304.

Fujiwara, Y., Lee, J.Y., Tokumotot, M., Satosh, M. 2012. Cadmium renal toxicity via apoptotic pathways. *Biol. Pharm. Bull*. 35(11), 1892-1897.

Garrett SH, Somji S, Sens MA, Zhang K, Sens DA. Microarray analysis of gene expression patterns in human proximal tubule cells over a short and long time course of cadmium exposure. *J Toxicol Environ Health A*. 2011;74(1):24-42.

Garrett, S.H., Somji, S., Todd, J.H., Sens, D.A. 1998. Exposure of human proximal tubule cells to cd^{2+} , zn^{2+} , and Cu^{2+} induces metallothionein protein accumulation but not metallothionein isoform 2 mRNA. *Environ. Health. Perspect*. 106(9), 587-95.

Gilbert RE. Proximal Tubulopathy: Prime Mover and Key Therapeutic Target in Diabetic Kidney Disease. *Diabetes*. 2017 Apr;66(4):791-800.

Greider, C. W. (1990), Telomeres, telomerase and senescence. *Bioessays*, 12: 363-369. doi:10.1002/bies.950120803

He L, Wang B, Hay EB, Nebert DW. Discovery of ZIP transporters that participate in cadmium damage to testis and kidney. *Toxicol Appl Pharmacol*. 2009 Aug 1;238(3):250-7.

Hodgson, Ernest. A textbook of modern toxicology. Appleton & Lange, 1987. Print.

Hoppensack, A., Kazanecki, C. C., Colter, D., Gosiewska, A., Schanz, J., Walles, H., & Schenke-Layland, K. (2014). A Human In Vitro Model That Mimics the Renal Proximal Tubule. *Tissue Engineering. Part C, Methods*, 20(7), 599–609.

Humphreys BD, Valerius MT, Kobayashi A, Mugford JW, Soeung S, Duffield JS, McMahon AP, Bonventre JV. Intrinsic epithelial cells repair the kidney after injury. *Cell Stem Cell*. 2008 Mar 6;2(3):284-91.

Itokawa, Y., Abe, T., Tabei, R., Tanaka, S. 1974. Renal and skeletal lesions in experimental cadmium poisoning. *Arch. Environ. Health*. 28, 149-154.

Järup L. Cadmium overload and toxicity. *Nephrol Dial Transplant*. 2002;17 Suppl 2:35-9.

Juan A. Oliver and Qais Al-Awqati. 2013. Stem Cells and Generation of New Cells in the Adult Kidney In Seldin and Giebisch's (5th edition), *The Kidney* (pp. 959-980). Retrieved from elsevierdirect.com

Kawamura, J., Yoshida, O., Nishino, K., Itokawa, Y. 1978. Disturbances in kidney functions and calcium and phosphate metabolism in cadmium-poisoned rats. *Nephron*. 20, 101-110.

Kempson, S.A., McAteer, J.A., Al-Mahrouq, H.A., Dousa, T.P., Dougherty, G.S., Evan, A.P. 1989. Proximal tubule characteristics of cultured human renal cortex epithelium. *J. Lab. Clin. Med*. 113, 285-296

Kim D, Garrett SH, Sens MA, Somji S, Sens DA. Metallothionein isoform 3 and proximal tubule vectorial active transport. *Kidney Int*. 2002 Feb;61(2):464-72.

Kim K, et al. (2011) Expression of stem cell marker CD133 in fetal and adult human kidneys and pauci-immune crescentic glomerulonephritis. *Histol Histopathol* 26(2):223–232.

Kotsonis, F.N., Klaassen, C.D. 1978. The relationship of metallothionein to the toxicity of cadmium after prolonged administration to rats. *Toxicol. Appl. Pharmacol*. 46, 39-54.

Lasagni, L., Serio, M., Romagnani, S., Romagnani, P. 2006. Isolation and characterization of multipotent progenitor cells from the Bowman's capsule of adult human kidney. *J. Am. Soc. Nephrol*. 17, 2443-2456.

Lazzeri, E., Crescioli, C., Ronconi, E., Mazzinghi, B., Sagrinati, C., Netti, G.S., Angelotti, M.L., Parente, E., Ballerini, L., Cosmi, L., Maggi, L., Gesualdo, L., Rotondi, M., Annunziato, F., Maggi, E., Lasagni, L., Serio, M., Romagnani, S., Vannelli, G.B., Romagnani, P. 2007. Regenerative potential of embryonic renal multipotent progenitors in acute renal failure. *J. Am. Soc. Nephrol*. 18(12), 3128-3138.

Lee, K. M., Choi, K. H., & Ouellette, M. M. (2004). Use of exogenous hTERT to immortalize primary human cells . *Cytotechnology*, 45(1-2), 33–38.

Lin F, Moran A, Igarashi P. Intrarenal cells, not bone marrow-derived cells, are the major source for regeneration in postischemic kidney. *J Clin Invest*. 2005 Jul;115(7):1756-64.

Lindgren D, Boström AK, Nilsson K, Hansson J, Sjölund J, Möller C, Jirström K, Nilsson E, Landberg G, Axelson H, Johansson ME. Isolation and characterization of progenitor-like cells from human renal proximal tubules. *Am J Pathol*. 2011 Feb;178(2):828-37.

- Liu J, Qu W, Kadiiska MB. Role of oxidative stress in cadmium toxicity and carcinogenesis. *Toxicol Appl Pharmacol.* 2009 Aug 1;238(3):209-14.
- Lombardi D, Becherucci F, Romagnani P. How much can the tubule regenerate and who does it? An open question. *Nephrol Dial Transplant.* 2016 Aug;31(8):1243-50.
- Loverre A, Capobianco C, Ditunno P, Battaglia M, Grandaliano G, Schena FP. Increase of proliferating renal progenitor cells in acute tubular necrosis underlying delayed graft function. *Transplantation.* 2008 Apr 27;85(8):1112-9.
- Lundberg AS, Hahn WC, Gupta P, Weinberg RA. Genes involved in senescence and immortalization. *Curr Opin Cell Biol.* 2000 Dec;12(6):705-9.
- Mandel L.J., and Balaban R.S. Stoichiometry and coupling of active transport to oxidative metabolism in epithelial tissues. *Am J Physiol* 1981; 240: pp. F357-F371
- Matlin K.S. & Caplan M.J. 2013. Epithelial Cell Structure and Polarity In Seldin and Giebisch's (5th edition), *The Kidney* (pp. 3-43). Retrieved from elsevierdirect.com
- McKee C, Chaudhry GR. Advances and challenges in stem cell culture. *Colloids Surf B Biointerfaces.* 2017 Nov 1;159:62-77.
- Misfeldt D.S., Hamamoto S.T., and Pitelka D.R.: Transepithelial transport in cell culture. *Proc Natl Acad Sci USA* 1976; 73: pp. 1212-1216
- Navas-Acien, A., Tellez-Plaza, M., Guallar, E., Muntner, P., Silbergeld, E., Jaar, B., Weaver, V. 2009. Blood cadmium and lead and chronic kidney disease in US adults: a joint analysis. *Am. J. Epidemiol.* 170, 1156-1164.
- Nouwen, E.J., Dauwe, S., van der Biest, I., De Broe, M.E. 1993. Stage- and segment-specific expression of cell adhesion molecules N-CAM, A-CAM, and L-Cam in the kidney. *Kidney Int.* 44(1), 147-158.
- Nürnbergger, J., Feldkamp, T., Kavapurackal, R., Opazo Saez, A., Becker, J., Hörbelt, M., Kribben, A. 2010. N-cadherin is depleted from proximal tubules in experimental and human acute kidney injury. *Histochem. Cell. Biol.* 133(6), 641-649.
- Peres LC, Sethuraman C, Al-Adnani M, Cohen MC. Necrotic epithelial cells in proximal renal tubules of 2nd trimester fetuses: is this "acute tubular necrosis"? *Int J Clin Exp Pathol.* 2012;5(4):326-30.
- Prigge, E. 1978. Early signs of oral and inhalative cadmium uptake in rats. *Arch. Toxicol.* 40, 231-247.
- Prozialeck WC, Edwards JR. Early biomarkers of cadmium exposure and nephrotoxicity. *Biometals.* 2010 Oct;23(5):793-809.

Prozialeck WC, Edwards JR. Mechanisms of cadmium-induced proximal tubule injury: new insights with implications for biomonitoring and therapeutic interventions. *J Pharmacol Exp Ther.* 2012 Oct;343(1):2-12.

Prozialeck WC, Niewenhuis RJ. Cadmium (Cd²⁺) disrupts Ca(2+)-dependent cell-cell junctions and alters the pattern of E-cadherin immunofluorescence in LLC-PK1 cells. *Biochem Biophys Res Commun.* 1991 Dec 31;181(3):1118-24.

Prozialeck WC, Vaidya VS, Liu J, Waalkes MP, Edwards JR, Lamar PC, Bernard AM, Dumont X, Bonventre JV. Kidney injury molecule-1 is an early biomarker of cadmium nephrotoxicity. *Kidney Int.* 2007 Oct;72(8):985-93.

Racusen L. Chronic transplant glomerulopathy: need for further assessment. *Clin J Am Soc Nephrol.* 2007 Nov;2(6):1108-9.

Romagnania P. and Remuzzi G. 2014. CD133+ renal stem cells always co-express CD24 in adult human kidney tissue. *Stem cell research*, ISSN: 1876-7753, Vol: 12, Issue: 3, Page: 828-9

Rosen S, Stillman IE. Acute tubular necrosis is a syndrome of physiologic and pathologic dissociation. *J Am Soc Nephrol.* 2008 May;19(5):871-5.

Ryan MJ, Johnson G, Kirk J, Fuerstenberg SM, Zager RA, Torok-Storb B. HK-2: an immortalized proximal tubule epithelial cell line from normal adult human kidney. *Kidney Int.* 1994 Jan;45(1):48-57.

Sagrinati, C., Netti, G.S., Mazzinghi, B., Lazzeri, E., Liotta, F., Frosali, F., Ronconi, E., Meini, C., Gacci, M., Squecco, R., Carini, M., Gesualdo, L., Francini, F., Maggi, E., Annunziato, F., Sallustio, F., Costantino, V., Cox, S.N., Loverre, A., Divella, C., Rizzi, M., Schena, F.P. 2013. Human renal stem/progenitor cells repair tubular epithelial cell injury through TLR2-driven inhibin-A and microvesicle-shuttled decorin. *Kidney. Int.* 83, 392-403.

Satarug S, Moore MR. Adverse health effects of chronic exposure to low-level cadmium in foodstuffs and cigarette smoke. *Environ Health Perspect.* 2004 Jul;112(10):1099-103.

Scholzen T, Gerdes J. The Ki-67 protein: from the known and the unknown. *J Cell Physiol.* 2000 Mar;182(3):311-22.

Shrestha S, Somji S, Sens DA, Slusser-Nore A, Patel DH, Savage E, Garrett SH. Human renal tubular cells contain CD24/CD133 progenitor cell populations: Implications for tubular regeneration after toxicant induced damage using cadmium as a model. *Toxicol Appl Pharmacol.* 2017 Sep 15;331:116-129.

Simon BR, Wilson MJ, Blake DA, Yu H, Wickliffe JK. Cadmium alters the formation of benzo[a]pyrene DNA adducts in the RPTEC/TERT1 human renal proximal tubule epithelial cell line. *Toxicol Rep.* 2014 Jul 14;1:391-400.

Simon BR, Wilson MJ, Wickliffe JK. The RPTEC/TERT1 cell line models key renal cell responses to the environmental toxicants, benzo[a]pyrene and cadmium. *Toxicol Rep.* 2014;1:231-242.

Slusser A, Bathula CS, Sens DA, Somji S, Sens MA, Zhou XD, Garrett SH. Cadherin expression, vectorial active transport, and metallothionein isoform 3 mediated EMT/MET responses in cultured primary and immortalized human proximal tubule cells. *PLoS One.* 2015 Mar 24;10(3)

Smeets B, Boor P, Dijkman H, Sharma SV, Jirak P, Mooren F, Berger K, Bornemann J, Gelman IH, Floege J, van der Vlag J, Wetzels JF, Moeller MJ. Proximal tubular cells contain a phenotypically distinct, scattered cell population involved in tubular regeneration. *J Pathol.* 2013 Apr;229(5):645-59.

Smeets, B. , Boor, P. , Dijkman, H. , Sharma, S. V., Jirak, P. , Mooren, F. , Berger, K. , Bornemann, J. , Gelman, I. H., Floege, J. , van der Vlag, J. , Wetzels, J. F. and Moeller, M. J. (2013), Proximal tubular cells contain a phenotypically distinct, scattered cell population involved in tubular regeneration. *J. Pathol.*, 229: 645-659. doi:10.1002/path.4125

Somji, S., Garrett, S.H., Sens, M.A., Gurel, V., Sens, D.A. 2004. Expression of metallothionein isoform 3 (MT-3) determines the choice between apoptotic or necrotic cell death in Cd+2-exposed human proximal tubule cells. *Toxicol Sci.* 80(2), 358-66.

Somji, S., Garrett, S.H., Sens, M.A., Sens, D.A. 2006. The unique N-terminal sequence of metallothionein-3 is required to regulate the choice between apoptotic or necrotic cell death of human proximal tubule cells exposed to Cd+2. *Toxicol. Sci.* 90(2), 369-376. Sharfuddin AA, Molitoris BA. Pathophysiology of ischemic acute kidney injury. *Nat Rev Nephrol.* 2011 Apr;7(4):189-200.

Sommar, J.N., Svensson, M.K., Bjor, B.M., Elmstahl, S.I., Hallmans, G., Lundh, T., Schon, S.M., Skerfving, S., Bergdahl, I.A. 2013. End-stage renal disease and low level exposure to lead, cadmium and mercury; a population-based, prospective nested case-referent study in Sweden. *Environ. Health.* 12:9.

Srinivasan B, Kolli AR, Esch MB, Abaci HE, Shuler ML, Hickman JJ. TEER measurement techniques for in vitro barrier model systems. *J Lab Autom.* 2015 Apr;20(2):107-26.

States, B., Foreman, J., Lee, J., Segal, S. 1986. Characterization of cultured human renal cortical epithelia. *Biochem. Med. Metab. Biol.* 36, 151-161.

Suzuki E, Fujita D, Takahashi M, Oba S, Nishimatsu H. Adult stem cells as a tool for kidney regeneration. *World J Nephrol.* 2016 Jan 6;5(1):43-52.

Taub, M, Chuman, L, Saier, M.H. Jr, Sato, G. 1979. Growth of Madin-Darby canine kidney epithelial cell (MDCK) line in hormone supplemented, serum-free medium. *Proc. Natl. Acad. Sci. U S A.* 76(7), 3338-3342.

- Taub, M., Sato, G. 1980. Growth of functional primary cultures of kidney epithelial cells in defined medium. *J. Cell. Physiol.* 105(2), 369-378.
- Taub, M., Sato, G.H. 1979. Growth of kidney epithelial cells in hormone-supplemented, serum-free medium. *J. Supramol. Struct.* 11(2), 207-216.
- Tejera D, Varela F, Acosta D, Figueroa S, Benencio S, Verdaguer C, Bertullo M, Verga F, Cancela M. Epidemiology of acute kidney injury and chronic kidney disease in the intensive care unit. *Rev Bras Ter Intensiva.* 2017 Oct-Dec;29(4):444-452.
- Templeton, D.N., Liu, Y. 2010. Multiple roles of cadmium in cell death and survival. *Chem. Biol. Interact.* 188(2), 267-275.
- Todd, J.H., Sens, M.A., Hazen-Martin, D.J., Bylander, J.E., Smyth, B.J., Sens, D.A. 1993. Variation in the electrical properties of cultured human proximal tubule cells. *In Vitro. Cell. Dev. Biol. Anim.* 29A(5), 371-378.
- Trifillis, A.L., Regec, A.L., Trump, B.F. 1985. Isolation, culture and characterization of human renal tubular cells. *J Urol.* 133(2), 324-329.
- Vogetseder A, Picard N, Gaspert A, Walch M, Kaissling B, Le Hir M. Proliferation capacity of the renal proximal tubule involves the bulk of differentiated epithelial cells. *Am J Physiol Cell Physiol.* 2008 Jan;294(1):C22-8.
- Waisberg M, Joseph P, Hale B, Beyersmann D. Molecular and cellular mechanisms of cadmium carcinogenesis. *Toxicology.* 2003 Nov 5;192(2-3):95-117.
- Wieser M, Stadler G, Jennings P, Streubel B, Pfaller W, Ambros P, Riedl C, Katinger H, Grillari J, Grillari-Voglauer R. hTERT alone immortalizes epithelial cells of renal proximal tubules without changing their functional characteristics. *Am J Physiol Renal Physiol.* 2008 Nov;295(5):F1365-75.
- Wilson, P.D., Dillingham, M.A., Breckon, R., Anderson, R.J. 1985. Defined human renal tubular epithelia in culture: growth, characterization, and hormonal response. *Am. J. Physiol.* 248, F436-F443.